UNIVERSITY OF OKLAHOMA

GRADUATE COLLEGE

SOLID ACID CATALYZED POLYSACCHARIDE HYDROLYSIS

A DISSERTATION

SUBMITTED TO THE GRADUATE FACULTY

in partial fulfillment of the requirements for the

Degree of

DOCTOR OF PHILOSOPHY

By

LUISA MARIA ARCHULETA SMALLWOOD
Norman, Oklahoma
2012

SOLID ACID CATALYZED POLYSACCHARIDE HYDROLYSIS

A DISSERTATION APPROVED FOR THE
DEPARTMENT OF CHEMISTRY AND BIOCHEMISTRY

BY

_____
Dr. Robert White, Chair

_____
Dr. Shaorong Liu

_____
Dr. Wai Tak Yip

_____
Dr. Charles Rice

_____
Dr. Lance Lobban

Acknowledgements

As a child my mother suggested I become a PhD like her, and I responded with, "No mom I want to become a REAL doctor"; I was obviously confused. There are several people that I must thank because without them I would not have become a REAL doctor.

I would like to thank Dr. Robert White for all his guidance, support, and stimulating discussions. It was a privilege to work in his lab. I learned several new techniques and gained valuable quantitative and qualitative analytical skills. I would also like to thank my graduate committee Dr. Shaorong Liu, Dr. Wai Tak Yip, Dr. Charles Rice, and Dr. Lance Lobban for giving me constructive feedback and the opportunity to defend my research in completion of the PhD program in analytical chemistry.

I would like to thank my parents Roberto and Melecita Archuleta for all their love and support. They have always inspired me and encouraged me to pursue my dreams. I would like to thank my wonderful husband Chuck Smallwood for his patience, encouragement, and words of wisdom. I would also like

Table of Contents

List of Tables

List of Figures

Abstract

In addition to the rising costs of gasoline and the depletion of fossil fuels, air pollution caused by burning fossil fuels has increased the need to develop alternative renewable fuels. One possible alternative is the conversion of renewable biomass to fuels. The ability to use cellulosic biomass instead of starch for ethanol production makes bioethanol an even more attractive renewable alternative fuel. The focus of the research described here is on the study and optimization of polysaccharide hydrolysis by using solid acid catalysts. Solid acid catalyst (SAC) candidates were identified for polysaccharide hydrolysis and then tested in both an aqueous medium and in an ionic liquid medium. Higher activities for amorphous SACs (sulfated zirconia, Nafion® SAC-13, and Nafion® NR50) were observed compared to the zeolites tested (HY and HZSM-5) for starch hydrolysis in aqueous media. However, Na^+ enhancement of the aqueous media significantly increased the activity of HY and HZSM-5 for starch hydrolysis. Thus, it was determined that for zeolites to be active for cellulose hydrolysis,

acid equivalents must be transported from the catalyst inner channels to the aqueous media, which can be accomplished by ion exchange. For polysaccharide hydrolysis in ionic liquid media, ion exchange induced proton release resulted in an observed catalytic activity for cellulose hydrolysis for all SACs tested (HY, HZSM-5, sulfated zirconia, Nafion® SAC-13, and Nafion® NR50). The mmol H^+ transferred from each solid to the medium was found to be dependent on the catalyst acid site location and its availability to the ionic liquid cations. After protons are released into the medium, the resultant catalytic activity is comparable to adding the equivalent amount of a liquid strong acid, and this activity is not dependent upon the structure of the SAC from which the acid equivalents are derived. This irreversible release of acidic protons make reuse of these catalysts impractical. Necessary structural features that should be incorporated into the design of future reusable catalysts with greater activity were identified by the fundamental studies described here.

Chapter 1 : BACKGROUND

Fossil fuels (e.g. coal, oil, and natural gas) make up 85% of the fuels used in the United States [1]. Of the total oil consumed in the United States, 71% is used for transportation [1]. An increase in the demand for fossil fuels has caused gasoline prices to drastically increase. In 2011, the average cost of gasoline in the United States was $3.48 per gallon, which is more than two times what it was in 2000 ($1.46 per gallon) [1]. As the cost of fossil fuels increases, alternative energy resources will become more cost competitive. Furthermore, the high dependency on non-renewable fossil fuels as energy sources is depleting these fuel resources. Fossil fuels are a non-renewable resource because they are derived from dead plants and animals that have been heated (140°C – 250°C) under extremely high pressures between 7,500 to 15,000 feet below the surface of the earth for millions of years. In addition to the rising cost of gasoline and the depletion of fossil fuels, air pollution caused by burning fossil fuels has increased the need to develop alternative renewable fuels.

Extensive research has been devoted to the development of alternatives to fossil fuels. One possible alternative is the conversion of renewable biomass to fuels [2, 3]. There are two major types of biofuels: biodiesel, which is typically made from vegetable oil, and bioethanol, which is made from the fermentation of sugars [2].

The research proposed here focuses on bioethanol as an alternative renewable fuel. Not only is bioethanol renewable, it also burns cleaner than fossil fuels. By releasing the same amount of carbon dioxide into the atmosphere as the starting biomass had removed, bioethanol is considered to be a carbon neutral fuel [2]. According to the Renewable Fuels Association, ethanol is blended in 80% of the gasoline used in the United States [4]. In 2009, the substitution of ethanol for gasoline decreased the need to import oil by 364 million barrels [4]. Newer model cars can accept up to 10% ethanol mixed with gasoline, whereas Flex fuel vehicles use E85, which is a mixture of 15% gasoline and 85% ethanol. Recent advancements have significantly decreased the amount of energy needed to produce ethanol so that only 30,000 British

Thermal Units (BTU) is needed to produce one gallon of ethanol, which can provide 77,000 BTU of energy [4].

The current method of ethanol production predominately utilizes food crop feedstocks such as corn (starch) and sugar cane (sucrose) as the source of sugars for fermentation. An obvious concern of using food crops to produce fuel would be a shortage of food due to increasing needs for fuel. Sugars can alternatively be obtained from lignocellulosic biomass (non-food sources) such as agricultural residues, wood residues, dedicated energy crops, and municipal paper waste. Agricultural residues consist of corn stover (e.g. leaves and stalk of corn) and sugar cane bagasse (e.g. sugar extraction remnants). Wood residues consist of sawmill and paper mill discards. These substrates cannot be used as food, which makes them good feedstocks for ethanol production.

1.1 Lignocellulosic Biomass

The process of making ethanol from food source feedstocks (e.g. corn and sugar cane) is much more simple than for processes using lignocellulosic biomass feedstocks. Lignocellulosic biomass is mainly composed

of 35-50% cellulose, 25-30% hemicellulose, and 15-30% lignin [5, 6]. Lignin is a highly branched, hydrophobic material consisting of phenylpropane units that binds cellulose and hemicellulose. There are no sugar molecules available from lignin, and therefore it is not useful for bioethanol production. Hemicellulose has an amorphous branched structure and is composed of various sugar monomers (50-300 monomers) such as xylose, mannose, glucose, galactose, and arabinose [6]. Hemicellulose can be hydrolyzed to produce monosaccharides (e.g. hexose and pentose), which can then be fermented into ethanol. Hexose monosaccharides have six carbon atoms and 3-4 chiral centers (ketohexose and aldohexose respectively), whereas pentose monosaccharides have five carbon atoms and 2-3 chiral centers (ketopentose and aldopentose respectively). Examples of these monosaccharides are shown in figure 1.1. Specific monomers are differentiated by the stereochemistry at the chiral centers. Cellulose is a highly crystalline unbranched polymer comprised of glucose monomers (1,000-10,000 monomers). Cellulose can be hydrolyzed to produce glucose, which can then be fermented into ethanol.
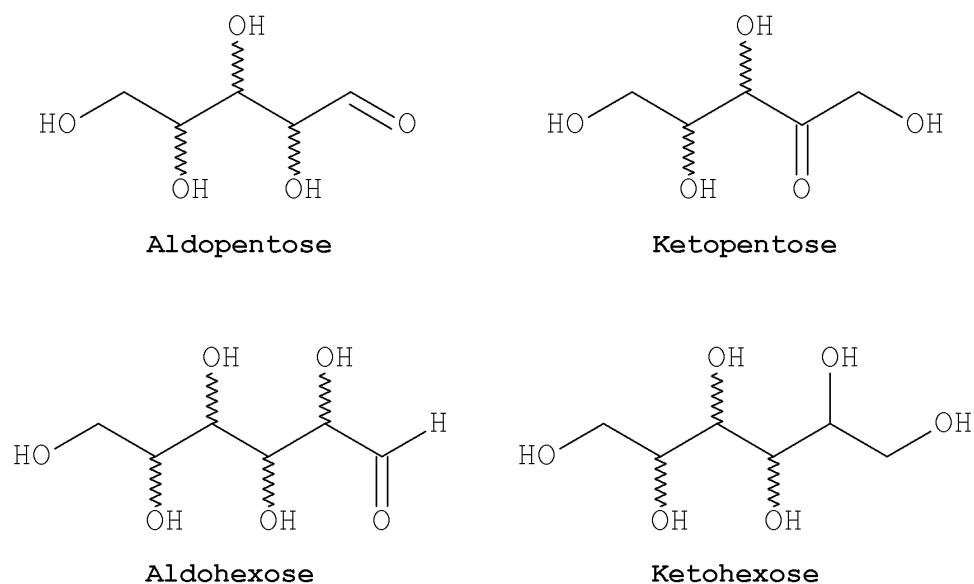
Figure 1.1 sugar monosaccharides

A variety of biomass pretreatment processes have been developed to separate and isolate the lignin, cellulose, and hemicellulose fractions from biomass. Each of these methods offers inherent advantages and disadvantages and can be classified as physical, chemical, and biological, based on their underlying mechanisms. Following pretreatment, biomass polysaccharides from cellulose and hemicellulose are decomposed into their constituent sugars by chemical or enzymatic means. The saccharifying procedure used for this conversion step should achieve efficient sugar release with minimal formation of byproducts. This is important because common byproducts, such as acetic

acid, furfural, and 5-hydroxyl-methyl furfural, are toxic to the microorganisms used for subsequent fermentation reactions [6]. Consequently, just as for all steps involved in biomass to biofuels conversion processes, intense research is underway to find better methods for saccharifying the polysaccharides derived from biomass feedstocks.

1.2 Polysaccharides

Because cellulose is the major component of lignocellulosic biomass materials, developing an efficient and cost effective hydrolysis process for the conversion of cellulose to glucose, which can then be fermented into ethanol, would be beneficial for the production of ethanol. However, the production of bioethanol from cellulose is a more difficult task than the production of ethanol from starch based materials.

Although both starch and cellulose are polysaccharides consisting of glucose monomers linked by glycosidic bonds, the type of linkage in these polymers is responsible for significant differences in properties. Starch contains between 15-30% amylose and 70-85% amylopectin. Amylose is a linear glucose

polymer with 1,4-alpha glycosidic bond linkages whereas amylopectin is a glucose polymer containing mainly 1,4-alpha glycosidic bond linkages with some branching via 1,6-alpha glycosidic bond linkages. The alpha linkages found in starch make it less rigid and with fewer hydrogen bonds than cellulose (figure 1.2). In this case "alpha linkage" is characterized as two glucose molecules linked by an oxygen from an axial OH of one monomer to another at the C(1) position.
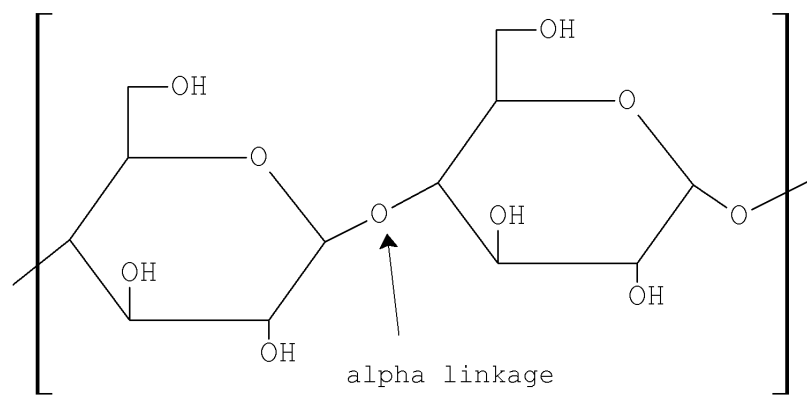
Figure 1.2 alpha-glycosidic bond linkage

Cellulose, on the other hand, is highly crystalline, unbranched, and polymers are involved in extensive intermolecular hydrogen bonding. Cellulose consists of glucose molecules linked by 1,4-beta glycosidic bonds (figure 1.3). In this case "beta

linkage" is characterized by two glucose molecules linked by an oxygen at an equatorial OH of one monomer to the C(1) position of the next monomer. In cellulose, every other glucose molecule in the chain is rotated 180°, which allows the polymer to assume a straight chain orientation. When these straight chains are stacked on top of each other, they align so that OH groups participate in extensive hydrogen bonding. This hydrogen bonding allows cellulose to be physically rigid and resistant to chemical hydrolysis.
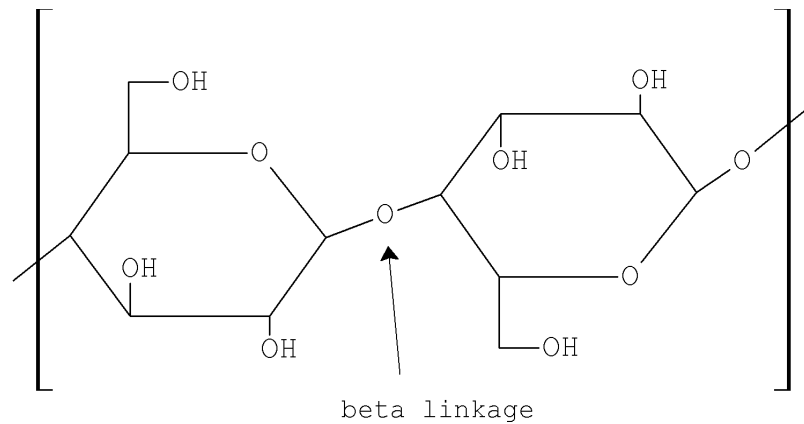
Figure 1.3 beta-glycosidic bond linkage

Polysaccharide solubility is thermodynamically favored when solvent-polysaccharide interactions effectively compete with the intermolecular hydrogen bonding between polymer chains. For polysaccharides,

the extent of intermolecular hydrogen bonding increases in the following order: starch < hemicellulose < cellulose. Consequently, more extreme conditions are required to dissolve cellulose than hemicellulose and starch. Although starch can be dissolved in water at low concentrations, cellulose is, for practical purposes, not soluble in water. For example, Strachan found that cellulose could be dissolved in water at 15°C only to the extent of 1.4 parts per 100,000 [7]. Cellulose dissolution in water is difficult because it requires the simultaneous breaking of numerous hydrogen bonds between adjacent cellulose molecules [8-14]. Although cellulose can be dissolved in water heated above 280°C, maintaining this temperature during hydrolysis results in decomposition of the glucose product [15-17]. Thus, in order to perform cellulose hydrolysis in an aqueous medium at lower temperatures, cellulose pretreatment methods are required.

The purpose of the pretreatment step is to break down the cellulose crystal structure and make it more accessible to hydrolyzing agents. Some complex pretreatments have been proposed, which often have a corrosive nature, require disposal of hazardous

byproducts and waste, and typically necessitate long pretreatment times [18]. The use of carbon dioxide explosion (supercritical carbon dioxide) to pre-treat cellulose (35°C, 3000 psi) provides higher glucose yields when enzyme catalysis is subsequently performed [19]. Supercritical carbon dioxide (SCD) is compressed at temperatures above its critical point (31.1°C, 1073 psi), and explosive release of the SCD is thought to disrupt the cellulose structure. This method requires the use of high pressures and buffer solutions. Ball milling (grinding) is another method that has been used to pretreat cellulose prior to hydrolysis. Although ball milling is environmentally friendly, it requires long pretreatment times (>24 hours). Research has shown that cellulose crystallinity decreases by 25% after ball milling for 48 hours [20, 21].

The current research focus for cellulose dissolution involves the use of ionic liquids, which are salts in liquid form at or below 100°C. Several studies have shown that cellulose can be dissolved in ionic liquids at moderate temperatures. Therefore, pretreatment steps are not required [22-28]. Ionic

liquids have not only been used for cellulose dissolution, but also as a hydrolysis medium [29–32].

1.3 Polysaccharide Hydrolysis Process

Polysaccharide molecules contain internal and terminal glycosidic bonds. It has been suggested that the terminal bonds are more reactive because it is easier to hydrolyze polysaccharides with a higher degree of branching (e.g. starch) compared to polysaccharides with no branching (e.g. cellulose) [33]. An overview of the hydrolysis mechanism of starch by acid catalysis is shown in figure 1.4. The mechanism starts with protonation of the glycosidic oxygen that links two glucose monomers. When one of those glucose monomers is terminal, cleaving of the glycosidic linkage forms one glucose molecule and a cyclic carbocation. Nucleophilic attack of water on the cyclic carbocation allows for the formation of a hydroxyl (OH) group at the carbon 1 position of the glucose monomer. Although the reaction mechanism is essentially the same for both starch and cellulose, increased hydrogen bonding in cellulose makes accessing the glycosidic bonds more difficult.
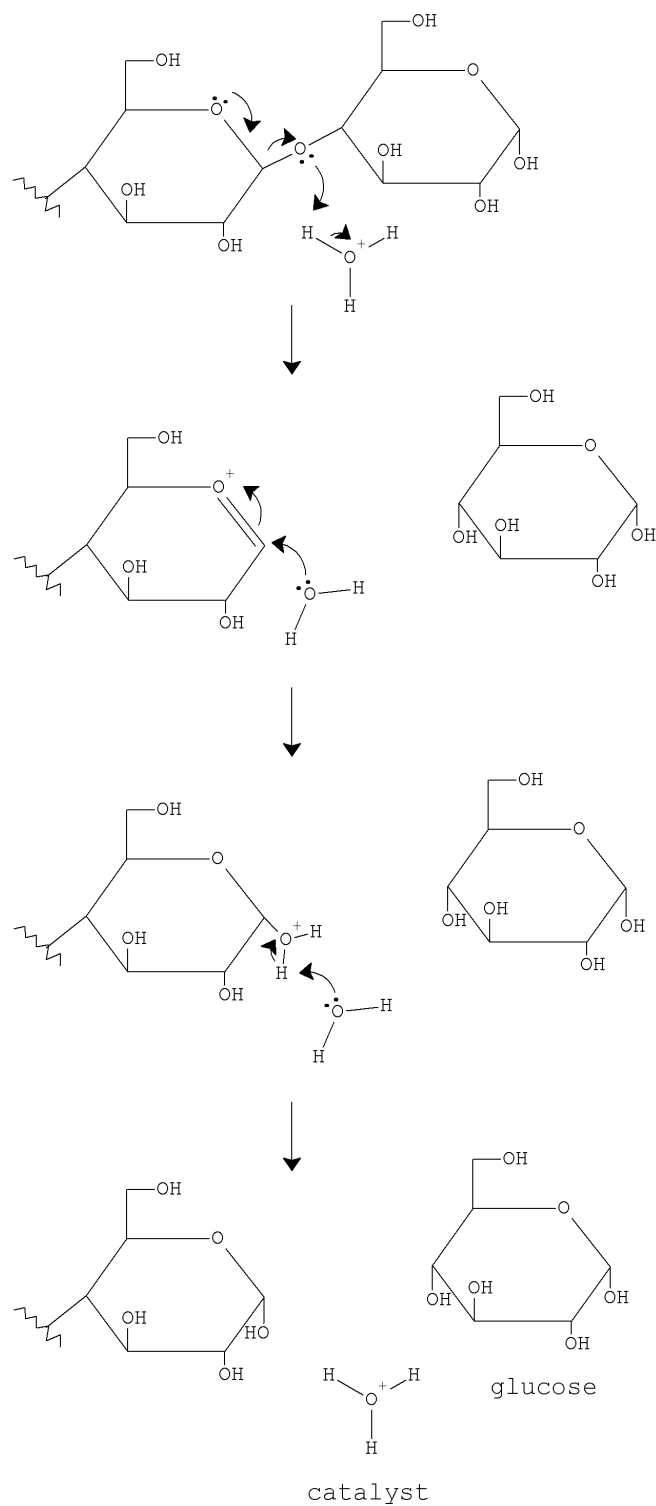
Figure 1.4 starch hydrolysis mechanism by acid catalysis

The research described in this dissertation focuses on the polysaccharide hydrolysis portion of the biomass to bioethanol production process. The most commonly researched processes for hydrolyzing polysaccharides to sugars include: liquid acid catalysis, hot compressed water treatment, enzymatic catalysis, and solid acid catalysis.

1.4 Liquid Acid Catalysis

Liquid acids (e.g. sulfuric acid) have a long industrial history for ethanol production from corn feedstocks [6, 34-40]. A simplified schematic of ethanol production from cellulose hydrolyzed by liquid acids is shown in figure 1.5. Cellulose is exposed to liquid acids and acid catalyzed hydrolysis results in sugars that can be fermented to create ethanol. However, before fermentation can occur, the liquid acid, which is detrimental to the yeast, must be neutralized.

Rinaldi and Schutch have reviewed acid catalyzed cellulose hydrolysis [5]. Two approaches are commonly employed: dilute acid catalysis and concentrated acid catalysis [6]. Hydrolysis using concentrated acid

catalysis is carried out at temperatures below 100°C, and requires long reaction times (e.g. hours). Hydrolysis using dilute acid catalysis is conducted at temperatures above 200°C, and requires shorter reaction times (e.g. minutes). However, high temperatures cause decomposition of sugar products that can adversely affect the fermentation process. According to Hamelinck et al. (2005), dilute acid (<1% sulfuric acid) catalyzed cellulose hydrolysis at 215°C for 3 minutes produced 50-70% glucose, whereas concentrated acid catalysis (30-70% sulfuric acid) at 40°C for 2-6 hours produced up to 90% glucose [41].
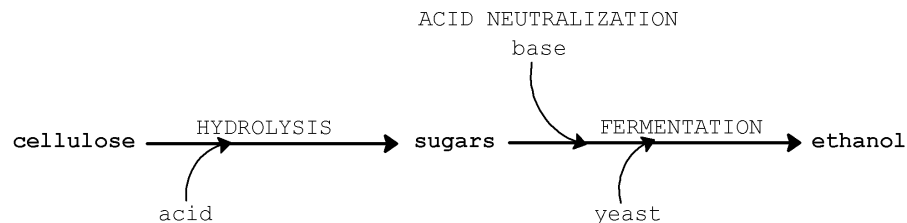
Figure 1.5 simplified schematic of cellulose hydrolysis by liquid acid catalysis

Although high sugar yields can be obtained with acid catalysis, there are many disadvantages to this method. The acids are corrosive, requiring expensive corrosion resistant steel reactors. Acid recovery is

costly and requires large energy consumption. Without acid recovery, acids must be neutralized before fermentation, requiring the disposal of large amounts of salts, making this method costly and environmentally hazardous. Under acidic conditions, the primary glucose decomposition pathway yields 5-hydroxyl-methyl furfural [42], which is toxic to the yeast used later in the ethanol production process.

1.5 Hot Compressed Water Treatment

Hot compressed water (HCW) is water that has been heated above the boiling point (100°C) under high pressure to maintain a liquid phase [43]. HCW treatment has been successfully utilized for polysaccharide hydrolysis [16, 44-46]. Under HCW conditions, water becomes more acidic and hydrolysis can occur. There are two main types of treatments: supercritical and subcritical water. In supercritical water, the temperature is above the critical point (>374°C), whereas in subcritical water, the temperature is below the critical point but above the boiling point (100°C - 374°C). The vapor-liquid critical point for

water occurs at 374°C and 22 MPa. Under these conditions no phase boundaries exist [47].

Hot compressed water is a favorable treatment method because there are minimal environmental and corrosion problems, low operational cost, and high reaction rates. Although this is an environmentally friendly technique, the yields of sugar for both supercritical (30-47%) and subcritical (14-23%) hot compressed water treatments do not compare to those obtained with liquid acid catalyzed hydrolysis [15, 16]. A disadvantage of this method is that high temperatures promote glucose decomposition after hydrolysis. In hot compressed water without added catalyst, glucose decomposition effective activation energies of 96 and 121 kJ mol^{-1} have been reported [48, 49].

1.6 Enzyme Catalysis

Enzyme catalysis is a newer technique that is currently the main focus of research for cellulose hydrolysis. A simplified schematic of cellulose hydrolysis by enzymatic catalysis is shown in figure 1.6. Cellulose is first mixed with water to create a

mash, which is then exposed to cellobiohydrolase enzymes (e.g. β-1,4-endoglucanases and β-1,4-exoglucanases). These enzymes break native cellulose into cellobiose, which is a disaccharide of glucose (figure 1.7). The resulting cellobiose can then be cleaved using cellulase enzymes (e.g. β-glucosidase) to obtain glucose [50]. The glucose is then fermented to produce ethanol.
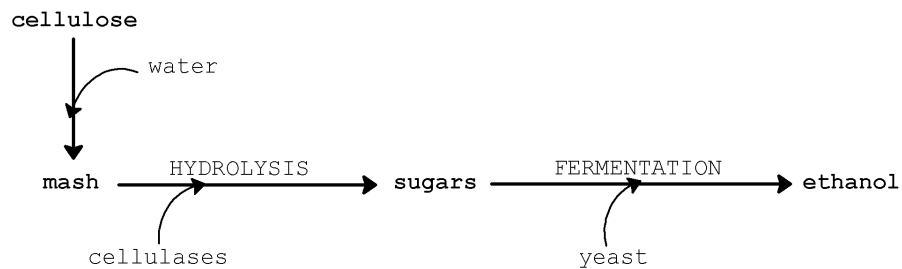
Figure 1.6 simplified schematic of cellulose hydrolysis by enzyme catalysis
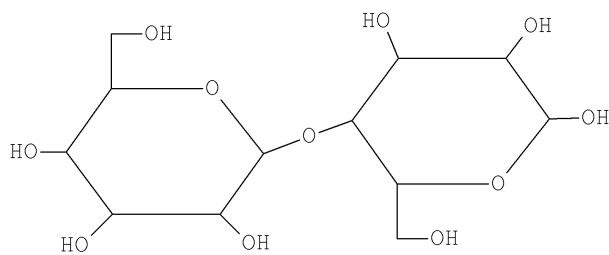
Figure 1.7 structure of cellobiose

Temperature requirements for enzyme catalysis (100°C) are milder than for dilute acid catalysis methods (200°C). Furthermore, enzyme catalysis involves minimal corrosion and produces sugar yields that are comparable to acid catalyzed hydrolysis (75-95%) with minimal byproducts [15, 41, 51]. Although high conversion can be obtained, there are several drawbacks to enzyme catalysis. Most importantly, the cellulases and cellobiohydrolase used for hydrolysis are costly [52]. Recent studies suggest that enzymes used for fermentation can cost $0.68-1.47 per gallon of ethanol produced, depending on the saccharification and fermentation yields [53]. This has led to intense research in the development of cheaper enzymes that can be recovered and reused. In addition, enzyme catalysis typically requires days to achieve high conversions, instead of hours or minutes, which are typical for liquid acid catalyzed hydrolysis.

1.7 Solid Acid Catalysis

Instead of using strong homogeneous liquid acids (e.g. sulfuric acid) for polysaccharide hydrolysis, this dissertation evaluates using solid acid catalysts

(SACs). Polysaccharide hydrolysis based on using solid acid catalysis is an option that hasn't been thoroughly investigated. The problems of corrosion and salt disposal that are characteristics of liquid acid catalyzed hydrolysis can be avoided by using SACs. Minimizing corrosion and eliminating the need for salt disposal makes the use of SACs a more environmentally friendly option. Thus, solid acid catalyzed hydrolysis has potential to be competitive with enzyme-catalyzed hydrolysis. Furthermore, because solid acid catalysts do not dissolve in water, they can potentially be recovered by filtration and reused.

1.7.1 Solid Acid Catalysts in Aqueous Media

Because surfaces of SACs have relatively low acid site densities, SACs perform much like a dilute acid catalyzed system. However, instead of the problems resulting from corrosion and acid neutralization, which are characteristic of homogenous strong acid catalysis methods, SACs can suffer from catalytic active site degradation. In addition, loss of catalytic activity can result from proton ion exchange with trace ions and

from residue accumulation on catalyst surfaces (e.g. char buildup).

Several solid acid catalysts have been found to be useful for hydrolyzing disaccharides (e.g. sucrose and cellobiose) dissolved in water, yielding up to 90% conversion (table 1.1). Tagusagawa et al. found that mesoporous niobium oxide (2 hr, 80°C) had high selectivity for the formation of glucose from sucrose, with sugar yields of 86% and essentially no degradation of the catalyst acid sites [54]. Table 1.1 indicates that several solid acid catalysts have high activity for hydrolyzing glycosidic bonds.

Table 1.1 disaccharide hydrolysis with SACs

Catalyst	Disaccharide	Time (h)	Temp (°C)	Converted (%)	Ref.
SE–MS[a]	Sucrose	4	80°C	86–90%	[55]
SP–MS[b]	Sucrose	4	80°C	81–83%	[55]
Sulfonated silica	Sucrose	4	80°C	64%	[55]
Amberlyst-15	Sucrose	4	80°C	88%	[55]
Nafion®	Sucrose	4	80°C	28%	[55]
PS–MS[c]	Cellobiose	0.5	175°C	90%	[56]
AS–MS[d]	Cellobiose	0.5	175°C	90%	[56]
SZ/SBA-15[e]	Cellobiose	1.5	160°C	80%	[57]

[a]sulfonated ethylene bridged mesoporous silica
[b]sulfonated phenlyene bridged mesoporous silica
[c]propylsulfonic acid functionalized mesoporous silica
[d]arenesulfonic acid functionalized mesoporous silica
[e]sulfated zirconia modified amorphous mesoporous silica (SBA-15)

The use of solid acid catalysts for the hydrolysis of polysaccharides in an aqueous medium has only recently been investigated (table 1.2). Although starch conversions ranged from 20-90%, cellulose conversions were significantly lower with typical conversions ranging from 1-45%, with the exception of one outlier at 74%, when acid functionalized carbonaceous spheres were utilized. Onda et al. evaluated several solid acids for hydrolysis of milled

cellulose in aqueous media, and reported low (<25%) glucose yields for the following solid acid catalysts that they tested: SiO_2, $\gamma-Al_2O_3$, H-mordenite, H-beta, HZSM-5, activated carbon (AC), Amberlyst-15, and sulfated zirconia [20]. Differences in relative activities were explained based on varying size restricted access of cellulose to SAC acid sites. In addition, sulfonated activated-carbon catalyst ($AC-SO_3H$) was found to provide approximately the same amount of glucose yield (40%) with fewer byproducts than 0.01 M sulfuric acid under the same reaction conditions [20, 21].

Table 1.2 polysaccharide hydrolysis with SACs

Catalyst	Disaccharide	Time (hr)	Temp (°C)	Converted (%)	Ref.
CS[a]	Starch	4	120°C	90%	[58]
Amberlyst-15	Starch	4	120°C	15%	[58]
HZSM-5	Starch	4	120°C	20%	[58]
CS[a]	Cellulose[b]	0.7	150°C	74%	[58]
Amberlyst-15	Cellulose[b]	0.7	150°C	25%	[58]
HZSM-5	Cellulose[b]	0.7	150°C	1%	[58]
SiO_2	Cellulose[c]	24	150°C	<5%	[20]

Table 1.2 polysaccharide hydrolysis with SACs

(continued)

Catalyst	Disaccharide	Time (hr)	Temp (°C)	Converted (%)	Ref.
γ-Al$_2$O$_3$	Cellulose[c]	24	150°C	<5%	[20]
H-mordenite (Si/Al=10)	Cellulose[c]	24	150°C	5-10%	[20]
H-beta (Si/Al=12)	Cellulose[c]	24	150°C	5-10%	[20]
HZSM-5 (Si/Al=45)	Cellulose[c]	24	150°C	5-10%	[20]
H-beta (Si/Al=75)	Cellulose[c]	24	150°C	5-10%	[20]
AC[d]	Cellulose[c]	24	150°C	5-10%	[20]
AC-SO$_3$H[e]	Cellulose[c]	24	150°C	40-45%	[20]
Sulfated Zirconia	Cellulose[c]	24	150°C	10-15%	[20]
Amberlyst-15	Cellulose[c]	24	150°C	25-30%	[20]
None	Cellulose[c]	24	150°C	<5%	[20]

[a]Carbonaceous spheres
[b]milled 24 hours
[c]milled 48 hours
[d]activated carbon
[e]sulfonated activated carbon

1.7.2 Solid Acid Catalysts in Ionic Liquid Solvent

The use of ionic liquids to dissolve cellulose eliminates the need for a pretreatment step, lowers required reaction temperatures, and the reaction medium

can potentially be reused. A simplified schematic of cellulose hydrolysis in ionic liquid with solid acid catalysis is shown in figure 1.8. Cellulose is first dissolved in ionic liquid and then water and SAC are added to the mixture. Hydrolysis of cellulose results in sugars, which can be fermented into ethanol. Prior to fermentation, the solid acid catalyst and ionic liquid are removed from the aqueous hydrolysis products.
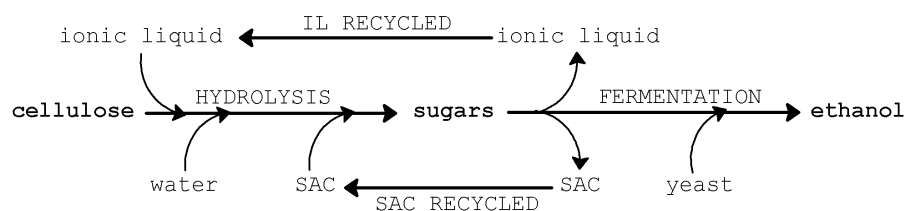
Figure 1.8 simplified schematic of cellulose hydrolysis by solid acid catalysis

The reaction mechanisms involved with using solid acid catalysts for polysaccharide hydrolysis in an ionic liquid medium (ILM) have not been thoroughly investigated. Rinaldi et al. evaluated several solid acid catalysts for their ability to depolymerize cellulose into cellooligomers when cellulose was dissolved in 1-butyl-3-methylimidazolium chloride ([BMIM]Cl) ionic liquid at 100°C for 1 hour [59].

Amberlyst-15 and Amberlyst-35 were reported to cause a significant decrease in the degree of polymerization (DP) of cellulose (table 1.3). Whereas cellulose treated with Amberlyst-15 and Amberlyst-35 had a DP of 125, DP values for the same cellulose treated with other SACs was significantly higher (1300-2200). The higher activities of Amberlyst-15 and Amberlyst-35 were suspected to be a result of high surface area and large pore sizes (36 nm and 28 nm respectively) for these catalysts relative to the other SACs studied. Amberlyst-70 was believed to have a lesser effect on the cellulose DP because it has significantly lower surface area than the Amberlyst-15 and Amberlyst-35 catalysts. Thus, although only a few studies involving solid acid catalysts have been reported, published results suggest that they may be useful as an alternative to concentrated acid catalysis methods for the hydrolysis of cellulose in ionic liquids.

Table 1.3 effectiveness of SACs on the degree of polymerization of cellulose

Catalyst	Degree of Polymerization[a]
Amberlyst-15	125
Amberlyst-35	125
Nafion® NR50	1800
Sulfated Zirconia	1700
HY	2100
HZSM-5	2200
Amberlyst-70	1700
γ-Al_2O_3	1300
SiO_2-Al_2O_3	2200

[a]approximated from ref [59].

1.8 Solid Acid Catalyst Acidity

In the presence of water, strong liquid acids ionize (e.g. HCl → H^+ + Cl^-), and the resulting proton (H^+) strongly interacts with the nonbonding electron pairs of water to form a hydronium ion (H_3O^+).

Therefore, in dilute aqueous solutions (pH 0-14), the predominant acid species is H_3O^+. For solid acid catalysts, acidic protons are found on or near the surface of the catalyst. Although H_3O^+ can also be formed, the only way for the coordinating hydronium ion to leave the catalyst surface and freely move through the medium would be if another cation takes its place through an ion exchange mechanism.

Assuming that there is no cation to exchange with the proton in an aqueous hydrolysis medium, solid acid catalysts should retain their acidity and be reusable. The catalytic activity of an SAC in water will be dependent on the surface acid sites that are accessible to the hydrolysis substrate. Acid sites located within volumes with size-restricted access will only be active for substrates small enough to pass into the restricted volume.

Ionic liquid media, on the other hand, provide cations that can replace catalyst protons by ion exchange. In this case, the ionic liquid would allow for the proton to be released into the hydrolysis medium, where large substrates that cannot pass into the restricted volume can be protonated. Under these

conditions, acid catalyzed reactions should proceed at rates similar to those for a liquid catalyst containing a similar number of protons as those provided by ion exchange from the SAC. Unfortunately, using SACs in this manner decreases the likelihood that they can be removed from the reaction medium and reused for subsequent reactions.

1.9 Solid Acid Catalysts Studied

The properties of three types of solid acid catalysts (SACs) were studied, which included: sulfated zirconia, ion exchange resins (Nafion® SAC-13 and Nafion® NR50), and zeolites (HY and HZSM-5). These catalysts were selected for their various properties: sulfated zirconia has randomly dispersed acid sites; the ion exchange resins are polymers with acid functionalities; and zeolites have pores with most acid sites located inside the pores.

1.9.1 Sulfated Zirconia

Sulfated zirconia (SZ) was discovered in 1962 by Holm and Bailey [60], and has been found to be a useful catalyst in reactions involving isomerization,

alkylation, cracking, and acylation [61, 62]. Several detailed reviews of sulfated zirconia have been published [62-64]. Sulfated zirconia has been reported to be a solid superacid, because its acid strength exceeds that for 100% sulfuric acid [65]. Yamaguchi proposed that the surface sulfur species is responsible for the highly acidic properties of SZ and that the surface structure is independent of the starting sulfur material used to synthesize the catalyst [66]. Although the structure of the sulfated zirconia acid site is still not known, several models have been proposed [65, 67-76]. All proposed models include sulfur bound to at least one oxygen from the metal oxide (ZrO_2), but the number of oxygens bonded to the sulfur species (S) varies. Several acid site models include a sulfur species with two single bonded oxygens to zirconium and two double bonded terminal oxygens (figure 1.9a) [61, 65, 68, 69, 74-76]. Laizet et al. proposed that a similar structure forms only when the S/Zr ratio is high. When the S/Zr ratio is low, the sulfur was thought to have one double bonded terminal oxygen and four oxygens singly bonded to zirconium (figure 1.9b) [75]. Other models have proposed a sulfur species with

one double bonded oxygen and three single bonded oxygens (figure 1.9c) [70-72]. More recently, Hino et al. proposed a mixture of these models, where the sulfur species can have either two double bonded terminal oxygens and two single oxygen to zirconium bonds, or one double bonded terminal oxygen and three single oxygen to zirconium bonds [67]. It has also been proposed that the S/Zr molar ratio plays a role in the surface structure and determines the number of double bonded oxygens [76].
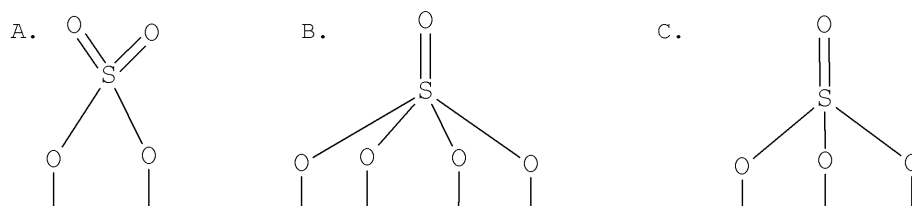
Figure 1.9 three of the most commonly proposed structures of sulfur species bound to oxygen from a metal oxide found in sulfated zirconia (simplified for clarity)

1.9.2 Nafion® Ion Exchange Resins

Nafion® is a sulfonated tetrafluoroethylene polymer developed by DuPont in the 1960s (figure 1.10) [77]. Nafion® has been shown to be a useful catalyst in reactions involving alkylation, acylation,

isomerization, phosphorylation, esterification, and nitration [78]. Nafion® is considered to be a superacid with an acid strength similar to that of 100% sulfuric acid [79]. It is believed that the electron withdrawing forces of the perfluoronated carbon chains neighboring the sulfonic acid group (SO_3H) develops a positive charge on the sulfonic acid group which is responsible for the superacidity [80].

$$-(CF_2CF_2)_m-(CF_2CF)_n-$$
$$|$$
$$(OCF_2CF)_p-OCF_2CF_2SO_3H$$
$$|$$
$$CF_3$$
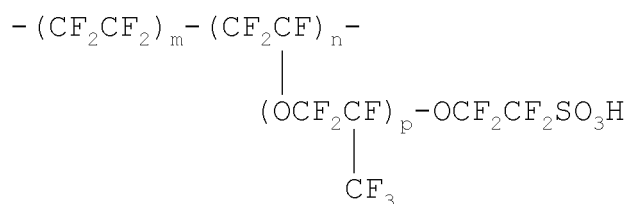
Figure 1.10 structure of Nafion® with the —(CF_2CF_2)– region hydrophobic, and the —SO_3H region hydrophilic [81]

Although the acid functionalities for both Nafion® NR50 and Nafion® SAC-13 have the same general structure, Nafion® SAC-13 is bound to amorphous silica and Nafion® NR50 is comprised of unsupported Nafion® polymer (figure 1.11). The amorphous silica used for Nafion® SAC-13 has pore diameters greater than 10nm, resulting in a larger surface area compared to Nafion®

NR50. Rajagopal found that Nafion® SAC-13 required shorter reaction times than Nafion® NR50 for the activation of hexamethyldisilazane used for alcohol silylation. It was suggested that the Nafion® SAC-13 provided better accessibility because of the amorphous silica, thereby enhancing the overall acidity [79]. Other studies have reported that although Nafion® SAC-13 is significantly more active than Nafion® NR50 for reactions involving nonpolar molecules (e.g. butane isomerization) [82, 83], there is no significant difference in catalytic activity for reactions involving polar molecules (e.g. Fries rearrangement of phenyl acetate) [84].
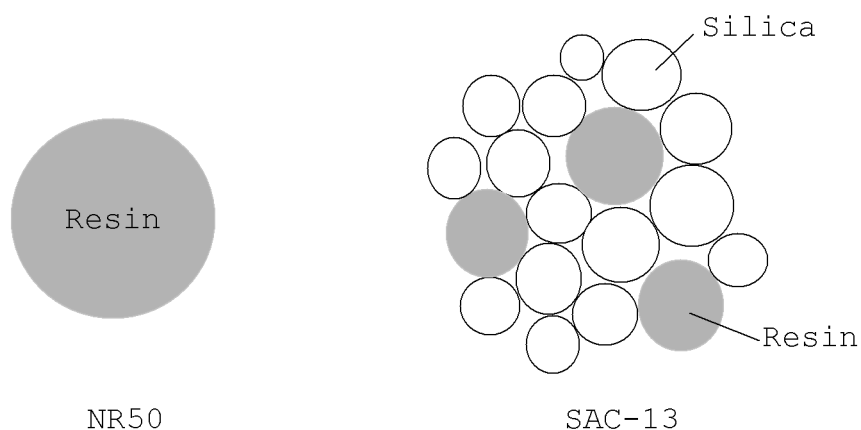
Figure 1.11 cartoon depiction of Nafion® NR50 and Nafion® SAC-13 derived from ref.[85]

1.9.3 Zeolites

Zeolites are microporous crystalline aluminosilicates characterized by their crystal structure, pore size (range from 3-10Å), and Si/Al ratio, which is chemically represented by $M_{2/n}O \cdot Al_2O_3 \cdot ySiO_2 \cdot wH_2O$ [86]. In this empirical formula, M is the charge balancing cation, *n* is the cation valence, *y* can range from 2-200, and *w* is the amount of water. In zeolites, substitution of Si^{4+} for Al^{3+}, results in a negative charge associated with an oxygen of the AlO_4 group, which is balanced by the presence of a cation. When the balancing charge is a proton, the zeolite will have an acid functionality. It has been found that the number of Al atoms incorporated into a protonated zeolite is directly proportional to the number of acid sites, so a higher Si/Al ratio results in a decrease in acid site density [87]. Zeolites have been shown to be useful catalysts for isomerization, alkylation, and hydrocracking reactions [88-91]. A study by da Silva et al. suggested that the hydrophobic nature of zeolites protected the acid sites from reacting with water in aqueous media, thereby preserving the acidity of the solid acid catalyst. Young et al. used

thermogravimetry and IR spectroscopy to suggest that this hydrophobic character is due to the nonpolar Si-O-Si groups, which do not adsorb water; whereas water can be absorbed to the Si-OH groups [92].

The Y zeolite has a Faujausite (FAU) framework, which consists of truncated octahedra linked by double 6-member rings, which form a supercage. The large cavity supercage is accessible through 12-member rings that have a 7.4 Å diameter [93, 94]. A detailed drawing of the FAU structure can be found in the "Atlas of Zeolite Framework Types" [95]. Although acid sites can be found throughout the FAU framework, the most easily accessible are those found in the supercage [96].

ZSM-5 is a zeolite with an MFI framework, which consists of straight channels with 10-member ring openings having dimensions of 5.3 Å x 5.6 Å and perpendicular intersecting sinusoidal channels with 5.1 Å x 5.5 Å openings [93, 94, 97]. A detailed drawing of the MFI structure can also be found in the "Atlas of Zeolite Framework Types" [95]. Acid sites are primarily found in the 10-member ring channels and near the intersections of the two channels [94, 98]. MFI

frameworks are highly siliceous and therefore, the number of acid sites are typically low.

1.10 Research Objectives

Solid acid catalysts have the potential to be cost effective, environmentally friendly, and non-corrosive, provided that they provide high biomass reaction rates, high sugar yields, and have the ability to be reused or regenerated. A variety of solid acid catalysts were selected to represent a range of characteristics. Sulfated zirconia was selected for its superacid strength. Nafion® has also been shown to exhibit superacidity. However, unlike sulfated zirconia, Nafion® is a polymer with terminal acid sites. Nafion® SAC-13 and NR50 were both tested to better understand the effects of binding the polymer to silica and how this more ordered structure may affect hydrolysis. Zeolites HY and HZMS-5 were selected to study the effects of pore size and Si/Al ratio on hydrolysis reactions.

The purpose of the experiments described here is two-fold. The first focus was to identify good solid acid catalyst candidates for polysaccharide hydrolysis

in both an aqueous medium and an ionic liquid medium. Solid acid catalysts were tested to determine their relative activities in both water and ionic liquid. The second focus was to investigate the mechanisms by which solid acid catalysts facilitate polysaccharide hydrolysis. Based on the literature, zeolites exhibit little to no activity for polysaccharide hydrolysis in aqueous media. In contrast, results obtained from the experiments described here reveal that zeolites can be highly active for polysaccharide hydrolysis in an ionic liquid medium.

Chapter 2 : EXPERIMENTAL

2.1 Chemicals and Reagents

Ion exchange resin Dowex 50WX4-200 (422096[A]) and cellulose (~20μm, 31,069-7) were purchased from Sigma-Aldrich (St. Louis, MO, USA).   All HPLC grade solvents, which included: ethyl acetate (E195SK-1), methanol (MX0475-1), and acetonitrile were purchased from Fisher Scientific (Pittsburgh, PA, USA).   All other chemicals, such as silicone oil (S159-500), copper sulfate (CX2185-1), sodium chloride (7581), glacial acetic acid (A38), sodium hydroxide (7708), oxalic acid dihydrate (A219), D(+)-glucose monohydrate (4074-2), ethanol, dimethylformamide, as well as certified ACS grade sodium citrate (SX0445-1), sodium carbonate anhydrous (SX0395-1), sulfuric acid (287648), hydrochloric acid (A144S-212), dimethyl sulfoxide (D1281), ammonium nitrate (3436-12), 2-propanol (A416SK-4), and 1-propanol (A414-1) were purchased from Fisher Scientific (Pittsburgh, PA, USA).   Solid acid catalysts: Nafion® SAC-13 (474541) and Nafion® NR50

[A] Catalog numbers are listed in parenthesis for each item purchased

(70150) were purchased from Sigma-Aldrich (St. Louis, MO, USA).

The use of reagent grade chemicals and distilled water was used for reactions to minimize contaminant cations that could cause a loss in catalytic activity as a result of ion exchange, resulting in a catalyticly active proton being replaced by a non-reactive cation.

2.2 Ionic Liquid

The ionic liquid (IL) that was evaluated as a polysaccharide hydrolysis medium was 1-ethyl-3-methylimidazolium chloride [EMIM]Cl, which has a melting point of 77-79°C and a flash point of 186°C. [EMIM]Cl (30764) was used as purchased from Sigma-Aldrich without additional purification. Cellulose dissolution could be obtained at 120°C in this ionic liquid after 30 minutes (ambient pressure) with ca. 20 wt% solubility.

2.3 Catalyst Properties, Preparation, and Acidity

The solid acid catalysts (SACs) evaluated in the studies described here included: sulfated zirconia, ion

exchange resins (Nafion® SAC-13 and Nafion® NR50), and zeolites (HY and HZSM-5). A summary of the catalyst properties is given in table 2.1.

Table 2.1 SACs properties

SAC	Physical	Pore Size (Å)	Structure
Sulfated Zirconia	Powder	n/a	Amorphous
Nafion® SAC-13	Powder	>100	Amorphous
Nafion® NR50	Pellet	n/a	Amorphous
HY	Powder	7.4	Crystalline
HZSM-5	Powder	5.3 x 5.6 5.1 x 5.5	Crystalline

Weingarten et al. evaluated the acid concentration of several solid acid catalysts ($Zr-PO_4$, $SiO_2-Al_2O_3$, HY, and WO_x/ZrO_2) using both ammonia temperature programed desorption (NH_3-TPD) and acid-base titrations. Their results showed that higher acid concentrations were obtained by acid-base titrations than by NH_3-TPD [99]. They also reported varying acid concentration differences (ranging from 0.5-2.9 mmol g^{-1}) between NH_3-

TPD and acid-base titration results for each catalyst [99]. Trends in these differences could not be explained based on SAC properties and no correlations were reported for the two methods (NH_3-TPD and acid-base titration). Whereas the NH_3-TPD method is commonly used to determine the acid concentrations of SACs used for gas phase reactions [61, 63, 100, 101], this method may not be an appropriate for determining acid concentrations when SACs are utilized for aqueous reactions. Other published studies that have included evaluations of SACs for aqueous phase applications have employed acid-base titration as the method for determining acid concentrations [55, 102]. Therefore, it seems reasonable to use titrations rather than NH_3-TPD to determine acidity for the studies described here.

The acid concentration for each SAC was determined by using a back titration method with phenolphthalein as the color indicator. The indicator was prepared by dissolving phenolphthalein (0.1 g) in 25 mL ethanol prior to the addition of distilled water (25 mL). Sodium hydroxide solution (0.01 M, 25 mL) was mixed with each SAC (0.1 g) for 10 minutes under constant

stirring; Nafion® NR50 was also mixed for 2 hrs prior to titration to allow for swelling and access to internal acid sites. Mixtures were centrifuged and the liquid was removed. Phenolphthalein indicator (10 drops) was added to an aliquot (10 mL) of the liquid and it was then titrated with oxalic acid (0.01 M) to a pink to clear color change end point. The acid concentration (mmol H^+ g^{-1}) for each SAC was calculated from the titration results by using equation 2.1. In this equation, the value 2.5 represents the dilution factor resulting from removing a 10 mL aliquot from the starting 25 mL volume.

Equation 2.1

$$\frac{\left[[(M\ NaOH)(25\,mL\ NaOH)]-[(M\ OA)(mL\ OA)\left(\frac{2\ mmol\ NaOH}{1\ mmol\ OA}\right)(2.5)]\right]\left[\frac{1\ mmol\ H^+}{1\ mmol\ NaOH}\right]}{0.1\ g\ SAC}$$

2.3.1 Sulfated Zirconia

Sulfated zirconia used for this research was prepared according to the method described by Sikabwe [103]. A paste was created by combining zirconium hydroxide (1 g) and ammonium sulfate (1 M, 0.9 mL). The mixture was dried at 110°C for 1 hour, and then

41

calcined in a Thermolyne 47900 furnace (Thermo Scientific, USA) at 600°C for 4 hours.

2.3.2 Nafion® Ion Exchange Resins

Nafion® NR50 (70150, pellet size 7-9 mesh) and Nafion® SAC-13 (474541) were purchased from Sigma-Aldrich (St. Louis, MO, USA) and were received in pellet and rod form respectively. Nafion® NR50 was used as received for all studies. Nafion® SAC-13 was ground to a fine powder by using a mortar and pestle.

2.3.3 HY Zeolite

The sodium form Y zeolite (NaY) was obtained from Honeywell UOP (Y-54, Si/Al=5.30, Des Plaines, IL). The procedure used for preparing HY by NaY protonation was slightly modified from the method outlined by Hesse [104]. The modified procedure involved mixing NaY (1 g) with ammonium nitrate (0.25 mol) in water and refluxing with constant stirring for 4 hours. The solid was then removed from the mixture by filtering with a Buchner funnel containing qualitative filter paper (Whatman™, 1001), and a filtering flask under vacuum. The solid catalyst was air dried prior to

calcination in a Thermolyne 47900 furnace (Thermo Scientific, USA) at 550°C for 3 hours to produce the final HY product.

2.3.4 HZSM-5 Zeolite

HZSM-5 (Si/Al=19) zeolite was synthesized by Rong Lin and Jesse Cooper according to the procedure described in the Mobil Oil U.S. Patent (US 3702886) [105]. HZSM-5 was used as prepared by Lin and Cooper [106].

2.4 Testing for Reducing Sugars

The Benedict's reagent method for testing for the presence of reducing sugars was discovered in 1908 by Stanley R. Benedict [107]. Reducing sugars are sugars containing an aldehyde functional group (i.e. glucose, ribose, and xylose) or sugars that contain a ketone functional group that can isomerize to an aldehyde form (i.e. fructose) (figure 2.1). Therefore, fructose only reacts with Benedict's reagent when it is in an aldehyde configuration.
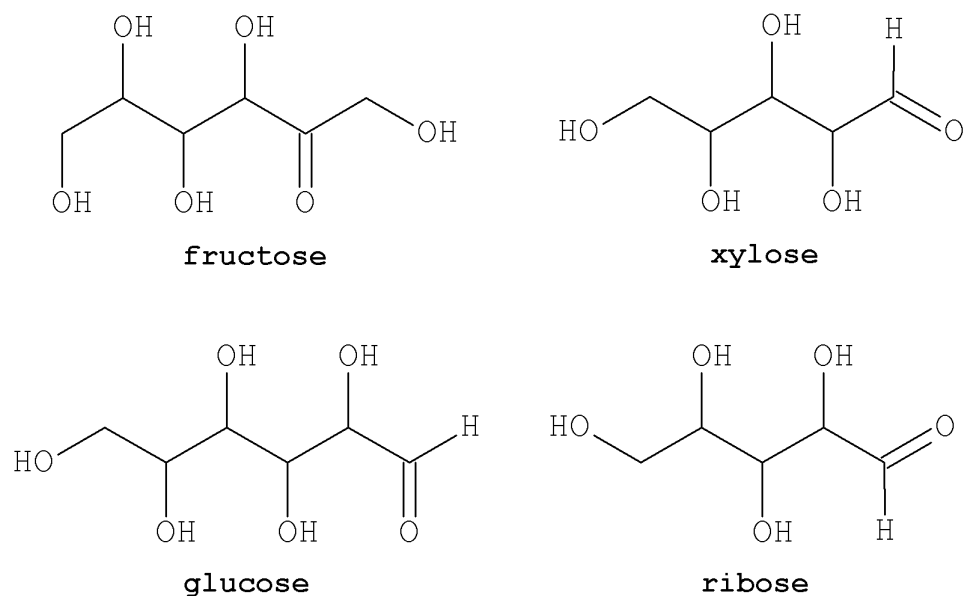
Figure 2.1 structures of reducing sugars

2.4.1 Benedict's Reagent

Benedict's reagent was made according to the procedure outlined in the literature [107]. Sodium citrate (86.5 g) and sodium carbonate (50 g) were dissolved in distilled water (300 mL) with heating. Separately, copper sulfate (8.7 g) was dissolved in distilled water (100 mL). After dissolution, the copper sulfate solution was slowly added to the sodium citrate and sodium carbonate mixture in a 500 mL volumetric flask, and filled to the mark with distilled water.

The Benedict's reagent method works on the basis that copper (Cu^{2+}) will selectively react with the aldehyde ends of reducing sugars, oxidizing them to carboxylic acids, whereas the Cu^{2+} is reduced to copper (I) oxide (Cu_2O), which can be detected as a red precipitate and simultaneous loss of the blue color of the solution (figure 2.2). Analysis of the solution color intensity by ultraviolet — visible spectroscopy (UV-VIS) allows for quantitative determination of reducing sugar yields.
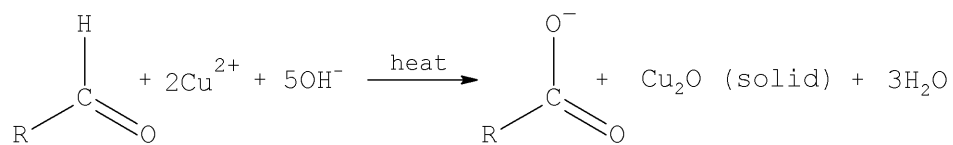
Figure 2.2 Benedict's reagent reaction with reducing sugars

UV-VIS spectroscopy can probe molecules containing π-electrons or non-bonding electrons, which can be excited from a ground state. Absorbance in the visible range is directly related to the color intensity of the solution, and this property was used for analyzing polysaccharide hydrolysis samples that had been reacted with the Benedict's solution. When samples contained

45

more reducing sugars, the blue color became lighter, and the UV-VIS measured absorbance was lower. In UV-VIS, the ratio of the light intensity (I/I_0) after passing through the reference (I_0) and the sample (I) is expressed as the percent transmittance (%T). Absorbance (A) can be calculated based on the transmittance (T) by using equation 2.2.

$$A = -\log\left(\frac{\%T}{100\%}\right) = -\log(T) \qquad \textbf{Equation 2.2}$$

2.4.2 Calibration Standards Preparation

A stock glucose solution (5 mM) was prepared by dissolving glucose (0.1 g) in distilled water (100 mL). From the stock solution, a series of calibration standards were prepared according to the dilutions listed in table 2.2. Each standard was heated in an oil bath at 100°C for 15min, and then cooled to room temperature in a water bath. After cooling, the standards were centrifuged and the liquid portion was analyzed by UV-VIS. Using a linear best-fit line derived from measurements of the calibration standards (figure 2.3), total reducing sugar concentrations in polysaccharide hydrolysis samples could be determined.

Table 2.2 Benedict's test calibration standards

Concentration (mM)	5mM Glucose (mL)	Water (mL)	Benedicts (mL)
2.0	2.0	2.0	1.0
1.5	1.5	2.5	1.0
1.0	1.0	3.0	1.0
0.5	0.5	3.5	1.0
0.0	0.0	4.0	1.0
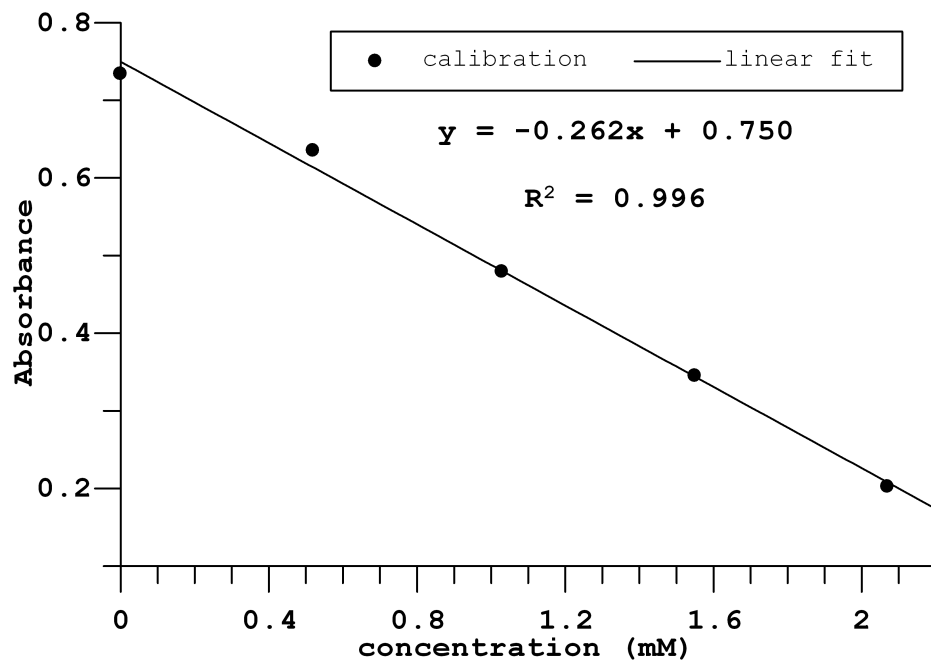
Figure 2.3 sample calibration curve for the Benedict's test

2.4.3 Polysaccharide Hydrolysis Sample Preparation

An aliquot (0.05 mL) of the hydrolysis sample was mixed with water (4 mL) and Benedict's reagent (1 mL),

for a total volume of 5.05 mL. The solution was then heated in an oil bath at 100°C for 15 min, and then cooled in a room temperature water bath. Samples were then centrifuged and the liquid portion was analyzed by UV-VIS.

2.4.4 Validation of the Benedict's Reagent Method by HPLC Analysis

The Benedict's test for reducing sugars was used to analyze samples after starch hydrolysis in an aqueous media (section 3.3) because high performance liquid chromatography (HPLC) was not initially available. When an HPLC instrument became available, polysaccharide hydrolysis products were analyzed by HPLC to determine glucose. A Shimadzu solvent delivery module (LC-10ADVP, Columbia, MD) was attached to a Waters 410 differential refractive index detector, and this combination was used to validate the results obtained by the Benedict's test. Samples were passed through a Cosmosil™ Sugar-D packed HPLC column (05394-81, 4.6 x 10 mm) at a flow rate of 1 mL min^{-1}.

Qualitative studies of polysaccharide hydrolysis products analyzed by HPLC confirmed the presence of

glucose. In a quantitative comparison of the same polysaccharide hydrolysis products analyzed by both HPLC and Benedict's reagent, there was less than 5% difference between the total glucose yield (TGY) calculated by HPLC and by the Benedict's reagent method. The Benedict's test was easier to implement than HPLC and therefore it was used for the remaining polysaccharide hydrolysis experiments.

2.5 Instruments

An Ainsworth 24N (Denver, Colorado) analytical balance was used to weigh solid chemicals. Weights to the nearest 0.01 mg could be obtained with this balance. An American Scientific Z210 (Columbus, Ohio) balance was used to weigh the ionic liquid. Weights to the nearest 1 mg could be obtained with this balance.

2.5.1 Hydrolysis Reactor

Initially, a commercially available, 4842 Parr high-pressure stirred reactor (Moline, IL, USA) was used for aqueous media hydrolysis reactions. The reactor system consisted of a steel reactor cylinder, which housed a Teflon sample holder, a magnetic drive

attached to a stirrer, gas inlet valve used to pressurize the system, a pressure gauge, and a heater. Pressures up to 20.68 MPa and a maximum temperature of 350°C could be attained with the 4842 Parr reactor. However, due to the size of the reactor vessel, large sample volumes (50 mL) were required for experiments. In addition, long heating times (45-60 min) were required to reach reaction temperatures because of the size of the reactor vessel. Due to the limited availability of some SACs and the long heating times, the Parr 4842 reactor was not suitable for the systematic evaluations of various SACs that was planned.

To replace the Parr 4842, a much smaller high-pressure stirred reactor (or mini-reactor) was fabricated for carrying out hydrolysis reactions in smaller volumes. The mini-reactor not only greatly reduced the sample size, but also reduced the heating times to a few minutes. Temperature profiles (figure 2.4) show that a constant temperature could be attained in the mini-reactor, even without stirring (NS), after about 10 minutes, whereas the Parr reactor required 45-60 minutes to reach a constant temperature. The mini-

reactor was used for all substrate hydrolysis reactions
carried out in aqueous media.
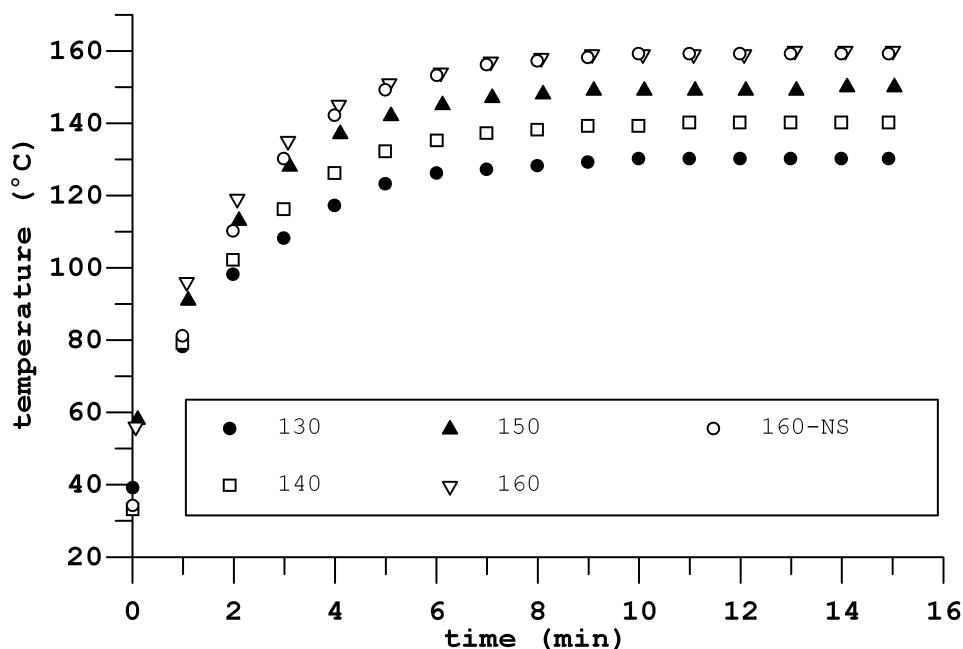
**Figure 2.4 mini-reactor initial heating times to reach
set temperature; "NS" denotes that no stirring was used**

The mini-reactor was used in conjunction with an
Agilent 6890 gas chromatograph (GC) oven heating
source, a cam and piston apparatus for shaking (figure
2.5), and a novel reactor vessel (figure 2.6). The
aluminum reactor vessel held a small quartz sample tube
(max volume 0.5 mL), which was spring loaded so that
the top of the tube was flush with the top of the
aluminum reactor vessel, to minimize movement of the

tube when the apparatus was shaken. A small stainless steel pin was placed in the quartz sample tube and served as a mixing device. The o-ring attached to the Swagelok male fitting face pushed against the flat surface of the reactor vessel, and when screwed into the Swagelok female nut, an airtight seal was created. The mini-reactor vessel was pressurized to at least 300 psi with nitrogen gas, which was added to ensure that the water remained in liquid form when heated above 150°C.
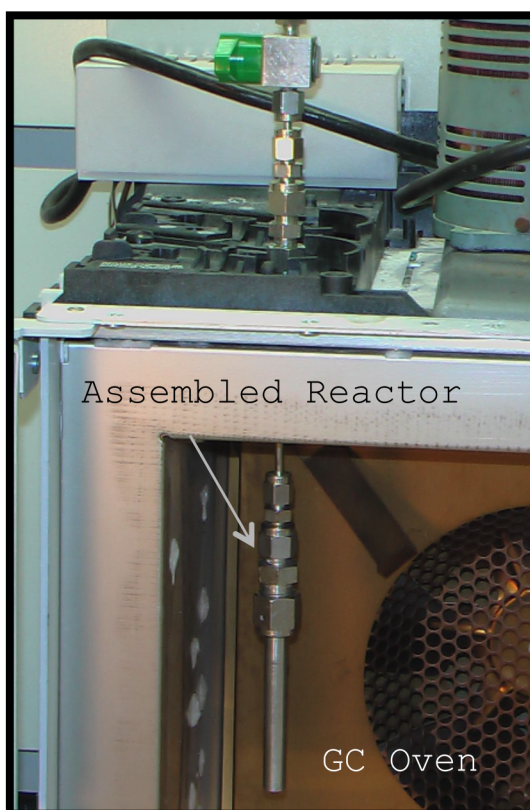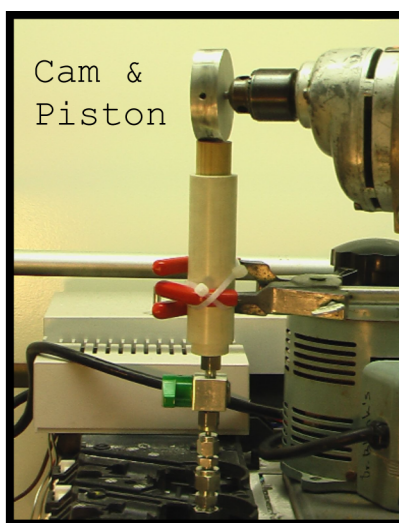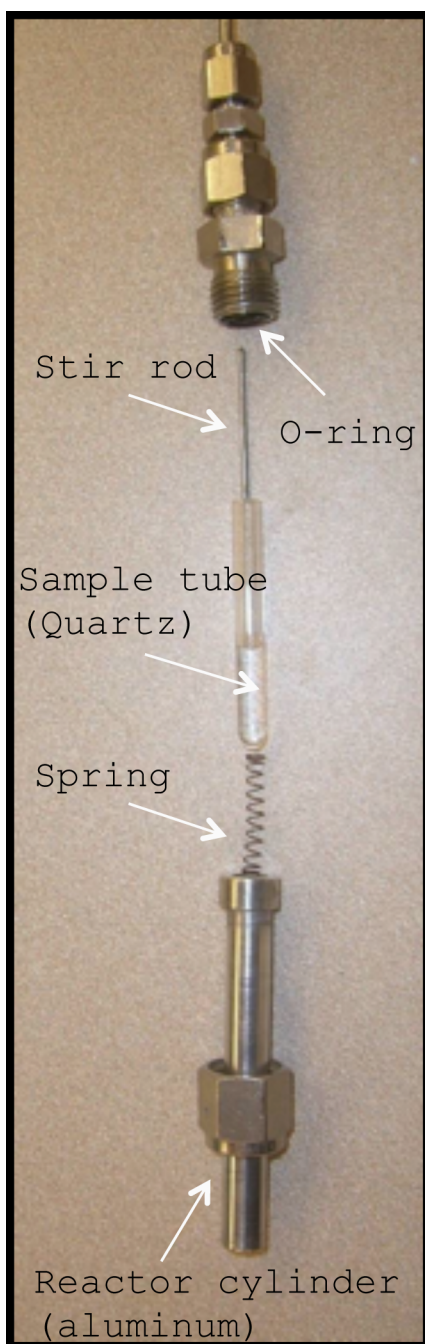
Figure 2.5 miniature high-pressure stirred reactor

Swagelok face
seal male fitting

o-ring

metal stirring rod

quartz sample tube

spring

aluminum reactor
vessel

Swagelok face
seal female nut
fitting
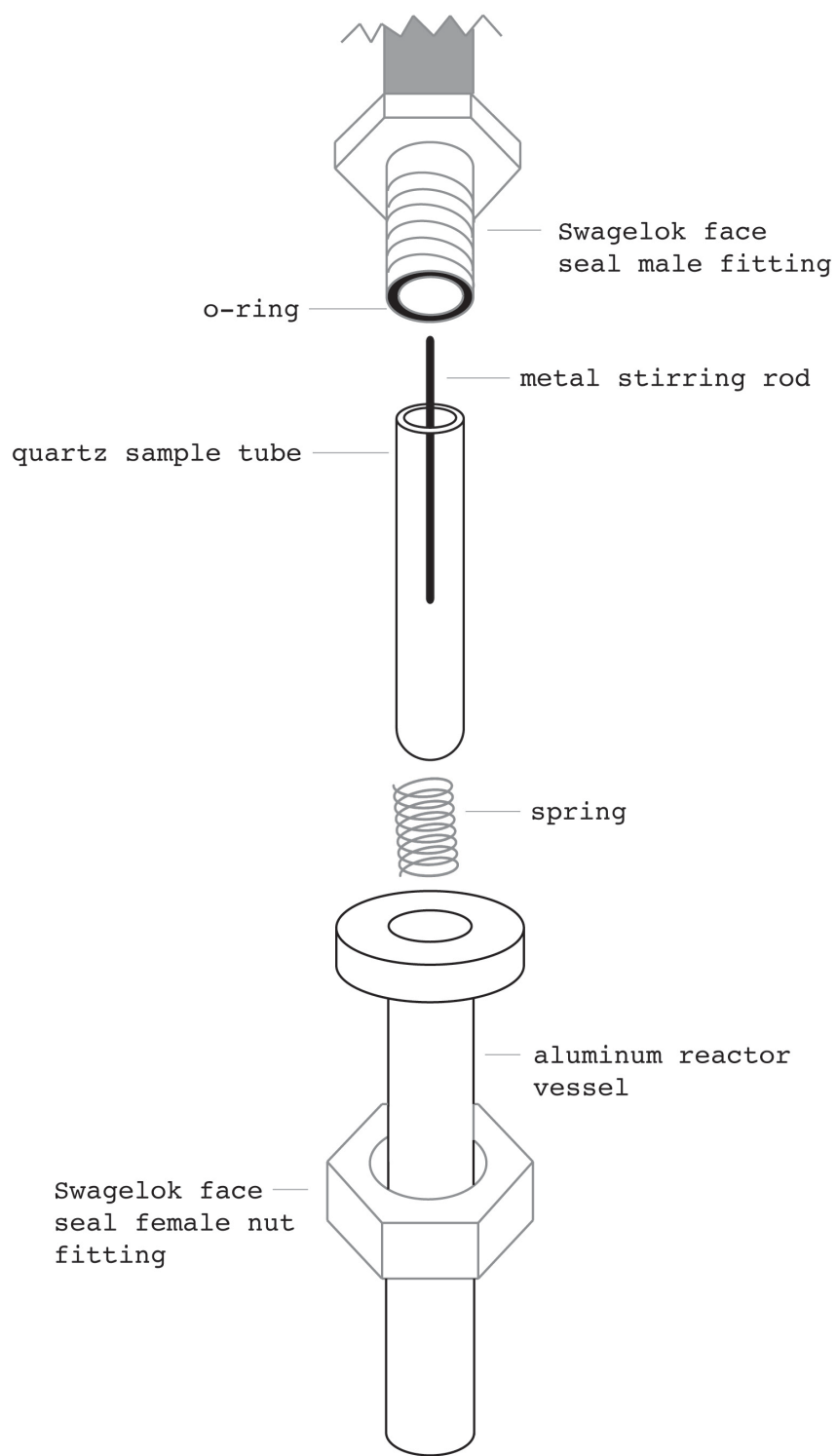
Figure 2.6 schematic of mini-reactor sample vessel

2.5.2 Oil Bath

A temperature controlled oil bath was used for heating polysaccharide hydrolysis samples containing ionic liquid media and for all Benedict's total reducing sugar assays. The apparatus consisted of the following equipment: Thermolyne Type 1000 stirring plate (Thermo Scientific, USA), Power Stat 3PN116C Variac (The Superior Electric Company, Bristol, CT), Omega CN3240 temperature controller (Omega Engineering Inc, Stamford, CT), heating element, stirring bar, and silicone oil. A metal guide held sample tubes in place within the oil bath. One large magnetic stirring bar was placed in the oil bath and small stirring bars were placed in each sample tube. The variac was set to 98 V and stirring was set to high to provide even heat distribution.

2.5.3 Ultraviolet-Visible Spectroscopy

Polysaccharide hydrolysis samples and standards were analyzed for reducing sugars content by first reacting them with Benedict's reagent (described in section 2.4) and then measuring the absorbance of the liquid by using a Shimadzu (Columbia, MD, USA) UV-

2101PC ultraviolet-visible spectrophotometer (UV-VIS). The background, calibration standards, and hydrolysis samples were all scanned from 800-400 nm to generate spectra. The absorbance was measured at 741 nm in each spectrum, which corresponds to the λ_{max} of the copper sulfate used in the Benedict's reagent, and these absorbance values were used for all calculations.

2.5.4 Gas Chromatography with Flame Ionization Detection

Ethyl acetate hydrolysis products (chapter 3) were analyzed by gas chromatography (GC) with flame ionization detection (FID). Samples were injected into an HP5890 GC-FID. The column used for separation was a 30 meter long Carbowax fused silica column with a film thickness of 0.25 μm, and an internal diameter of 0.32 mm (Agilent 113-2132). The injector temperature was set to 250°C, detector temperature was set to 275°C, and the oven temperature program used was: initial temperature 30°C, hold for 2 minutes, then ramp at 50°C min^{-1} to a final temperature of 200°C and hold for 2 minutes. A ramp rate of 50°C min^{-1} was used to decrease the sample run time. Although the oven had difficulty

maintaining this ramp rate, it was reproducible. The

helium carrier gas was maintained at 1 ml min^{-1} with a

column head pressure of 11.2 psi. All analyses were

performed in splitless mode. These settings provided

baseline separation of all peaks (figure 2.7).
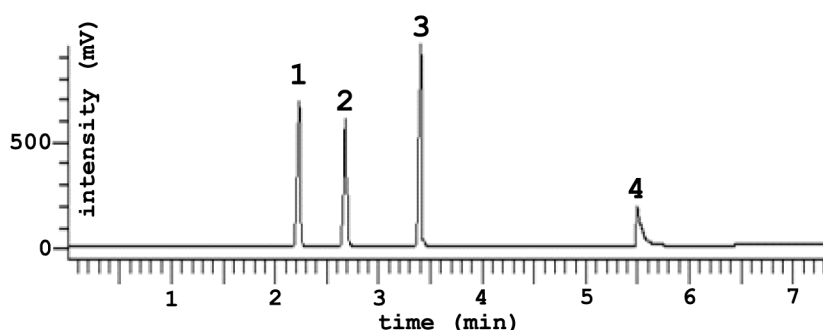
Figure 2.7 sample GC-FID spectra of ethyl acetate (1), ethanol (2), propanol (3), and acetic acid (4)

2.5.5 Gas Chromatography with Mass Spectrometry

Gas chromatography (GC) with mass spectrometry

(MS) detection was used to determine the amount of

ethanol produced by fermenting cellulose hydrolysis

products (chapter 5). A Carbowax (30 m x 0.25 μm x 0.32

mm) fused silica column was used for these studies.

The GC injector temperature was set at 200°C, the

detector temperature was set at 250°C, and the oven was

programed to start at 80°C and ramp to 200°C at 30°C

min^{-1}. The helium carrier gas flow rate was 1 mL min^{-1} and samples were injected by using splitless mode. Mass spectral information was obtained by monitoring m/z 45 and m/z 59 signals. Calibration standards were prepared with 0.1, 0.3, 0.5, 0.7, and 1.0% ethanol. All standards and samples were also spiked with 0.5% propanol, which was used as an internal standard. By measuring reference samples containing 0.5% propanol (m/z 59) and 0.5% ethanol (m/z 45), it was determined that there was no interference at the respective m/z values.

2.5.6 Diffuse Reflectance Infrared Fourier Transform Spectroscopy

Zeolites HY and HZSM-5 were analyzed by Diffuse reflectance infrared Fourier transform spectroscopy (DRIFTS), which was used to detect slight structural changes after exposure to ionic liquid. The DRIFTS FTIR instrument was a Mattson Nova Cygni 120 (Madison, WI) and DRIFTS measurements were made using a Harrick Scientific Inc. (Ossining, NY) praying mantis diffuse reflection accessory with environmental chamber. The number of signal averaged scans was set to 16 at 8 cm^{-1}

resolution and a frequency range from 1000–4000 cm^{-1}.
Prior to DRIFTS analysis, solid acid catalysts were
ground to a fine powder and then mixed in a 1:1 ratio
with silver powder diluent. Because [EMIM]Cl is a
solid at room temperature, it was also mixed in a 1:1
ratio with silver powder. The sample temperature was
held at 200°C for 45 min to remove adsorbed water from
catalyst surfaces, and then spectra were measured while
maintaining the sample temperature at 200°C.

Chapter 3 : RELATIVE ACTIVITY AND WATER TOLERANCE OF SOLID ACID CATALYSTS

3.1 Background

When using a solid acid catalyst (SAC) for polysaccharide hydrolysis, polysaccharide molecules must have access to catalyst protons and water must be readily available to react with and break protonated glycosidic linkages. Thus, solid acid catalysts must be mixed with water and polysaccharides should ideally be dissolved. For solid acid catalysts to be good candidates for polysaccharide hydrolysis, they should remain active when exposed to water and should be reusable with minimal loss of catalytic activity. The SACs used in this work are more commonly used in either a gaseous medium [61, 62, 78] or a non-polar liquid [99], so little is known about their properties in aqueous solutions. Characterization methods for surface properties of SACs used for gas phase reactions have been well established [108]. However, few reports of SACs being used to catalyze reactions in water have been published. Exposure of a solid acid catalyst to water can potentially alter the surface properties of

the catalyst. For example, it has been proposed that adsorption of hydroxyl ions (OH^-) from water molecules onto Lewis acid sites (M^{n+}) of an SAC create BrØnsted acid sites [99, 109]. Thus, detailed studies of the water tolerances of sulfated zirconia, Nafion®, HY zeolite, and HZSM-5 zeolite under conditions needed for polysaccharide hydrolysis were conducted to determine their water stabilities at elevated temperatures.

Previously published studies have evaluated the water tolerance of selected solid acid catalysts [87, 110-115]. Table 3.1 lists some solid acid catalysts that have been previously used to catalyze the aqueous phase hydrolysis of ethyl acetate. Test reactions for the SACs reported in table 3.1 were conducted in a batch reactor at 70°C for 2 hours. Values listed as %EA conversion are assumed to be the amount of ethyl acetate converted to ethanol and acetic acid. However, details of the calculations used for each study (%EA converted) were not given in the literature and therefore, it may not be fair to compare the catalysts on an absolute scale. As shown in table 3.1, water tolerant solid acid catalysts have been found to exhibit a wide range of activity for ethyl acetate (EA)

hydrolysis. This variation in %EA converted is most likely due to differences in acid site locations, acid strengths, and the acid site densities of the SACs.

Table 3.1 summary of published results for ethyl acetate hydrolysis by solid acid catalysis

Catalyst	%EA converted	Reaction Temp (°C)	Ref.
SiO_2-APS-$Cs_{2.5}H_{0.5}PW_{12}O_{40}$	42	70	[111]
Aciplex-SiO_2	27	70	[87]
Nafion-SiO_2	12	70	[87]
HZSM-5	15	70	[87]
MoO_3/ZrO_2	13	70	[114]
$ZrPO_4$	10	70	[112]
$ZrPO_4$	8	70	[110]

Under the same reaction conditions used to obtain the results reported in table 3.1 (70°C, 2 hr), sulfated zirconia was also found to be active for ethyl acetate hydrolysis. The activity (20% conversion) falls within the range of %EA converted values given in table 3.1 (8-42%), suggesting that it had some water tolerance. Rather than testing all the SACs under the reaction conditions cited in the literature (70°C, 2 hr),

conditions that were more relevant to polysaccharide hydrolysis were chosen. Although polysaccharide hydrolysis reactions require temperatures greater than 70°C, reaction temperatures should be kept below 150°C to minimize glucose decomposition. Under acidic conditions at this temperature, the primary glucose decomposition pathway yields 5-hydroxymethyl furfural (5-HMF), in addition to fructose, formic acid, levulinic acid, and char [42]. 5-HMF is proposed to be an intermediate in the char formation pathway, because increasing 5-HMF yield was found to be linked to increased char formation at subcritical water temperatures (350°C) [116]. Thus, maintaining lower reaction temperatures (≤150°C) should minimize glucose decomposition, thereby minimizing char formation, which can cause catalyst deactivation.

Furthermore, water at elevated temperatures can also cause poisoning of acid sites, depending upon SAC hydrophobicity [87]. In this case, "poisoning" is defined as acid sites covered by water, preventing adsorption of organic molecules. SACs that tend to be hydrophilic are more susceptible to this type of poisoning.

3.2 Ethyl Acetate Hydrolysis

A water tolerance study was used to evaluate the performance of solid acid catalysts in water at various temperatures (70-150°C) and to evaluate their activities after repeated use at 150°C. Ethyl acetate rather than a polysaccharide was used as the hydrolysis substrate for these studies. Ethyl acetate hydrolysis reactions have previously been used to evaluate the innate ability of a catalyst to donate a proton in aqueous media [87, 110-114]. Hydrolysis of ethyl acetate is a simple reaction yielding ethanol and acetic acid (figure 3.1). The general mechanism of ethyl acetate hydrolysis by acid catalysis (H_3O^+) can be explained by four steps: 1) a proton attaches to an electron lone pair on the double bonded oxygen, causing a delocalized positive charge; 2) water attaches to the carbon through an electron lone pair on the oxygen; 3) a proton is transferred to the oxygen with the ethyl group attached; and 4) ethanol is released and a proton is removed to yield acetic acid.
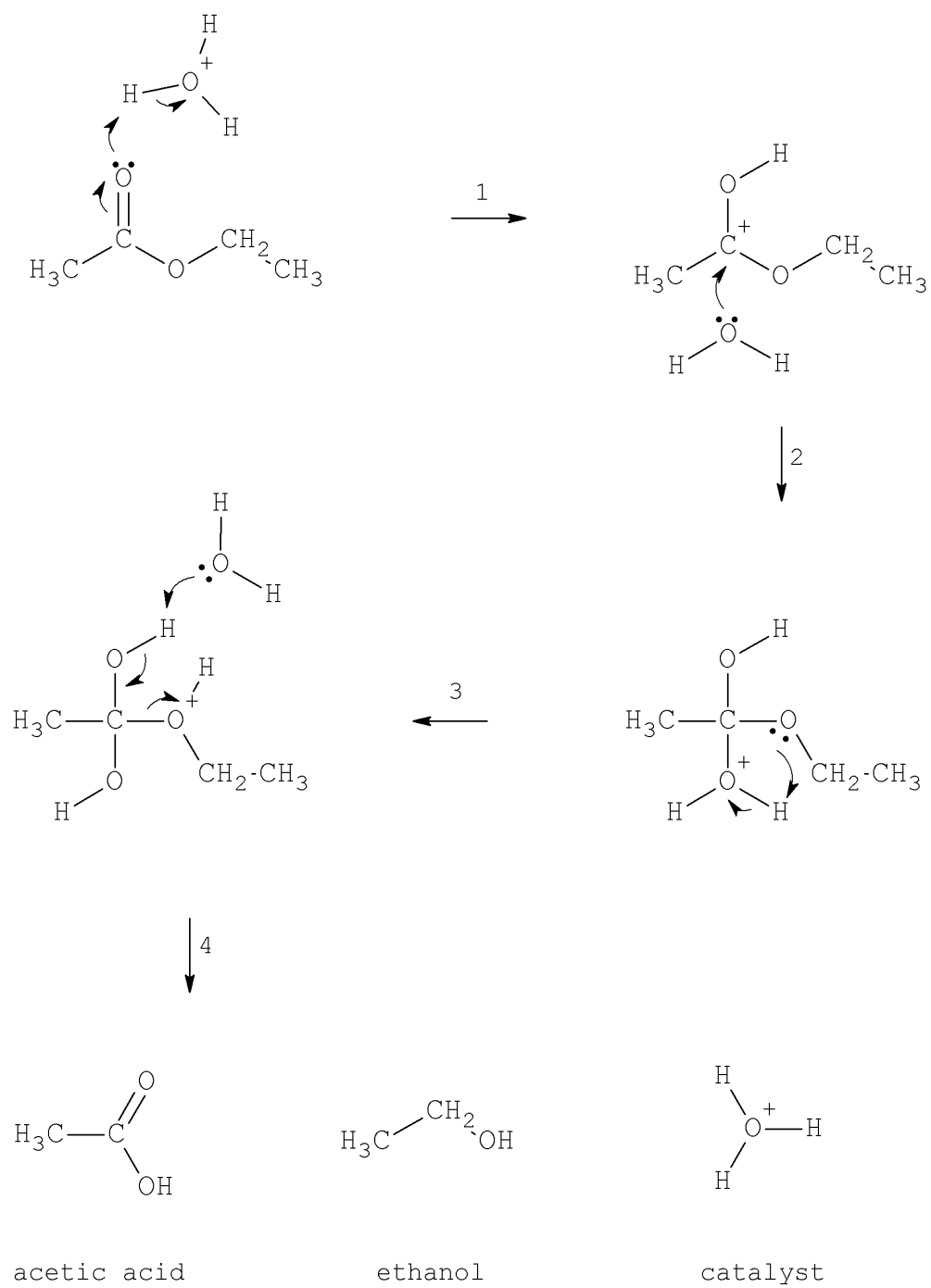
Figure 3.1 acid catalyzed ethyl acetate hydrolysis mechanism

3.2.1 Ethyl Acetate Hydrolysis Sample Preparation

Propanol was not expected to react with the SACs under the water tolerance reaction conditions, and was therefore used as an internal standard to permit quantitative analyses of reaction product mixtures. 5% propanol in water was mixed with each catalyst (0.01 g SAC or 10 µL HCl solution) and then heated at 150°C for 2 hours to confirm that propanol did not react. The liquid was then analyzed by gas chromatography with flame ionization detection (GC-FID). The propanol chromatogram peak areas obtained by analysis of the 5% propanol solution before and after exposure to the catalyst were less than 1% different and no additional peaks appeared, which confirmed that propanol did not react with the SACs.

To evaluate the effects of using a stirring rod to mix reactants, SACs were used for ethyl acetate hydrolysis with and without a stirring rod and hydrolysis results were compared. Visual inspection of the samples revealed a significant loss of solution when the stirring rod was used. This was mostly due to the low viscosity of the solution. The stirring rod would cause the solution to splash out of the sample

tube. Furthermore, visual inspection of the sample tube indicated that adequate mixing could be achieved by shaking when no stirring rod was used. Based on these results, it was determined that shaking the sample tubes without a stirring rod provided adequate mixing with minimal sample loss.

The hydrolysis test solution was a mixture of 5% (vol) ethyl acetate (EA) and 5% (vol) propanol (P) in distilled water, which will be referred to as 5% EA/P. The catalyst (0.01 g SAC, 10 µL HCl solution, or 24 µL H_2SO_4 solution) and 5% EA/P solution (0.4 mL) were placed into the quartz sample tube of the mini-reactor. A reference sample (i.e. blank) was prepared in the same manner, except that no catalyst was added. Although the minimum pressure required to maintain water in the liquid phase at 150°C is only 0.5 MPa, samples were pressurized to at least 2 MPa with nitrogen gas to ensure no loss of sample due to volatilization. The mini-reactor was heated isothermally for 30 minutes to temperatures ranging from 70°C to 150°C, with shaking but without the stirring rod. To quench the reaction, samples were immersed in a cold-water bath immediately after

removing them from the oven. The quartz sample tubes were then centrifuged to separate the SACs from the liquid prior to analysis of the liquid by gas chromatography with flame ionization detection (GC-FID).   The instrument conditions used for GC-FID analysis are described in section 2.5.4.   The GC-FID instrument relative standard deviation was typically about 5% and was determined by calculating chromatogram peak areas obtained by repeated injections of the same sample.

3.2.2 Ethyl Acetate Conversion

To determine the amount of ethyl acetate converted, an aliquot (1 µL) of the ethyl acetate mixture (5% EA/P) in water was analyzed by GC-FID before and after hydrolysis.

$$\%\text{EA converted} = \frac{\frac{A_{ea}^{0}}{A_{p}^{0}} - \frac{A_{ea}}{A_{p}}}{\frac{A_{ea}^{0}}{A_{p}^{0}}} \text{ x } 100\% \qquad \textbf{Equation 3.1}$$

In equation 3.1, A_{ea}^{0} represents the ethyl acetate peak area before hydrolysis, A_{p}^{0} is the propanol peak area before hydrolysis, A_{ea} is the ethyl acetate peak area

after hydrolysis, and A_p is the propanol peak area after hydrolysis.

3.2.3 Temperature Profiles for Various Catalysts

Results were obtained for ethyl acetate hydrolysis (catalyst weight kept constant at 0.01 g SAC) as a function of temperature for the following SACs: sulfated zirconia, HY, HZSM-5, and Nafion® SAC-13. Table 3.2 lists the average ethyl acetate conversions (values determined by equation 3.1) and standard deviations (average ± standard deviation) for the SACs tested. The standard deviation for each SAC assay was determined based on triplicate runs and ranged from 0.4-5% ethyl acetate converted.

Table 3.2 results for ethyl acetate hydrolysis by solid acid catalysis

Temp(°C)	Sulfated Zirconia	Nafion® SAC-13	HY	HZSM-5	None
	% ethyl acetate converted				
70	12±2	12±5	10±2	13±1	9±1
80	18±2	15±3	12±3	18±2	10±1
90	22±0.4	21±3	16±1	23±1	9±3
100	31±2	26±2	13±2	30±1	10±2
110	47±1	32±1	17±2	35±3	15±2
120	59±0.4	44±2	21±2	43±2	17±1
130	75±1	52±1	23±2	45±1	30±4
140	86±3	62±2	35±2	58±2	35±2
150	94±1	79±1	42±5	64±2	36±2

The SAC activity trends when the catalyst weight was kept constant at 0.01 g are shown in figure 3.2. The blank measurement (i.e. no catalyst) showed activity for ethyl acetate hydrolysis, with up to 36% ethyl acetate converted at 150°C (30 min). The acidity

of the blank measurement comes from the formation of the hydronium ion, where: $2H_2O \leftrightarrow H_3O^+ + OH^-$ and the equilibrium constant (K_W) for this equilibrium is represented as $K_W = [H_3O^+][OH^-]$. The K_W value changes with temperature and therefore, the H_3O^+ concentration changes with temperature. Calculated K_W values at various temperatures have been reported. For example: 25°C ($K_w=1x10^{-14}$), 150°C ($K_w=2.28x10^{-12}$), and 250°C ($K_w=6.37x10^{-12}$) [117–119]. Consequently, the concentration of H_3O^+ is $1x10^{-7}$, $1.5x10^{-6}$, and $2.5x10^{-6}$ at 25°C, 150°C, and 250°C respectively, indicating that water becomes more acidic as its temperature increases. If the acidity of water did not increase with temperature, ethyl acetate conversions for the blank would not have been expected to increase with temperature when all other conditions were held constant.

The highest conversion of ethyl acetate was obtained with sulfated zirconia at 150°C after 30 minutes, which yielded 94% conversion. On the other hand, HY activity was found to be comparable to no catalyst being added (i.e. blank measurement) for ethyl acetate hydrolysis at temperatures between 70°C and

71

150°C. Kamiya et al. and Okuhara et al. also found that HY (Si/Al=2.4) was inactive for ethyl acetate hydrolysis at 70°C and 60°C respectively after 2 hours [110, 120]. Our results indicate that HZSM-5 and Nafion® SAC-13 have similar activity for ethyl acetate hydrolysis under these reaction conditions. These results are consistent with those reported by Okuyama et al., who found that HZSM-5 and Nafion® SAC-13 had similar activities for ethyl acetate hydrolysis at 70°C after 2 hours [115].
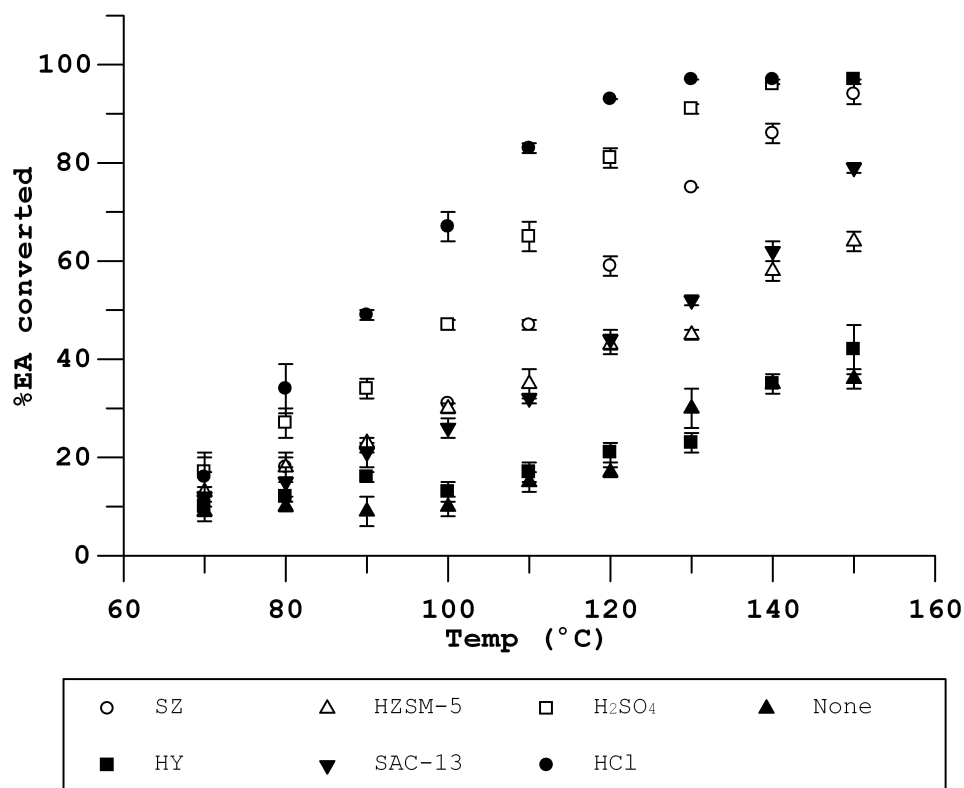
Figure 3.2 ethyl acetate hydrolysis in aqueous medium at various temperatures using solid acid catalysis

Sulfated zirconia gave the highest ethyl acetate conversions (110-150°C, 30 min) when compared to the other SACs tested. Below 100°C, sulfated zirconia activity was comparable to HZSM-5 and Nafion® SAC-13. Kamiya et al. reported that HZSM-5 (Si/Al=40) was slightly more active than sulfated zirconia when ethyl acetate hydrolysis was performed at 70°C for 2 hours, yielding 29% conversion compared to 22% for sulfated zirconia [110]. Although the EA conversion values

reported by Kamiya et al. cannot be compared to those reported here because experimental conditions were different, they reported that HZSM-5 was slightly more active than sulfated zirconia. Assuming that the results presented here, which indicated that HZSM-5 was less active than sulfated zirconia above 100°C, are statistically different from their results, a possible explanation for this difference may involve the HZSM-5 Si/Al ratio for the catalyst employed here compared to the one used by Kamiya et al. Namba et al. have suggested that the Si/Al ratio of zeolites affects the hydrophobicity of the solid, which plays a significant role in their catalytic activity for ethyl acetate hydrolysis. They carried out aqueous phase ethyl acetate hydrolysis at 60°C catalyzed by HZSM-5, HY, and H-mordenite zeolites, which had been subjected to de-alumination to produce samples with varying Si/Al ratio. For each catalyst, activity increased when the Si/Al ratio increased relative to the catalyst with the lowest Si/Al ratio until a maximum was reached. For samples containing Si/Al ratios higher than this optimum, catalytic activity decreased. This increase in activity with increasing Si/Al ratio was explained

by an increase in the hydrophobicity of the catalyst surface, which enhances the catalyst surface affinity for ethyl acetate. Although this effect increased the likelihood (i.e. rate) that ethyl acetate would be hydrolyzed, the increase in Si/Al ratio also resulted in a decrease in the number of acid sites, which would be expected to decrease catalytic activity. Thus, when the Si/Al ratio exceeded an optimal value, the loss in acid sites more than offset the reaction rate increase associated with higher hydrophobicity, and the observed catalytic activity decreased. Their research revealed a lower activity for HZSM-5 with Si/Al=29 compared to HZSM-5 with Si/Al=47, with measured rate constants reported to be 1.15×10^3 min^{-1} g^{-1} and 1.78×10^3 min^{-1} g^{-1} respectively [121]. Thus, it seems reasonable that the HZSM-5 with a Si/Al ratio of 19 used for studies described here may exhibit lower activity than sulfated zirconia, whereas the HZSM-5 used by Kamiya et al., which had a Si/Al ratio of 40 (closer to the optimum of 47 reported by Namba et al.) may have exhibited higher catalytic activity than sulfated zirconia [110].

Although the amount of catalyst used (0.01g) was kept constant, the amount of acid (mmol H^+ g^{-1}) varied

for each catalyst. For the purpose of comparing the activities of the solid and liquid acid catalysts, %EA converted was scaled by the mmol H^+ employed. The mmol H^+ employed was determined by titrations of fresh catalysts as described in section 2.3 yielding: H_2SO_4 (0.0072) HCl (0.0077), sulfated zirconia (0.0079), HY (0.0162), HZSM-5 (0.0110), and Nafion® SAC-13 (0.0061), where values in parentheses are mmol H^+ provided to the reaction mixture. When compared based on activity per mmol H^+, the catalysts separated into four main groups (figure 3.3). These four groups were designated based on catalyst structure: 1) liquid acids, 2) amorphous SACs, 3) crystalline SAC (HZSM-5 Si/Al=19), and 4) crystalline SAC (HY Si/Al=5.3).
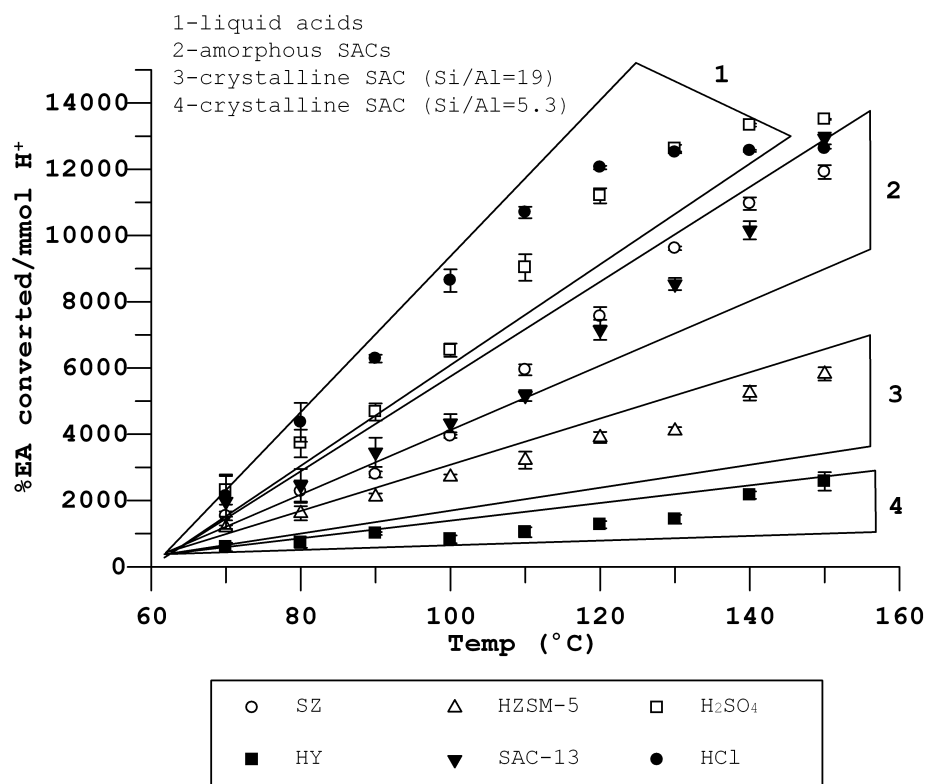
Figure 3.3 percent ethyl acetate converted scaled by the mmol H^+ added based on titrations of fresh SAC

The same trends are observed for increasing ethanol formation when the GC-FID peak area ratio of ethanol/propanol is scaled by the mmol H^+ added (figure 3.4).
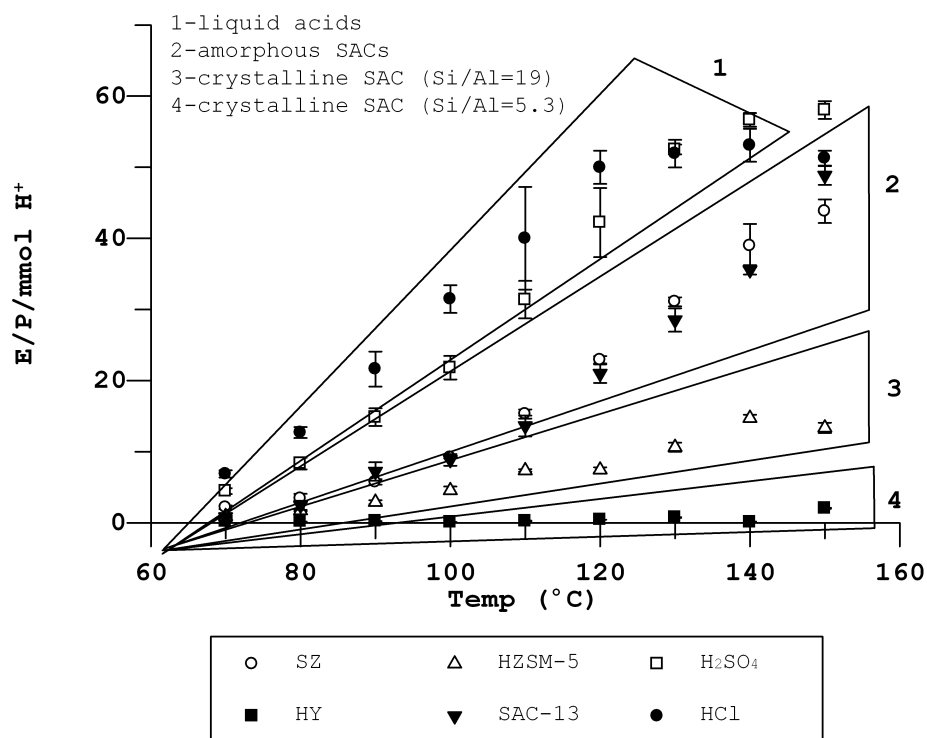
Figure 3.4 ratio of the GC–FID spectra peak area of ethanol and propanol (E/P) scaled by the mmol H^+ added based on titrations of the fresh SAC

There may be several reasons why the liquid acids performed better than the solid acid catalysts. Although hydrolysis samples were thoroughly mixed, the SAC containing samples were still heterogeneous. The participating acid sites in heterogeneous catalysts are restricted to those accessible to the hydrolysis substrate. On the other hand, all of the acidic protons in homogeneous catalysts can participate in hydrolysis. Thus, substrate access to acidity for

solid catalysts would be more limited than for homogeneous acid catalysts (e.g. HCl).

Furthermore, the mmol H^+ used for scaling the SACs can be over estimated. The mmol H^+ of the SACs was determined by an aqueous acid–base titration method (described in section 2.3). It has been suggested that Lewis acid sites (LAS) on SACs exposed to water will generate new BrØnsted acid sites (BAS) that were absent in the initial catalyst [109, 122], which would also occur during the hydrolysis reaction in aqueous media. Any acid site (originally BAS or LAS converted to BAS) that sodium hydroxide (titrant) can access will be counted by the acid–base titration method. This becomes a problem if these acid sites are accessible to the titrant, but not to the hydrolysis substrate, because this would lead to an over estimation of the mmol H^+ participating in hydrolysis reactions.

The amorphous solid acid catalysts: sulfated zirconia and Nafion® SAC–13, had similar activities for ethyl acetate conversion per catalyst acid equivalent. The acid sites of sulfated zirconia and Nafion® SAC–13 are mostly located on exposed surfaces that should be readily accessible to ethyl acetate molecules.

Although the proton is bound to the SAC framework by electrostatic forces, the degree to which it is bound will determine how far the proton can migrate from the surface while still balancing the negative surface charge. For example, in a strong acid site, the electrostatic force is weak and the proton can move farther away from the SAC surface than a proton at a weaker acid site. Assuming that no ion exchange occurs to release the proton into the medium while maintaining a balance for the negative surface charge, ethyl acetate molecules must come into contact with protons located near the surface of the SAC for hydrolysis to occur. The expected greater H^+ availability for the amorphous SACs may be the reason that they exhibited greater activity for ethyl acetate hydrolysis than the zeolites.

The zeolite solid acid catalysts (HY and HZSM-5) exhibited relatively lower activities for ethyl acetate conversion. It has been suggested that zeolite exposure to water can cause loss of BrØnsted acidity. Parker et al. suggested that water breaks the framework bonds to form AlOH and SiOH based on the new hydroxyl peaks that they detected in infrared (IR) spectra (3710

cm^{-1}, 3615 cm^{-1}) after HY and HZSM-5 were exposed to water vapor [123, 124]. Lohse et al. claimed that IR peaks near 3700 cm^{-1} and 3600 cm^{-1} were indications of non-framework AlOH in dealuminated Y type zeolite [125]. Parker et al. also suggested that when less than one water molecule was adsorbed per framework Al on HY, only partial removal of the Al occurred, which could be fully restored by heating at 100°C under dry nitrogen gas. On the other hand, when more than one water molecule is adsorbed per framework Al, more Al bonds are broken and higher temperatures (300°C) are required for removal of the water. In that case, the application of the higher temperatures cause loss of Al from the framework and therefore loss of BrØnsted sites [123]. It should be pointed out that these literature references were focused on the effects of water for reactions in the gas phase. In contrast, the research described here involves using zeolites in an aqueous phase; so heating the catalyst to remove water (which caused loss of framework Al) never occurred. Therefore, under the conditions used for the experiments described here, water may interact with both the framework (to form AlOH and SiOH) and with the

protons at BrØnsted acid sites (to form H_3O^+) [124], but loss of BrØnsted acidity should not occur.

The lower conversions obtained by using HY and HZSM-5 is more likely attributed to differences in acid site accessibility. The acid sites of zeolites are typically located within a size-restricting pore, and the ethyl acetate must diffuse into the zeolite pores to interact with the protons. Although the molecular size of ethyl acetate (4.95 Å) [126] is small enough to fit into the zeolite pores (5-7 Å), access to the acid sites would be expected to be more restricted for zeolites than for amorphous catalysts.

Manjare and Ghoshal studied the effect of pore size on the adsorption of ethyl acetate. The molecular sieves used for their study had similar properties except for the pore size. Molecular sieve 5A is made up of 8-member rings with 5 Å pore diameters, and molecular sieve 13X is made up of 12-member rings with 10 Å pore diameters. It was found that approximately 20-30% more ethyl acetate was adsorbed on molecular sieve 13x than on molecular sieve 5A [126]. This suggests that ethyl acetate should have more access to acid sites in zeolites with larger pores than in

82

zeolites with smaller pores. However, results described here show higher ethyl acetate conversions with HZSM-5 (10 member ring; pore sizes 5.3 x 5.5 Å and 5.1 x 5.5 Å), which has smaller pores than HY (12 member ring; pore diameter 7.4 Å). In fact, HY conversions were comparable to no acid being added (i.e. blank measurement).

Although unexpected based on pore size considerations, the finding that ethyl acetate conversion was greater for HZSM-5 than for HY is consistent with previous literature reports. Namba et al. and Kamiya et al. also found that HZSM-5 performed better than HY for ethyl acetate hydrolysis in water [110, 121]. Kerr reported that HY can lose 25% of its original BrØnsted acidity just by being exposed to water for 10-15 minutes [127]. However, they provided no experimental data to back up this claim, so its validity is questionable. Although loss in acidity would decrease the activity of the catalyst, it does not explain why HY was effectively inactive for ethyl acetate hydrolysis.

Zeolite catalyst hydrophobicity may be a better predictor of EA hydrolysis activity. Zeolite

frameworks are made up of oxygen sharing tetrahedral SiO_4 and AlO_4 groups. Young et al. studied the effects of water vapor on silica surfaces by infrared spectroscopy, and found that although water molecules adsorb to zeolite Si-OH surface groups (figure 3.5a), they do not adsorb to Si-O-Si groups. These framework groups (Si-O-Si) are thus suggested to be homopolar; they have no electrostatic force field and are considered hydrophobic [92]. However, substituting Al^{3+} for Si^{4+} results in a negative charge on the oxygen (AlO_4^-), and a cation (e.g. proton) can compensate for this charge (figure 3.5b). When a proton is the charge balancing cation, the site has acidic properties. The proton, which has a high affinity for water, decreases the overall hydrophobicity of the zeolite. A lower Si/Al ratio (fewer Si-O-Si groups) results in larger amounts of water being adsorbed on zeolite surfaces, making it less hydrophobic. In fact, Olson et al. found that the amount of gas phase water adsorbed on the surface was directly proportional to the aluminum content[128].

a. hydrogen-bonded model   b. protonated model
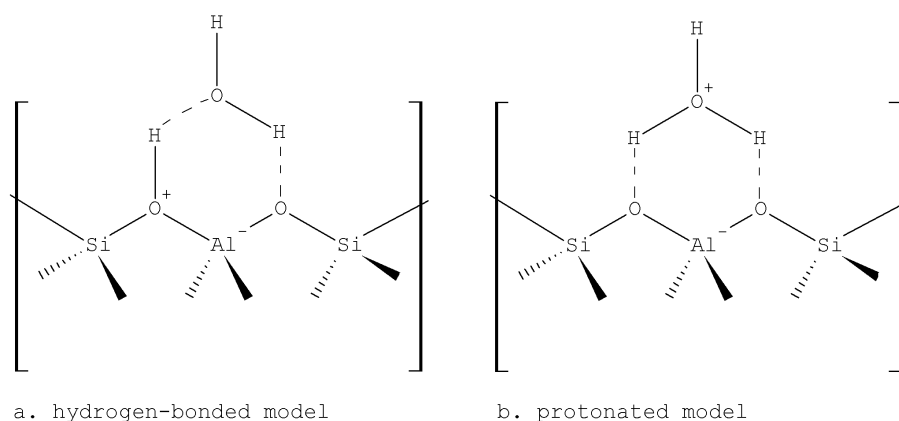
Figure 3.5 zeolite acid sites derived from ref. [87]

Several studies have evaluated the hydrophobicity of zeolites [87, 92, 128-131] and a correlation between Si/Al ratio and hydrophobicity has been found [91, 121, 132]. Hattori et al. suggested that a Si/Al ratio greater than 10 can be considered hydrophobic, because of an increase in adsorption of organics [133]. Namba et al. reported an increase in activity for ethyl acetate hydrolysis in aqueous media with increasing Si/Al ratio until a maximum was reached [121]. The optimum Si/Al ratio was determined based on the maximum ethyl acetate hydrolysis reaction rates at 60°C catalyzed by HY (Si/Al ratio range = 2.4-3.8) and HZSM-5 (Si/Al ratio range = 29-92). The observed maxima are most likely due to a tradeoff between catalyst acidity and hydrophobicity. Increasing the Si/Al ratio past

the optimum results in lower activity due to decreased acidity [121]. The optimum Si/Al ratio for catalyzing ethyl acetate hydrolysis, within the Si/Al ratio ranges studied, were reported for HZSM-5 (optimum Si/Al=47) and HY (optimum Si/Al=3) [121]. The optimum Si/Al ratio differs significantly with zeolite structure, but the reasons for this are still not understood. In general, HY catalysts tend to have lower Si/Al ratios than HZSM-5 catalysts. This may be attributed to the different methods used to synthesize the zeolites. HZSM-5 is synthesized by using organic cation templates, and tend to have lower aluminum content than HY, which is synthesized by using inorganic cation templates [134]. This is due to the higher volume to charge ratio of organic template cations, which limits the number of cations incorporated within the pore volume. As a result, fewer framework Al atoms are required to balance the template charge for HZSM-5. However, it should be pointed out that there are methods for modifying zeolite Si/Al ratios. Some of these methods involve varying the Al source concentration to obtain specific Si/Al ratios, whereas

other methods employ dealumination processes after synthesis to remove some Al atoms from the framework.

The HZSM-5 (Si/Al=19) used for experiments described here had a higher Si/Al ratio than the HY (Si/Al=5.3), and therefore contained more Si-O-Si groups. This resulted in less water poisoning on the HZSM-5 surface and a relative increase in affinity for organics. In the case of HY, relatively more Al-O-Si groups replace Si-O-Si groups, allowing for increased hydrogen bonding with water. Overlapping clusters of water molecules can form by hydrogen bonding, covering the acid sites and SAC surfaces (figure 3.6a). This buildup of water on the surface of the SAC makes it increasingly difficult for organic material (e.g. ethyl acetate) to access the acid sites. HZSM-5, on the other hand, has relatively fewer Al-O-Si groups. Therefore, smaller clusters of water molecules will form, making it easier for organic molecules to access the internal acid sites (figure 3.6b).
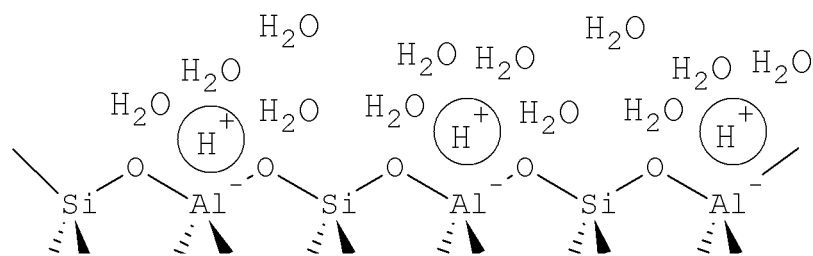
a. low Si-O-Si content
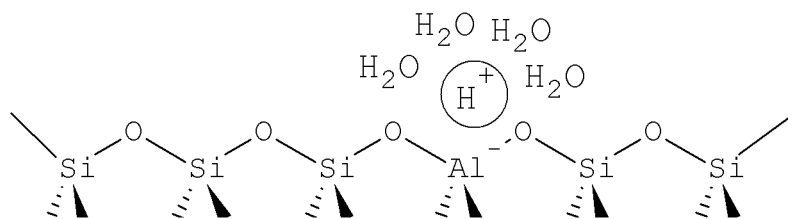
b. high Si-O-Si content

Figure 3.6 water adsorption on zeolite surfaces

3.2.4 Catalyst Reusability for Ethyl Acetate Hydrolysis

Hydrolysis of 5% EA/P (0.4 mL) using an SAC (0.01 g) was performed in the mini-reactor with the oven maintained at 150°C for 30 minutes, as described in section 3.2.1. After the first run, the quartz sample tube was centrifuged and the liquid was carefully removed and analyzed for ethyl acetate hydrolysis products (e.g. ethanol and acetic acid) by gas chromatography with flame ionization detection. The catalyst was then rinsed with distilled water,

centrifuged, and the liquid was discarded. This "washing" of the catalyst was repeated three times. Fresh 5% EA/P solution (0.4 mL) was added to the quartz sample tube containing the "washed" catalyst and the reaction was carried out again. This procedure was repeated until the same SAC had been used for three ethyl acetate (5% EA/P) hydrolysis runs.

In this manner, sulfated zirconia, Nafion® SAC-13, and HZSM-5 were tested for their ability to be reused (table 3.3). HY yielded results that were no different from the blank and was therefore not included in these tests.

Table 3.3 reusability of SACs for ethyl acetate hydrolysis

Catalyst	Run 1	Run2	Run3
	ethyl acetate converted (%)		
Sulfated zirconia	95%	65%	52%
HZSM-5	73%	66%	67%
Nafion® SAC-13	80%	62%	59%

HZSM-5 showed only a slight decrease, from 73% ethyl acetate converted in the first run to 67% ethyl acetate converted in the third run at 150°C after 30 minutes. Kimura et al. also reported nearly unchanged HZSM-5 activity for ethyl acetate hydrolysis after repeated use, and the hydrolysis medium after removal of HZSM-5 was found to be inactive [120]. This may be attributed to the hydrophobic nature of the surface of HZSM-5, which decreases the poisoning effect of water [135]. Nafion® SAC-13 showed a significant decrease in catalytic activity from 80% in the first run to 59% by the third run. Palinko et al. reported that Nafion® SAC-13 lost SO_3H groups (responsible for the acid sites) at temperatures above 150°C [136]. Loss of these groups would result in decreasing catalytic activity after repeated use.

Sulfated zirconia showed the greatest decrease in catalytic activity after three runs at 150°C for 30 minutes. In the first run, 95% conversion was obtained, but only 52% conversion was obtained by the third run. In fact, sulfated zirconia catalytic activity consistently decreased after repeated 30 minute runs at temperatures above 100°C (figure 3.7).

Temperatures below 100°C were not tested. The error bars on the graph in figure 3.7 are estimated from the highest error obtained by using fresh sulfated zirconia (table 3.3) for ethyl acetate hydrolysis (ca. 3%).
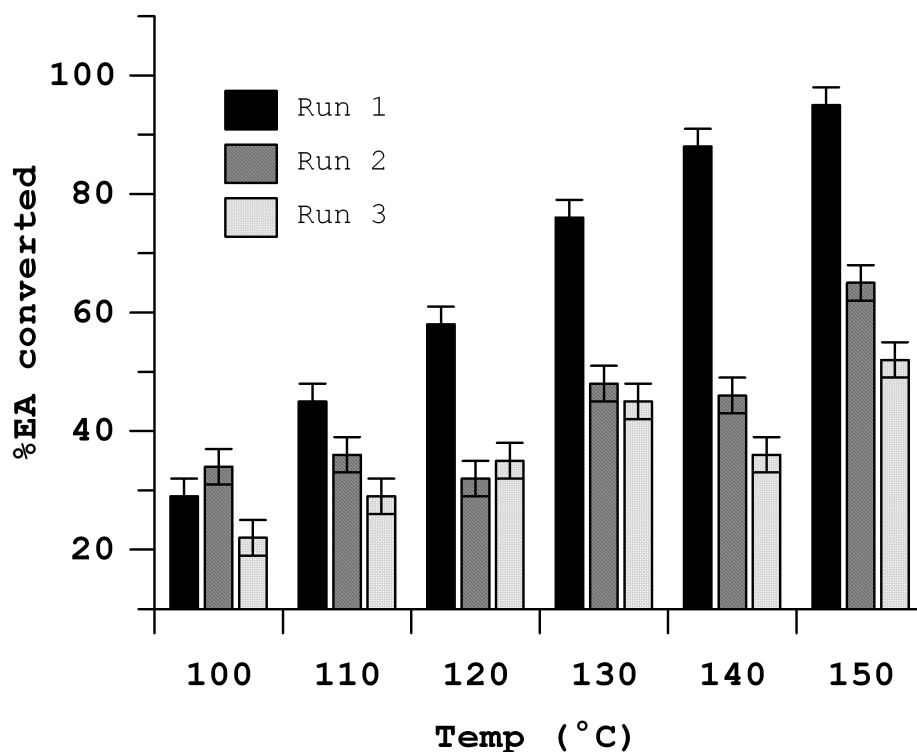
Figure 3.7 catalytic activity of sulfated zirconia after repeated use for ethyl acetate hydrolysis at various temperatures

Several other researchers have also found sulfated zirconia to deactivate after repeated use for ethyl acetate hydrolysis [110, 120, 135]. In the presence of water, sulfated zirconia has been suggested to lose

protons associated with the acid site to the medium
[120]. To test this theory, Kimura et al. removed the
SAC from the reaction medium, added fresh substrate
(ethyl acetate) to the used reaction medium, and
checked for activity. Continued activity would
indicate the presence of acidity leached from the SAC
to the reaction medium. Kimura et al. found that the
sulfated zirconia reaction medium was slightly active
for ethyl acetate hydrolysis; indicating leaching of
acidity. Omota et al. reported a drop in pH when
sulfated zirconia was exposed to water [137]. Char
build up on the catalyst surface can also cause
blockage or loss of acid sites. Based on these
findings, it seems reasonable that the activity of
sulfated zirconia would decrease with repeated use.

3.3 Starch Hydrolysis

The overall goal of this work is to perform
cellulose hydrolysis by using solid acid catalysts. It
would seem that if a catalyst is active for solvated
starch hydrolysis, it should also be active for
solvated cellulose hydrolysis. Although the mechanisms
for polysaccharide hydrolysis (figure 1.4) and ethyl

acetate hydrolysis (figure 3.1) involve addition of a water molecule so that one portion of the substrate gains a hydroxyl group (OH$^-$) and the other gains a hydrogen ion (H$^+$), the reaction mechanisms are different. For ethyl acetate, an ester is hydrolyzed to an acid and an alcohol. Polysaccharide hydrolysis, on the other hand, results in breaking glycosidic bonds to form glucose monomers. Therefore, it is not necessarily expected that the ethyl acetate hydrolysis results will correlate with those obtained for polysaccharide hydrolysis in water with the SACs. Furthermore, the relatively larger size of starch compared to ethyl acetate may make hydrolysis with zeolites, which have size restricted access to the acid sites, more difficult.

The remainder of this chapter describes an evaluation of the activities of various SACs for the hydrolysis of starch, which is a better model compound for cellulose hydrolysis than ethyl acetate. The mechanisms for acid catalyzed hydrolysis of cellulose and starch are almost identical. Both starch and cellulose are made of glucose monomers linked by glycosidic bonds. As discussed in section 1.2, the

difference between starch and cellulose lies in these glycosidic bonds. Starch is made of glucose linked by 1,4-alpha glycosidic bonds, which allows for polymer branching. On the other hand, cellulose is made of glucose linked by 1,4-beta glycosidic bonds, making it very rigid and without branching.

3.3.1 Starch Solution

A 1% starch solution was made by mixing 1 g of starch with approximately 5 mL distilled water in a 100 mL beaker. Boiling distilled water was then added to the beaker and the solution was heated an additional 2-3 minutes until it became clear. The solution was then quantitatively transferred to a 100 mL volumetric flask, and once cooled, the flask was filled to the mark with distilled water.

3.3.2 Starch Hydrolysis Sample Preparation

The catalyst (0.01 g SAC, 10 µL HCl solution, or 24 µL H_2SO_4 solution) and 1% starch solution (0.4 mL) were placed into the quartz sample tube of the mini-reactor. The mini-reactor was pressurized to at least 2 MPa with nitrogen gas and then heated isothermally at

150°C for various times. The temperature (150°C) was chosen to maximize starch conversion based on the results obtained for ethyl acetate hydrolysis. The reaction was quenched by immersion in cold water. The quartz sample tube was then centrifuged and the liquid was tested for reducing sugars with Benedict's reagent (as described in section 2.4) and analyzed by ultraviolet-visible spectroscopy (UV-VIS) as described in section 2.5.3. The starch conversion was calculated by using equation 3.1.

3.3.3 Starch Conversion

The percent total glucose yield (%TGY) was determined by calculating the ratio of the glucose (mmol) after hydrolysis (G) and the glucose (mmol) theoretically possible (G_0) assuming the starch had been converted to 100% glucose (equation 3.2). Starch is made up of glucose monomers. Assuming that starch is completely hydrolyzed to glucose, G_0 can be calculated by dividing the weight of the starch (0.004 g) by the molecular weight of the repeat unit (MW_{RU}=162 g mol^{-1}); which is calculated by subtracting the molecular weight of water (MW_{water}=18 g mol^{-1}) from the molecular weight of

glucose ($MW_{glucose}$=180 g mol^{-1}). Subtracting MW_{water} is required due to the loss of one water molecule for every glycosidic linkage found in the starch polymer. As an example, when 0.004 g of starch was used, G_0 is calculated to be 0.025 mmol. The value for G was calculated based on Benedict's test results and using a best-fit linear line of calibration standards (described in section 2.4.2).

$$\frac{G}{G_0} \text{x } 100\% = \% \text{ total glucose yield} \quad \textbf{Equation 3.2}$$

3.3.4 Starch Hydrolysis with Various SACs

In addition to the solid acid catalysts tested for ethyl acetate hydrolysis (sulfated zirconia, HY, HZSM-5, and Nafion® SAC-13), Nafion® NR50 was also used. Nafion® NR50 is an alternate version of Nafion® SAC-13. While both are sulfonated tetrafluoroethylene polymers, the polymer for Nafion® NR50 is unbound, whereas the polymer for Nafion® SAC-13 is bound to amorphous silica. Total glucose yield (values determined by equation 3.2) are listed in table 3.4. Standard deviations for these values were not obtained because each mixture was tested only once. The main purpose of

this experiment was to determine if the SACs tested for water tolerance with ethyl acetate hydrolysis would show similar relative activities for starch hydrolysis and to determine whether this activity was significantly greater than a blank measurement (i.e. no catalyst). Although not measured, errors could be estimated to be about 5% based on standard deviations of the starch hydrolysis results at various temperatures with sulfated zirconia (discussed in the next section). Sulfated zirconia had significantly higher activities than the blank at 150°C after 0.5 hr. Both Nafion® NR50 and Nafion® SAC–13 provided significant activities, but only after 2 hours.

Table 3.4 starch hydrolysis in aqueous medium by solid acid catalysis

Catalyst	150°C 0.5hr	150°C 1hr	150°C 2hr
	% total glucose yield[a]		
Sulfated zirconia	69	76	35
HY	11	19	13
HZSM-5	15	26	32
Nafion® SAC-13	19	33	67
Nafion® NR50	17	29	70
None	8	21	14

[a]calculated using equation 3.2
[b]acidity (mmol/g) was determined by titration as described in section 2.3

The trends for each SAC when the amount of catalyst was kept constant are shown in figure 3.8. Zeolite HY resulted in TGY that were comparable to the blank (i.e. no catalyst), which was similar to the results obtained for ethyl acetate hydrolysis. Nafion® SAC-13 and Nafion® NR50 exhibited similar activity for starch hydrolysis. However, their activities were lower than that found for sulfated zirconia. Like the ethyl acetate hydrolysis results, sulfated zirconia showed to have the highest activity when catalyst weight was kept constant, compared to the other SACs

tested for starch hydrolysis (150°C, 0.5 hr, 1 hr). The highest total glucose yield was obtained with sulfated zirconia after 1 hour, with 76% TGY. After 2 hours, %TGY decreased to 35% with the sulfated zirconia catalyst, which was attributed to glucose degradation. Visual inspection of the sample tube revealed a brown color to the solution, which likely resulted from side reactions involved with glucose degradation.
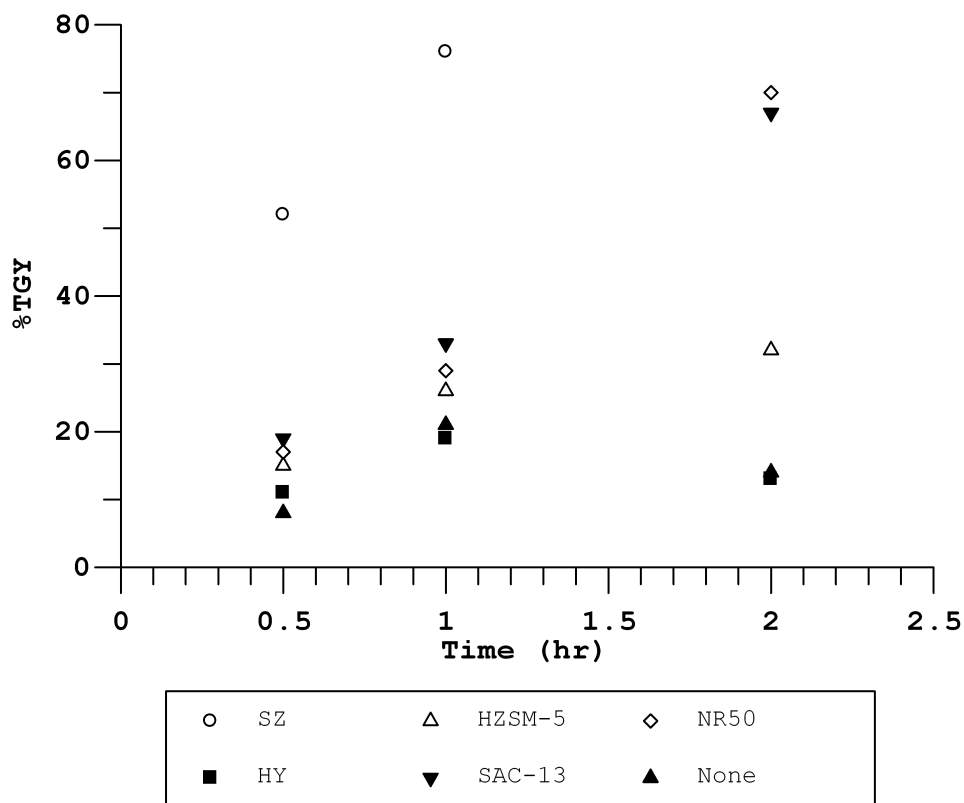
Figure 3.8 starch hydrolysis in water at 150°C for 0.5, 1, and 2hrs using solid acid catalysis

It is suspected that zeolite hydrophobicity played a role in the activity for ethyl acetate hydrolysis. However, starch would not be expected to be as hydrophobic as ethyl acetate, due to the many OH groups located throughout the starch framework. Therefore, based on hydrophobicity alone (ignoring steric effects, dissolution of starch, etc.), starch should be easier to hydrolyze with zeolite catalysis than ethyl acetate. It would seem that HY, which should be more hydrophilic than HZSM-5, should be more effective at hydrolyzing starch. However, this assumption is not supported in the results. Therefore, hydrophobicity does not appear to be a significant factor contributing to the activity of zeolites for starch hydrolysis.

The inability of HY to catalyze starch hydrolysis may instead be attributed to steric effects associated with the zeolite pores, which would restrict access of the large starch molecules to acid sites. Based on this reasoning, HZSM-5 would be expected to show even lower activity than HY, due to the even smaller pore size of HZSM-5. In contrast, our results indicated that HZSM-5 had higher activity compared to HY for starch hydrolysis after 2 hours at 150°C. Jiang et al.

also found that HZSM-5 (Si/Al=45) was active for starch hydrolysis (120°C, 4 hr, microwave reactor), resulting in a 22% glucose yield [58]. Unfortunately, HY was not tested in their study, so they made no comparisons.

The acid site locations in each zeolite may play a role in their activities for starch hydrolysis. HZSM-5 (MFI framework) is made up of straight 10-member ring channels intersected by zigzag 10-member ring channels. All acid sites are located within the channels. When a substrate is too large for the pores, the acid sites located near the opening of the channel may still be accessible. This would lead to fewer acid sites involved in the hydrolysis process, and may be responsible for the observed low starch hydrolysis activities.

The supercage (12-member ring) of HY (FAU framework) is composed of linked sodalite cages and double six-member rings (d6r). Acid sites located in the d6r and sodalite cages are only accessible through the 6-member ring openings. The two acid sites located in the supercage are not near the pore opening. One is located in the center of a hexagonal window connecting the sodalite cage and a supercage. The other is

located in the supercage on a square window of a sodalite cage between two d6rs. Therefore, acid sites in the supercage of HY are less likely to be accessible to large substrates. Consequently, no activity would be expected for starch hydrolysis. Although acid site locations may also be used to explain differences observed when HY and HZSM-5 were used for ethyl acetate hydrolysis, that discrepancy is better explained by the hydrophobic argument.

Although the amount of catalyst used (0.01 g) was kept constant, the concentration of acid (mmol g^{-1} H^+) varied for each catalyst. For the purpose of comparing the relative activities of the solid and liquid acid catalysts, %TGY was scaled by the mmol H^+ employed. The mmol H^+ added for HZSM-5 (0.0110 mmol H^+) and Nafion® SAC-13 (0.0061 mmol H^+) was the same as was listed for ethyl acetate hydrolysis. The other catalysts were remade for this study and the amounts of acid provided were as follows: sulfated zirconia (0.0108), HY (0.0147), H_2SO_4 solution (0.0042), and HCl solution (0.0070) where values in parentheses are mmol H^+ provided to the reaction mixture (figure 3.9). Nafion® NR50 swells in the presence of water, allowing access

to additional internal acid sites [138, 139]. Titrating Nafion® NR50 to determine acidity based on exposure to sodium hydroxide for 2hrs (described in section 2.3), yielded 1.6 mmol H^+ per gram which would result in 0.016 mmol H^+ for these experiments. Lopez et al. found a 60% volume increase when NR50 was exposed to water at 60°C [138]. Due to steric effects, sodium hydroxide (titrant) may be able to access more acid sites than starch (hydrolysis substrate) under the same conditions. To mimic access to surface acid sites only, a quick titration method was used (described in section 2.3). This method should give lower mmol H^+ values, because only some of the acid sites should be accessible. Assuming that starch cannot access internal acid sites (even with swelling), this may be a better predictor for the mmol H^+ participating in starch hydrolysis. Using this method, Nafion® NR50 was determined to provide 0.0063 mmol H^+.
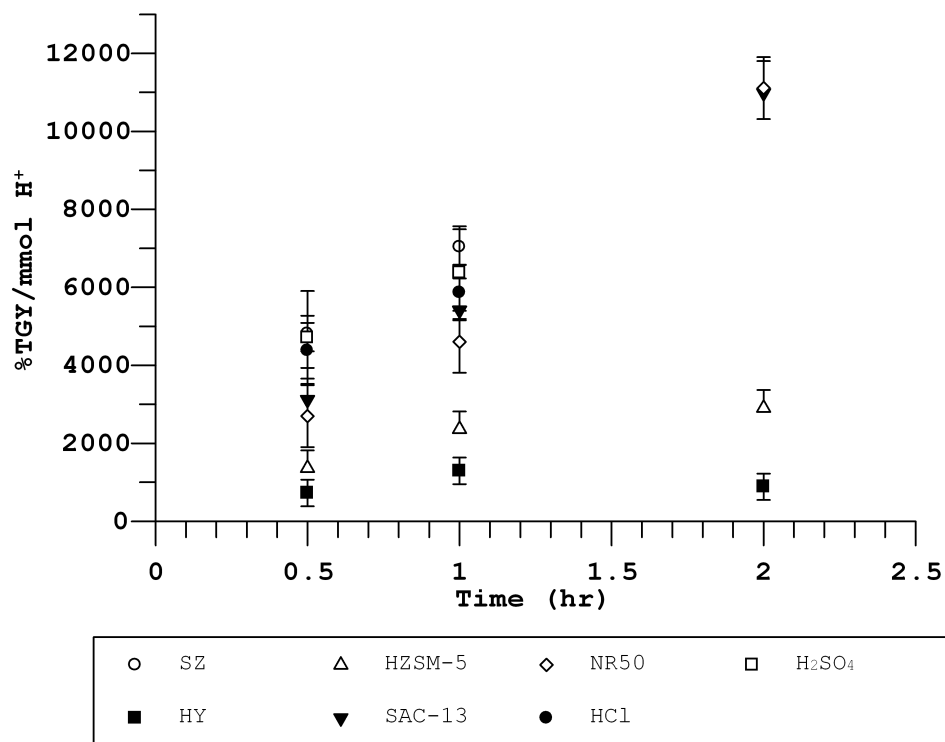
Figure 3.9 %TGY from starch hydrolysis scaled by the mmol H$^+$ added based on titrations of fresh SACs

When %TGY values were scaled by the mmol H$^+$ added, the activity of the liquid acids were found to be similar to the amorphous solid acid catalysts. Under similar reaction conditions (150°C for 30 minutes), this was also the case for ethyl acetate hydrolysis. When the reaction temperature was decreased to 130°C (30 min), liquid acids (HCl and H_2SO_4) performed better than sulfated zirconia for starch hydrolysis, a trend which was also found for ethyl acetate hydrolysis at temperatures below 150°C.

Similar to the ethyl acetate hydrolysis results, amorphous solid acid catalysts (sulfated zirconia and Nafion®) performed better for starch hydrolysis than the zeolites (HZSM-5 and HY). The lower %TGY values obtained by the zeolites may be attributed to the size of the starch molecule relative to the pore sizes of the zeolites, making hydrolysis in aqueous media with zeolites more difficult.

3.3.5 Starch Hydrolysis Reaction Rates with Sulfated Zirconia

The purpose of these experiments was to determine the energy of activation for starch hydrolysis catalyzed by sulfated zirconia and to compare this value to previously published results for liquid acids. Profiles for starch hydrolysis catalyzed by sulfated zirconia at various temperatures as a function of time were obtained and utilized for reaction rate calculations (figure 3.10). Sulfated zirconia was used because it was the best catalyst for both ethyl acetate and starch hydrolysis. It also appeared to perform almost as well as sulfuric acid at 150°C (when scaled by the mmol H^+ added).
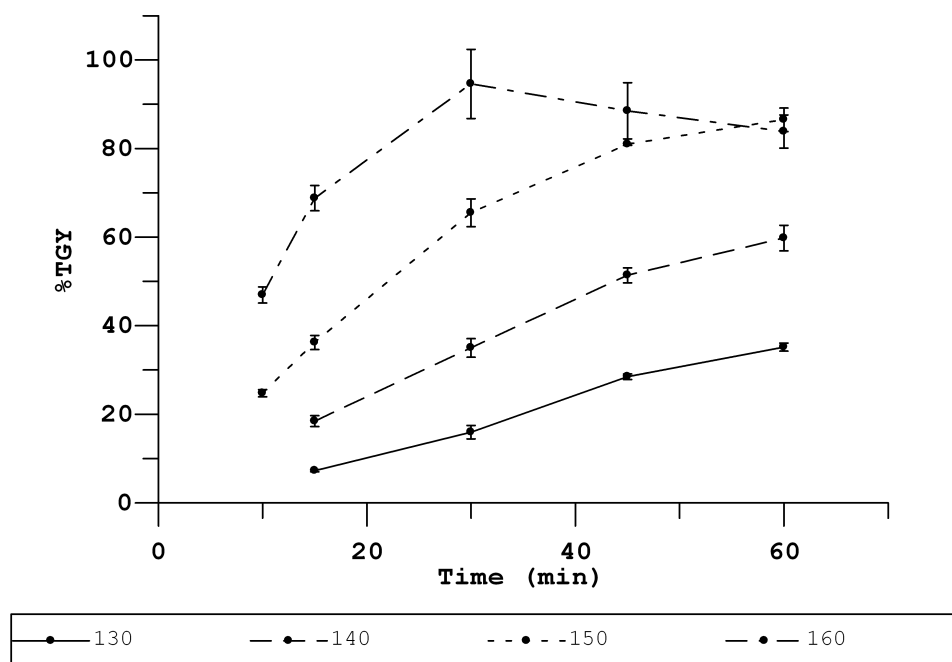
Figure 3.10 temperature profiles for starch hydrolysis catalyzed by sulfated zirconia

It is important to note that for starch hydrolysis at 160°C after 30 minutes, the %TGY decreased, which was attributed to glucose degradation. In fact, under similar conditions, Choi and Kim found that 5-hydroxymethyl furfural (5-HMF) forms, due to glucose dehydration in the presence of sulfuric acid. At 160°C, they reported that only a few minutes were required before 5-HMF was detected [37].

Using only the initial linear portions of the temperature profile data (figure 3.11), and assuming a first-order rate law (equation 3.3), sugar formation

rate constants were calculated for each temperature. In equation 3.3, M_0 is the initial amount of starch, M is the amount of starch after hydrolysis (1-S), where S is the amount of reducing sugars formed, t is time, and k is the rate constant.

$$\ln M= -kt+\ln M_0 \qquad \textbf{Equation 3.3}$$
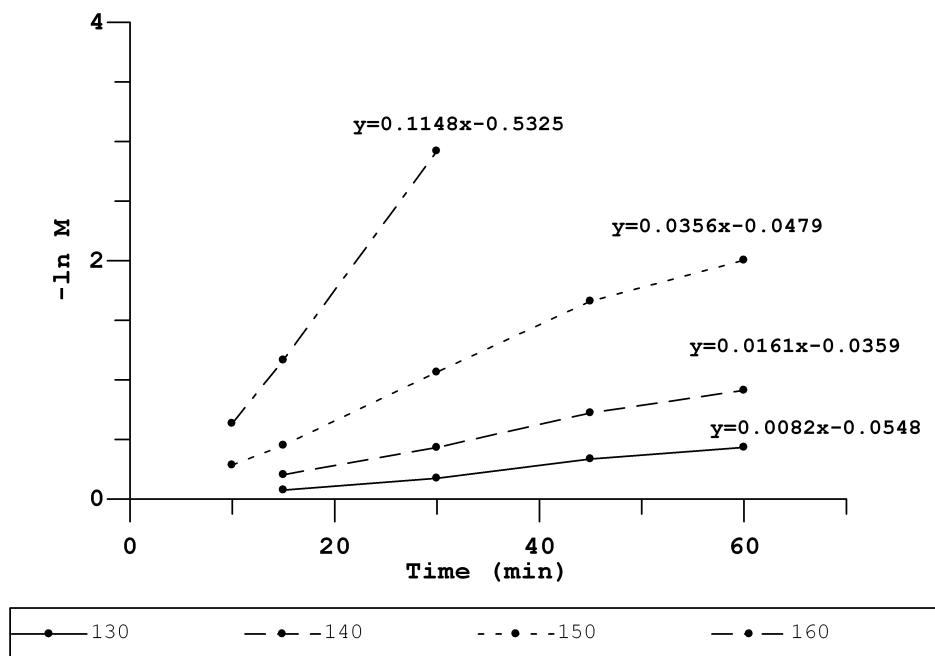
Figure 3.11 sulfated zirconia rate constants determined

As expected, the rate constants increased as the temperature increased: 130°C (0.0082), 140°C (0.0161), 150°C (0.0356), 160°C (0.1148) where the values in

parentheses are the rate constants (% TGY min^{-1}). Utilizing the Arrhenius equation (equation 3.4), a plot of ln k versus T^{-1} was used to obtain E$_A$ (figure 3.12). In equation 3.4, k is the rate constant, R is 1.987 cal K^{-1} mol^{-1}, T is temperature (K), C is the frequency factor and can be determined by the y-intercept, and the energy of activation (E$_a$) is determined by the slope (-E$_a$/R) of a plot of ln k versus T^{-1}. The energy of activation for sugar formation by starch hydrolysis by using sulfated zirconia was calculated to be 30.1 kcal mol^{-1}, which is similar to the activation energy reported for maltose hydrolysis in water by sulfuric acid (30.2 kcal mol^{-1}) [37]. Maltose is a disaccharide composed of two glucose molecules and therefore should be easier to hydrolyze than starch (many glucose molecules linked). Based on these findings, it appears that the sulfated zirconia activation energy for starch hydrolysis in aqueous media is likely comparable to that for sulfuric acid. This would suggest that protons on the surface of sulfated zirconia are readily accessible.

$$\ln k = -\left(\frac{E_a}{RT}\right) + \ln c \qquad \textbf{Equation 3.4}$$
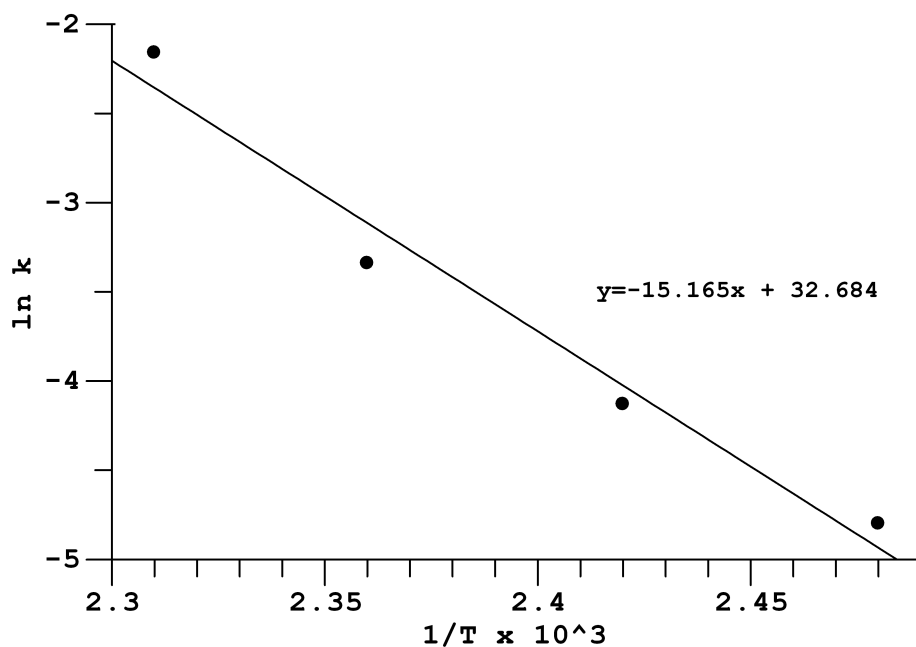
Figure 3.12 Arrhenius plot for starch hydrolysis catalyzed by sulfated zirconia

3.3.6 Sulfated Zirconia reusability for Starch Hydrolysis

Sulfated zirconia exhibited the greatest activity when catalyst weight was constant for both ethyl acetate and starch hydrolysis. However, it also exhibited the greatest decrease in catalytic activity when repeatedly used for ethyl acetate hydrolysis. Therefore, its ability to be reused for starch hydrolysis was evaluated. All other SACs tested for starch hydrolysis (HZSM-5, HY, Nafion® NR50, and Nafion® SAC-13) at 150°C after 30 minutes showed

activities only slightly higher than the blank (i.e. no catalyst) and therefore, they were not tested for reusability. Starch hydrolysis %TGY values for these SACs were ca. 16%, whereas the blank was ca. 8%. For comparison, sulfated zirconia was much higher (ca. 69%).

Hydrolysis of a 1% starch solution (0.4 mL) with sulfated zirconia (0.01 g) was performed in the mini-reactor at 150°C for 30 minutes as described in section 3.3. After the first run, the quartz sample tube was centrifuged and the liquid was removed and tested for reducing sugars by using the Benedict's reagent method. The catalyst was then rinsed with distilled water, centrifuged, and the liquid was discarded. This "washing" of the catalyst was repeated three times. Fresh 1% starch solution (0.4 mL) was added to the quartz sample tube containing the "washed" catalyst. This method was repeated until the same SAC was used for three starch (1%) hydrolysis runs under these conditions. While the catalyst could be reused, there was a significant decrease in activity after each use, as was the case with ethyl acetate hydrolysis. Fresh sulfated zirconia produced 73% TGY that dropped with

each successive use to 34% for the second and 20% for the third run.

It seems reasonable that the activity loss of sulfated zirconia for starch hydrolysis after repeated use can be attributed to the same reasons as the ethyl acetate hydrolysis activity loss. This was described as a loss of protons to the medium due to leaching of the ionic sulfur species from the sulfated zirconia surface. In addition to leaching, protonated organic molecules can replace H^+ on the catalyst surface, which likely happens during char buildup.

3.4 Ion Exchange Mechanism in Zeolites

Zeolites HY and HZSM-5 showed little to no activity for starch hydrolysis in an aqueous medium. This was attributed to the acid site locations, which are only accessible through size-restricted openings. Because starch is too large to access the protons inside the zeolites, these protons must be made more accessible in order to make zeolites a viable SAC for polysaccharide hydrolysis. One possibility would be to use ion exchange to release protons into the reaction medium from the zeolite pores and channels. For

zeolites immersed in an aqueous medium, the zeolite protons (H^+) balance the negative charge on the framework surface (SAC^-), which can be explained by a weak acid equilibrium model ($HSAC \leftrightarrows H^+ + SAC^-$). Sodium ions ($Na^+$) can be introduced to the zeolite and exchange for the charge-balancing protons, which allows protons (H^+) to move freely into the aqueous medium. This process can be described by an ion exchange equilibrium model ($HSAC + Na^+ \leftrightarrows NaSAC + H^+$). A relatively high concentration of Na^+ should cause a significant transfer of H^+ from zeolite surfaces to the aqueous medium, effectively decreasing the pH of the solution. The purpose of the experiments described in this section was to determine if ion exchange significantly increased the acidity of solutions containing HY and HZSM-5.

HY (0.2 g, 2.29 mmol g^{-1}) and HZSM-5 (0.2 g, 0.88 mmol g^{-1}) were each mixed with various concentrations (0, 0.25, 0.5, 0.75, 1, and 2 M) of sodium chloride (10 mL) in round bottom flasks. Samples were refluxed with constant stirring for one hour to promote ion exchange. Boiling was obtained with a setting of 80 volts on the variac, which was connected to a heating mantel that

held the round bottom flask. The liquid was filtered from the solid acid catalyst, and 5 mL of the liquid was titrated with sodium hydroxide (0.01 M) to determine acidity.

Adding 0.25 M Na^+ to the solution caused an increase in acidity of ca. 0.06 mmol H^+ and 0.17 mmol H^+ for HZSM-5 and HY respectively when compared to the blank (e.g. water only). This is consistent with other studies, which have shown that ion exchange with Na^+ causes a decrease in zeolite acidity [140, 141]. The ion exchange equilibrium would suggest that an increase in solution acidity should accompany a decrease in the number of protons present within zeolite channels. The relatively smaller increase in solution acidity for HZSM-5 could be explained by the difference in Si/Al ratios for the two zeolites. HY (Si/Al=5.3) has a lower Si/Al ratio than HZSM-5 (Si/Al=19), so there are fewer Al atoms present in HZSM-5. Therefore, HZSM-5 has fewer charge balancing cations (e.g. protons), which results in fewer H^+ available for ion exchange.

For comparison, the amount of solution acidity increase was scaled by the acid content of the fresh catalysts, which was determined by using the solid acid

titration methods described in section 2.3: HY (0.458 mmol H^+) and HZSM-5 (0.176 mmol H^+). Total ion exchange would result in a scaled value of 1, which corresponds to 100% ion exchange. However, only 65% (HY) and 40% (HZSM-5) were observed to ion exchange with Na^+, suggesting that acidity still remained in the solid (figure 3.13). This was confirmed by titration of the solid. If this methodology is correct, adding the scaled values corresponding to the solution and solid acidity for each Na^+ concentration should result in a total value of 1. In fact, HY and HZSM-5 resulted in average scaled values of 1.14 (±0.14) and 1.02 (±0.02) respectively.
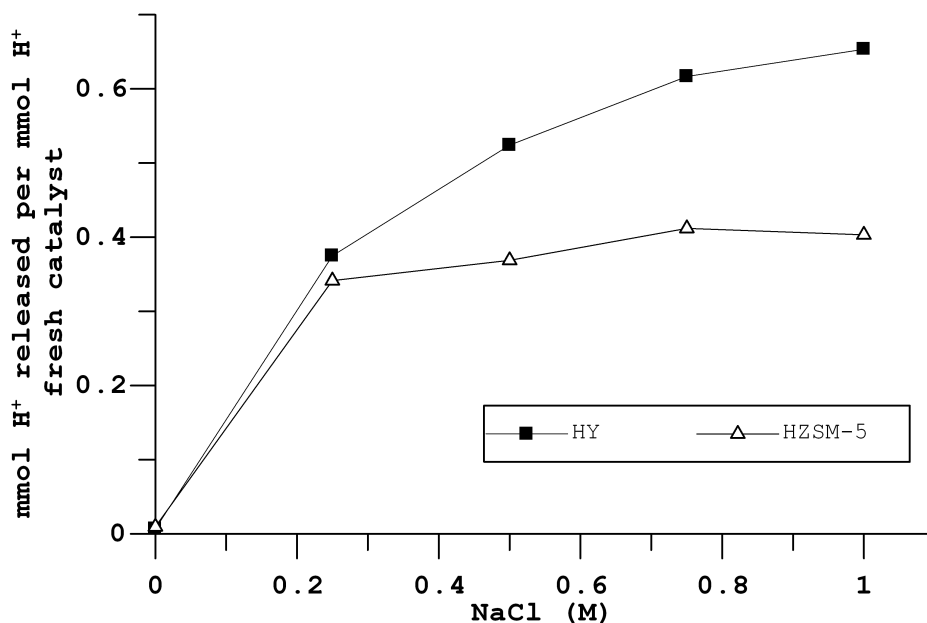
Figure 3.13 mmol H$^+$ released into the medium when HY and HZSM-5 were exposed to various concentrations of NaCl; based on titration of the medium

The increase in solution acidity for HZSM-5 after adding 0.25 M Na$^+$ was not significantly different from the increase observed when higher Na$^+$ concentrations were employed (figure 3.13). On the other hand, results for HY indicated that increasing the concentration of Na$^+$ from 0.25 M to 1 M produced an increase in the mmol H$^+$ released to the solution (figure 3.13). Although not shown in figure 3.13, the addition of 5 M Na$^+$ for HY resulted in similar solution acidity as found after adding 1 M Na$^+$, suggesting that the

amount of H^+ ion exchanged from HY had reached a maximum at 1 M Na^+.

Although the mmol H^+ transferred to the aqueous solution leveled off after 0.25 M NaCl was added to the solution containing HZSM-5, the corresponding solution containing HY did not level off until after 1 M NaCl was added. This difference in HY and HZSM-5 may be explained by the differences in acid concentrations. Fresh HY (0.458 mmol H^+) used for this experiment had more than double the mmol H^+ contained within the same weight of HZSM-5 (0.176 mmol H^+). Under these conditions, more sodium chloride should be required for ion exchange with HY compared to HZSM-5.

Zeolite acid site locations may also play a role in relative ion exchange properties. HZSM-5 acid sites are found within the channels (5.1 x 5.5 Å and 5.3 x 5.6 Å) of the zeolite, and therefore should be readily accessible to ion exchange with Na^+ (c.a. 4.7 Å hydrated radius [142, 143]). Based on the effective size of Na^+ relative to the HZSM-5 channels, minimal steric effects would be expected. On the other hand, acid sites in HY are located in the supercage, sodalite cage, and double six-member rings (d6r). Although the supercage (7.4 Å)

should not offer much of a steric hindrance towards Na^+ ion exchange, the acid sites located in the sodalite cage and d6rs are only accessible through 6-member rings (2.53 Å), which should effectively block hydrated Na^+ ions. However, theoretical and experimental studies have shown that zeolite ion exchange processes are complicated and not readily described by simple mechanisms [144-148]. For example, Alberti and Martucci suggested that protons in zeolites are not associated with one acid site, but rather move between various acid sites by a Grotthuss mechanism [144]. The Grotthuss mechanism describes a water mediated proton transfer; in which the proton moves through the water by making and breaking bonds with water molecules. Because all acid sites for HZSM-5 are located within Na^+ accessible channels, Grotthuss proton transfer would not be expected to play a significant role in the rate of ion exchange with Na^+. On the other hand, the ion exchange rate for some protons in HY might be dependent on the rate of proton transfer among negative surface sites located in the sodalite cage and d6rs.

3.5 Starch Hydrolysis in Na$^+$ Aqueous Media

Because adding sodium ions to the reaction medium increases aqueous acidity when solutions contain zeolites, it is important to determine how ion exchange may affect polysaccharide hydrolysis. Based on the results described in the previous section (3.4), it seems that zeolites should be more active for starch hydrolysis after adding Na$^+$ to the solution.

For comparison purposes, both a water only and Na$^+$ enhanced aqueous medium were used for starch hydrolysis with the following SACs: sulfated zirconia, HY, HZSM-5, Nafion® NR50, and Nafion® SAC-13. Experiments were performed in triplicate in a similar manner to the method described in section 3.3 and samples were heated in the mini reactor at 150°C for 30 minutes. Replicate sample standard deviations were below 5% for all catalysts except for samples containing Nafion® NR50 (water only medium) and sulfated zirconia (1 M NaCl medium), which yielded standard deviations of 9% and 11% respectively. No data points could be omitted at 90% confidence ($Q_{calc} < 0.941$) by using the Dixon's Q-test. It is possible that the various pellet sizes (c.a. 3-5 mm) of the Nafion® NR50 catalyst contributed

to the larger standard deviations. Due to the size range of these pellets, different numbers of the pellets (3-4) were often required for reactions. Consequently, the catalyst surface area varied for experiments, which could have changed the number of surface accessible acid sites available for experiments. However, it is still unclear as to why higher standard deviations were obtained for the sulfated zirconia experiments.

Except for sulfated zirconia, addition of Na^+ to the aqueous medium significantly increased the %TGY (table 3.5). Although the structure of the sulfated zirconia acid sites is not fully understood, it is considered to be a super acid, which means the charge balancing protons have weak interactions with the acid site. In this case, it is likely that the super acidity can cause protonation of the water without the need for ion exchangeable cations. Consequently, ion exchange does not significantly increase the availability of H^+ to the solution.

Table 3.5 starch hydrolysis in Na$^+$ enhanced aqueous medium

Catalyst	H$_2$O Medium (150°C)	Salt Medium (150°C)
	% total glucose yield	
Sulfated Zirconia	69±2	67±11
HY zeolite	23±5	80±2
ZSM–5 zeolite	15±5	82±4
Nafion® SAC–13	19±5	63±5
Nafion® NR50	17±9	79±2

The significant increase in the activity of the Nafion® NR50 catalyst after addition of Na$^+$ might be attributed to increased swelling of the polymer, which would expose more acid sites [138, 139]. Addition of Na$^+$ to the solution could then allow for ion exchange induced release of these otherwise buried protons to the reaction medium, resulting in higher catalytic activity. In the absence of ion exchange (e.g. water only medium), these internal acid sites would not be accessible to the hydrolysis substrate, resulting in lower total glucose yield. Unlike Nafion® NR50, Nafion® SAC–13 does not undergo swelling because polymer chains are attached to amorphous silica. However, the amorphous silica framework of Nafion®

SAC-13 may impose size restricted areas where acid sites are less accessible to larger molecules (e.g. starch, cellulose). However, smaller cations (e.g. Na^+) should be able to access these areas. The net result of these effects is that starch hydrolysis by Nafion® SAC-13 increased after addition of Na^+, but the increase was not as large as was detected for Nafion® NR50.

As previously described, zeolite acid sites are mostly located within size restricting pores. The increase in starch hydrolysis activity for zeolites when Na^+ was added to reaction mixtures suggests that a significant number of H^+ ions were transferred from zeolite channels to the aqueous solution by means of ion exchange.

3.6 Summary

The water tolerance of various SACs (e.g. HY, HZSM-5, sulfated zirconia, and Nafion® SAC-13) was systematically characterized based on the temperature dependence of catalyst activity for ethyl acetate hydrolysis. Scaling the ethyl acetate converted (%) by the amount of fresh solid acidity revealed higher activities for amorphous SACs (sulfated zirconia and

Nafion® SAC-13) compared to the zeolites tested (HY and HZSM-5). Surprisingly, HY was found to be inactive for ethyl acetate hydrolysis. Among the three SACs that were active for ethyl acetate hydrolysis (HZSM-5, sulfated zirconia, and Nafion® SAC-13), HZSM-5 was the only catalyst found to be reusable without a significant decrease in activity. Sulfated zirconia and Nafion® SAC-13 lost 43% and 21% activity respectively, for their second uses for ethyl acetate hydrolysis. Although ethyl acetate was a good predictor of the water tolerance of the SACs studied, the overall goal of this work is to study cellulose hydrolysis using SACs. Unfortunately, cellulose cannot be dissolved in aqueous media. Therefore starch hydrolysis in water was studied instead.

Whereas Nafion® NR50, Nafion® SAC-13, and sulfated zirconia exhibited significant activities for starch hydrolysis in both aqueous and Na^+ enhanced media, zeolites HY and HZSM-5 exhibited significantly higher activity when used in the Na^+ enhanced media. The observed little to no activity for HY and HZSM-5 catalyzed starch hydrolysis in aqueous media was attributed to steric hindrance due to the large size of

starch molecules relative to the smaller pore sizes, which restricts access to acid sites. Based on these results, in order for zeolites to be active for cellulose hydrolysis (discussed in chapter 4), acid equivalents must be transported from the catalyst inner channels to the aqueous media, which can be accomplished by ion exchange.

Chapter 4 : HYDROLYSIS IN AN IONIC LIQUID

4.1 Background

Cellulose has been proposed as an alternative to starch as a starting material for ethanol production [2, 41, 149]. However, cellulose is difficult to dissolve in water and is more resistant to hydrolysis. While hot compressed water has proven to be useful for the dissolution of cellulose [15, 17, 47, 118, 150], high temperatures and pressures must be maintained during the hydrolysis process, which leads to hydrolysis product (i.e. glucose) decomposition [15, 16, 46]. Alternatively, ionic liquids have been shown to dissolve cellulose under much milder conditions [23, 24, 151, 152].

4.1.1 Ionic Liquids

Ionic liquids are salts that are liquids at or below 100°C [151]. Ionic liquids have been used to dissolve cellulose at lower temperatures [23, 25–28, 153] (<150°C) than water (280°C). Furthermore, precipitation of cellulose that has been dissolved in an ionic liquid significantly lowers its degree of

crystallinity compared to untreated cellulose [31, 151, 152, 154-157]. Cellulose treated in this manner is more easily hydrolyzed, resulting in increased sugar yields. Another benefit of ionic liquids is that they have the potential to be recycled and reused [158].

Vitz et al. studied various 1-alkyl-3-methylimidazolium ionic liquids with various anions and found that chloride, acetate, and phosphate had good cellulose dissolving properties [159]. However, the ionic liquids containing acetate and phosphate were not appropriate for acid catalyzed hydrolysis of cellulose, because they were easily protonated by strong acids [158], reducing the number of acid equivalents available for hydrolysis.

Ionic liquids containing anions with no basic properties, particularly 1-butyl-3-methylimidazolium chloride [BMIM]Cl and 1-ethyl-3-methylimidazolium chloride [EMIM]Cl, have been shown to be a useful medium for cellulose hydrolysis [29, 30, 32, 160]. Li et al. hydrolyzed corn stalk, rice straw, pine wood, and bagasse in [BMIM]Cl using hydrochloric acid (7 wt%) at 100°C for 1 hour and obtained 66%, 74%, 81%, 68% total reducing sugars respectively [29]. Vanoye et al.

evaluated the kinetics involved with acid catalyzed cellobiose hydrolysis in [EMIM]Cl catalyzed by various liquid acids. They found that the hydrolysis reaction was much faster than the glucose degradation reaction when the acid pK_a was below 0.5 [161]. The energy of activation for cellobiose hydrolysis in [EMIM]Cl was found to be 26.5 kcal mol^{-1} and 68% glucose was obtained by using methane sulfonic acid catalyst (90°C, 2.5 hr) [161]. Binder and Raines dissolved cellulose in [EMIM]Cl prior to hydrolyzing with hydrochloric acid (105°C, 4 hr) and obtained 89% glucose [157]. Based on these results and commercial availability, [EMIM]Cl or [BMIM]Cl might be good solvents for large scale cellulose dissolution. The ionic liquid chosen for the studies described here was [EMIM]Cl. This selection was made primarily because the cost of this ionic liquid ($0.34 g^{-1}) was lower than the cost for [BMIM]Cl ($1.31 g^{-1}).

Before the work described here, only a few studies had been done using solid acid catalysis for cellulose hydrolysis in an ionic liquid medium [158, 162, 163]. Zhang et al. performed cellulose hydrolysis in [BMIM]Cl using microwave assisted heating with various solid

acid catalysts (SAC). Styrene based sulfonic acid resin (NKC-9), HY, and HZSM-5 exhibited activity for cellulose hydrolysis producing 38% (3.3 min), 48% (8 min), and 43% (9.5 min) total reducing sugars (TRS) respectively at a microwave irradiation of 240 W [162]. Rinaldi et al. evaluated the ability of several SACs to depolymerize cellulose in [BMIM]Cl and reported that their performance was related to the surface area and pore size of the SAC [59]. Apparently, high surface areas and large pore sizes allow better access to solid acid sites, which results in greater cellulose depolymerization.

4.2 Ionic Liquid Tolerance of Various SACs

Before using 1-ethyl-3-methylimidazolium chloride, which will be referred to as [EMIM]Cl, for polysaccharide hydrolysis, it was important to understand how the ionic liquid medium (ILM) might affect the stability of the SAC. The solid acid catalysts tested were: sulfated zirconia (SZ), HY, HZSM-5, Nafion® SAC-13, and Nafion® NR50.

The ILM was prepared by mixing [EMIM]Cl (2 g) with distilled water (0.3 mL). SAC (0.25 g) was exposed to

the ILM for 1 hr at 105°C using a temperature controlled oil bath. The catalyst was then removed by filtering, rinsed with distilled water, and dried at room temperature. The SAC (before and after ILM exposure) was titrated using the back titration procedure described in detail in section 2.3 to determine the number of acid equivalents, where excess sodium hydroxide was mixed for 10 min (except Nafion® NR50, 2 hr) with the SAC and an aliquot of liquid was titrated with oxalic acid using a color indicator. Results indicated that a significant loss in catalyst acidity (mmol H^+) occurred for all of the SACs tested (table 4.1). Titration of the ILM after removal of the SAC with sodium hydroxide using a color indicator was also performed. However, due to the yellow color of the [EMIM]Cl it was difficult to see the end point color change, which made it difficult to obtain reproducible results. Therefore, results for the liquid titrations are not reported in table 4.1, but were rather calculated based on the initial SAC acidity and the loss of acidity after exposure to the ionic liquid (shown as "difference" in table 4.1). Although quantitative data regarding loss of acidity after

exposure to the ionic liquid was not obtained, a color change for pH paper immersed in the ionic liquid after SAC removal verified the presence of increased ILM acidity after SAC removal.

Table 4.1 acidity of various SACs before and after exposure to ILM

Catalyst	SAC Before IL[a]	SAC After IL[a]	Difference[b]
	mmol H^+ on catalysts		
SZ	0.27	0.19	0.08
HY	0.73	0.29	0.44
HZSM-5	0.28	0.05	0.23
Nafion® SAC-13	0.15	0.05	0.10
Nafion® NR50[c]	0.16	0.05	0.11
Nafion® NR50[d]	0.40	0.15	0.25

[a]determined by titration of the solid acid catalyst
[b]calculated mmol H^+ added to the reaction medium
[c]based on 10 min NaOH mixing time
[d]based on 2 hr NaOH mixing time

Nafion® SAC-13 and HZSM-5 had less than 0.05 mmol H^+ remaining on the solid after being exposed to the

129

ILM. On the other hand, sulfated zirconia and HY lost only about half of their original acidities (mmol H^+). Based on the data from sections 3.4 and 3.5, it can be hypothesized that the most likely cause for the loss of acidity from these solid acids would be an ion exchange mechanism between the imidazolium cation ($EMIM^+$) and H^+. While having the ability to ion exchange could increase the activity of the catalyst by making the protons more readily available, it also decreases reusability. The protons removed from the solid remain in the ILM and thus would not be present in the used solid catalyst.

Compared to the other SACs, Nafion® NR50 interacted differently with the ILM. It swelled, exposing additional internal acid sites. Therefore, the ionic liquid cation could exchange with internal protons and the amount of this exchange could increase with time, depending on the degree of swelling. It was hypothesized that the same process could occur when Nafion® NR50 was exposed to the NaOH titrant. To test this, fresh and ILM exposed (1 hr) Nafion® NR50 were titrated using both a 10 min and 2 hr NaOH mixing time. A 10 min NaOH mixing time should permit titration of easily accessed surface acid sites and allow for

minimal swelling. Based on solid acidity titrations with a 10 min NaOH mixing time, Nafion® NR50 was found to start with 0.16 mmol H^+ and retain only 0.05 mmol H^+ after exposure to [EMIM]Cl. The 2 hr NaOH mixing time should allow for swelling, permitting access to internal acid sites. Based on solid acidity titrations using a 2hr NaOH mixing time, it was found that fresh Nafion® NR50 had 0.40 mmol H^+ and 0.15 mmol H^+ was still available after being exposed to [EMIM]Cl. Thus, the longer exposure to NaOH allowed for more access to internal acid sites. Based on these results, it was concluded that the amount of time Nafion® NR50 spends in an ion exchange capable medium would determine the amount of available protons.

4.2.1 EMIM$^+$ Ion Exchange in Zeolites

Unlike the other solid acid catalysts, zeolites have specific pore sizes, and most acid sites are located within these size restricted pore openings. Based on the increased activity of zeolites for starch hydrolysis in the presence of ion exchange cations compared to a water only medium (section 3.5), in addition to the results presented in this section, it

was hypothesized that EMIM⁺ could fit into the pores of the zeolites, allowing for ion exchange release of protons. The crystal size of EMIM⁺ was determined using CCDC Conquest 1.14 software and the Cambridge Structural Database and was performed by Douglas Powell, Ph.D. (Crystallography Lab, University of Oklahoma). The distances reported were based on measurements from the nuclei centers and measurements taking hydrogen into account (figure 4.1, table 4.2). Because ionic liquids are salts in liquid form, the crystal size of EMIM⁺ was used to approximate the actual size of EMIM⁺ in liquid form.
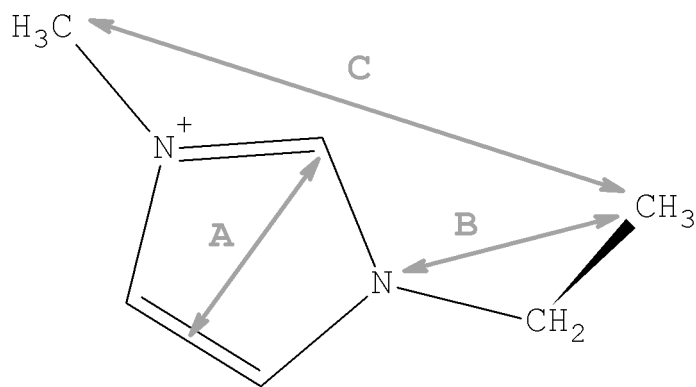
Figure 4.1 dimensions of crystal EMIM⁺

Table 4.2 dimensions of crystal EMIM

Distance	Crystal Measurement[a] (Å)	Estimated Actual Measurement[b] (Å)
A	2.2–2.25	3.5
B[c]	1.3	2.5–3
C	5.7–5.8	6–6.5

[a]measured from the nuclei center
[b]takes into account hydrogens and "puffiness" of molecules
[c]thickness

Based on the crystal size (accounting for hydrogen) of $EMIM^+$ (3.5 x 3 x 6.5 Å) and the size of the pore openings for HY (7.4 x 7.4 Å) and HZSM-5 (5.3 x 5.6 Å), it seems reasonable that an $EMIM^+$ ion exchange mechanism is possible with zeolites. Based on these dimensions, $EMIM^+$ should be able to fit into the HY pore at any angle. The smaller pore size of HZSM-5, on the other hand, will only allow $EMIM^+$ to fit in a specific orientation. Based on these assumptions, a faster rate of proton diffusion out of the pores and into the ILM would be expected for HY.

4.3 Ethyl Acetate Hydrolysis in [EMIM]Cl medium

The water tolerance of SACs was tested in chapter 3 by using ethyl acetate as the hydrolysis substrate. To allow for direct comparison with SAC hydrolysis results obtained in aqueous media, ethyl acetate hydrolysis was performed in the ILM (experiments were conducted by Dalia Maraoulaite, Department of Chemistry, University of Oklahoma, 2011). Based on the postulated ion exchange mechanism, it was expected that the activities for ethyl acetate hydrolysis catalyzed by zeolites would significantly increase in the ILM, as compared to aqueous media. In an aqueous media (chapter 3), ethyl acetate could only access zeolite acid sites after passing through 5-7 Å pores. When sodium ions were added, the zeolite protons were released into the medium. Ionic liquids consist entirely of cations and anions, so ion exchange would be expected to be an important process when most of the reaction medium consists of ions. The ionic liquid medium (ILM) consisted of 2 g of [EMIM]Cl mixed with 0.3 mL water (needed for hydrolysis reaction). The ILM (0.4 mL) was placed in the quartz sample tube of the mini-reactor, and ethyl acetate (30 μL), propanol (15

μL), and the SAC (0.01 g) were added. Propanol was used as an internal standard to quantify ethyl acetate conversion. Testing only propanol in the ILM yielded no additional GC peaks, verifying that it did not react under these conditions. Each sample was pressurized to 60 psi with nitrogen gas and then heated at 105°C for 1 hr. After 1 hr, the mini-reactor vessel was cooled in a cold-water bath. The quartz sample tube was removed from the mini-reactor vessel and centrifuged prior to analysis by GC-FID. Because the ionic liquid produced a large peak that overlapped the hydrolysis product peaks, the injector temperature was reduced to 130°C. Lowering the injector temperature minimized volatilization of the ionic liquid, effectively trapping it within the GC injector and eliminating the representative chromatogram peak. All other GC-FID parameters were the same as those used for ethyl acetate hydrolysis in aqueous media (described in section 2.5.3). The solid acid catalysts that were tested included: HY, HZSM-5, and sulfated zirconia.

While a loss of ethyl acetate was observed for HZSM-5, HY, and sulfated zirconia (SZ), ethanol and acetic acid were not detected in significant quantities

and results for ethyl acetate hydrolysis in [EMIM]Cl were not reproducible. The lack of chromatographic peaks corresponding to ethanol and acetic acid suggests that observed ethyl acetate losses were not associated with hydrolysis. Instead, ethyl acetate loss may have been caused by its volatility and the difficulty in dissolving it in the ionic liquid. Visual inspection of the sample tube revealed a small volume loss after heating, which may have been caused by ethyl acetate volatilization. In addition, mixing ethyl acetate and [EMIM]Cl and then leaving the mixture undisturbed for several minutes resulted in separation into two layers. In fact, Zhang et al. utilized various 1-alkyl-3-methylimidizolium chloride (alkyl = butyl, hexyl, octyl) ionic liquids for the separation of ethyl acetate and ethanol, because ethyl acetate was found to be immiscible with these ionic liquids [164, 165].

If ethyl acetate was not completely dissolved in [EMIM]Cl, samples would not be homogenous, which would result in inconsistent results. Furthermore, it would be very difficult to achieve ethyl acetate hydrolysis when it was not dissolved. This could explain the poor conversions to ethanol and acetic acid. Based on these

results, the use of ionic liquid as a medium for ethyl acetate hydrolysis was not deemed to be viable. Therefore, the effects of changing the hydrolysis medium from aqueous to ionic liquid could not be studied by using ethyl acetate hydrolysis.

4.4 Polysaccharide Hydrolysis in [EMIM]Cl

Although ionic liquids can dissolve cellulose, addition of water to the ionic liquid reduces solubility and causes precipitation [59, 154]. However, water is a necessary reactant in the hydrolysis reaction. Therefore, it was important to find the minimum amount of water required for complete hydrolysis as well as the maximum amount of water that could be added to the ionic liquid medium (ILM) without causing cellulose precipitation. The minimum amount of water required for polysaccharide hydrolysis, assuming that glucose was the only product, was calculated by using equation 4.1. The molecular weight of the repeat unit (MW_{RU}=162 g mol^{-1}) was determined by subtracting the molecular weight of water (MW_{water}=18 g mol^{-1}) from the molecular weight of glucose ($MW_{glucose}$=180 g mol^{-1}). Because cellulose is composed of dehydrated glucose

repeat units, dividing the weight of cellulose used (0.1 g) by the MW_{RU} yields the moles of the repeat unit that can be obtained if cellulose is completely hydrolyzed. In order to make one mole of glucose, one mole of water is needed. Based on equation 4.1, a minimum of 0.01 mL water would be required for hydrolysis of 0.1 g of cellulose.

Equation 4.1

$$\frac{0.1\,g \quad \text{cellulose}}{162\frac{g}{mol} \quad \text{repeat unit}} \times \frac{1 \text{ mol glucose}}{1 \text{ mol repeat unit}} \times \frac{1 \text{ mol } H_2O}{1 \text{ mol glucose}} \times \frac{18\,g}{mol} H_2O \times \frac{1\,mL}{g} H_2O$$

The maximum amount of water that could be added without causing cellulose precipitation was determined by a series of qualitative experiments. Using a temperature controlled oil bath, cellulose (0.1 g) was dissolved in [EMIM]Cl (2 g) with constant stirring at 120°C. After dissolution, water was added in various amounts, either incrementally or all at once. Samples were then visually inspected for cellulose precipitation. Under these conditions, it was determined that when water was added in small increments (c.a. 0.05 mL), up to 0.35 mL of water could be added without causing cellulose precipitation.

Based on these findings, it was determined that 0.3 mL of water would be added to the ILM to facilitate hydrolysis without causing cellulose precipitation.

Polysaccharide hydrolysis samples were prepared by dissolving the polysaccharide (0.1 g) in [EMIM]Cl (2 g) using a temperature controlled oil bath to maintain a temperature of 120°C. After complete dissolution, the temperature was lowered to 105°C and distilled water (0.3 mL) was added in increments of 0.05 mL. After a homogenous mixture was obtained, the SAC (0.25 g) was added to the sample while maintaining constant stirring. The hydrolysis reaction was carried out for 3 hours and the solution was sampled for analysis every 15 minutes. For each analysis, an aliquot (0.05 mL) was removed from the hydrolysis sample and tested for reducing sugars with the Benedict's test (described in section 2.4). The percent total glucose yield (%TGY) was calculated based on equation 3.2 (section 3.3.3).

4.4.1 Solid Acid Catalysis in [EMIM]Cl

The SACs tested included: sulfated zirconia, HY, HZSM-5, Nafion® SAC-13, and Nafion® NR50. Cellulose hydrolysis percent total glucose yield (%TGY) are

listed in table 4.3 and errors are based on triplicate data with the greatest error being 17%. It can be speculated that the large errors stem from the viscosity of the ionic liquid, which made reproducible aliquot removal difficult. Visual inspection of the pipet indicated that residual sample remained after sampling. For these reasons, attempts were made to perform cellulose hydrolysis in a consistent manner. As a blank measurement, cellulose hydrolysis was also performed at 105°C for 2hrs without a catalyst, and no reducing sugars were detected.

Table 4.3 cellulose hydrolysis in [EMIM]Cl

Time (hr)	HY	HZSM-5	SZ	SAC-13	NR50
		% total glucose yield			
0.25	29±8	9±9	8±8	2±3	6±5
0.50	55±8	20±6	9±9	6±2	21±2
0.75	62±8	36±7	10±10	10±2	40±8
1.00	68±10	46±9	11±9	13±1	54±4
1.25	65±5	59±12	16±13	16±4	67±8
1.50	62±2	59±9	16±14	18±2	73±7
1.75	59±1	70±16	22±14	25±5	76±6
2.00	54±2	69±12	25±12	27±2	81±5
2.25	55±3	70±17	26±11	32±3	77±9
2.50	49±2	69±8	31±15	33±2	76±9
2.75	48±1	73±9	33±15	32±10	73±12
3.00	43±1	76±12	35±14	36±1	70±10

When the catalyst weight was kept constant, the relative order of SAC activity for cellulose hydrolysis in [EMIM]Cl was found to be HY > HZSM-5 and Nafion® NR0 > Nafion® SAC-13 and sulfated zirconia. This order is the reverse of what was found for starch hydrolysis in aqueous media (section 3.3.4): sulfated zirconia > Nafion® SAC-13 and Nafion® NR50 > HZSM-5 > HY. Ion exchange effects introduced by the ionic liquid cation ($EMIM^+$) may explain these results. In fact, trends for the production of glucose by catalysis with a constant weight of the SACs could be separated into two categories.

Group 1 consists of HY, HZSM-5, and Nafion® NR50 (figure 4.2); all of which can exhibit increased hydrolysis when difficult to reach surface bound protons are released into solution by ion exchange. Acid sites of zeolites are located within size restricting pores that are too small for large polysaccharide molecules to access. Swelling of Nafion® NR50 causes the surface area of the pellets to increase, exposing internal acid sites. It should be noted that Nafion® NR50 swells in both ionic liquids [166] and water [85]. However, the presence of cations

142

from the ionic liquid allow for ion exchange with exposed internal acid sites revealed as a result of swelling, thereby increasing the number of protons participating in the hydrolysis reaction. Previously, Dwiatmoko et al. studied the effect of [BMIM]Cl on Nafion® NR50, and suggested that the activity for cellobiose hydrolysis significantly increased in the presence of [BMIM]Cl when compared to an aqueous medium [166]. This increased activity was attributed to a BMIM$^+$ induced release (e.g. ion exchange) of protons from the resin; which had been made more accessible by swelling [166]. In both the case of zeolites and Nafion® NR50, ion exchange with EMIM$^+$ can lead to release of H$^+$ to the reaction medium, which likely would have been inaccessible without ion exchange.

Group 2 consists of sulfated zirconia and Nafion® SAC-13 (figure 4.2); for which most acid sites are on the exterior surface of the catalyst and therefore should be accessible to the polysaccharide. Although the acid sites on these catalysts should also be subject to ion exchange, their activities may not substantially change because the catalyst surfaces were already more available to the hydrolysis substrate in

water. Consequently, ion exchange with EMIM$^+$ would not be expected to dramatically change polysaccharide hydrolysis activity. Thus, the change in the order of activity for the SACs in ionic liquid media compared to aqueous media may be explained by solution acidity changes resulting from ion exchange.
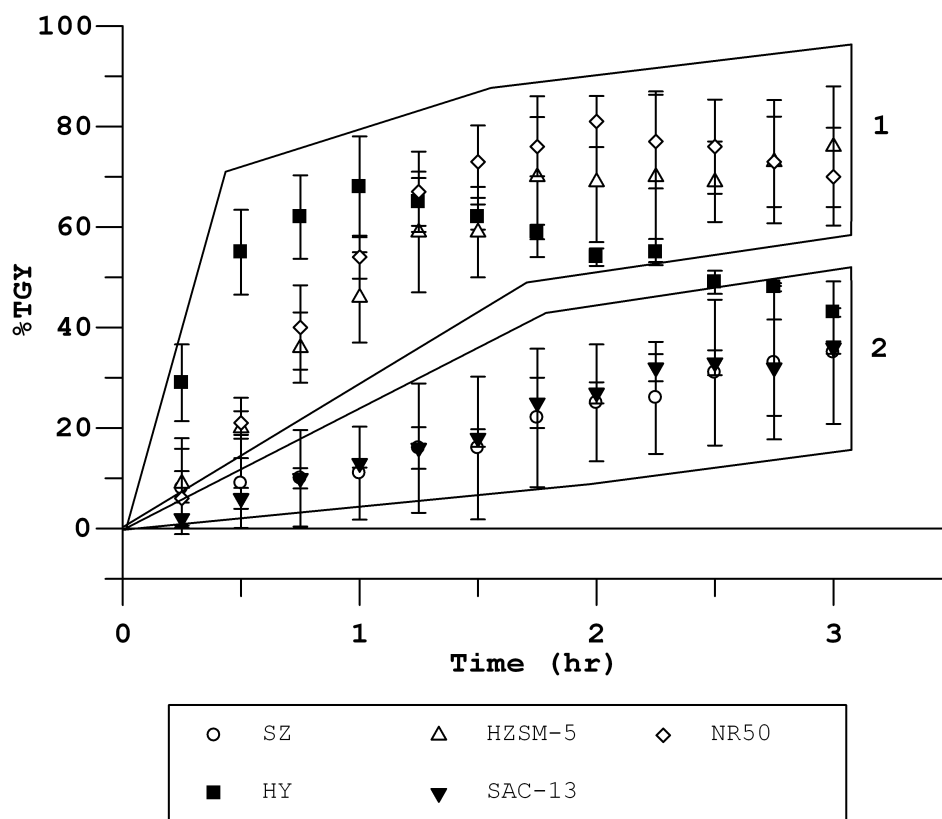
Figure 4.2 cellulose hydrolysis in ILM at 105°C with various solid acid catalysts

It should also be pointed out that after ca. 1hr, the activity of HY appears to cross from group 1 to

group 2. However, this apparent decrease is simply a loss of glucose caused by degradation. Visual inspection of the sample indicated the appearance of a brown color, which became darker with increasing reaction time. This brown color was likely associated with glucose degradation products. Although not as obvious as for HY, Nafion® NR50 and HZSM-5 profiles also exhibited decreases after ca. 1.5 hours. Visual inspection of these samples revealed slight brown coloring after 3 hours at 105°C. It is unclear why the rate of glucose degradation varied significantly for these catalysts. However, it can be speculated that because HY was a better catalyst for hydrolysis, it was also a better catalyst for glucose decomposition. Nafion® SAC-13 and sulfated zirconia exhibited lower %TGY, and glucose degradation was difficult to detect either by a decrease in %TGY or visually by formation of a brown color.

Although the crystal structures of starch and cellulose differ, once dissolved, the glycosidic bonds of both cellulose and starch should be hydrolyzed with relatively equal ease. Therefore, similar SAC activities for starch and cellulose hydrolysis in

[EMIM]Cl would be expected. To verify this prediction, starch hydrolysis was performed in a similar manner and under the same reaction conditions as cellulose hydrolysis. As expected, the same trends were seen for both starch and cellulose hydrolysis in [EMIM]Cl (figure 4.3), where two groups could be designated based on acid site availability (e.g. mostly internal and mostly external).
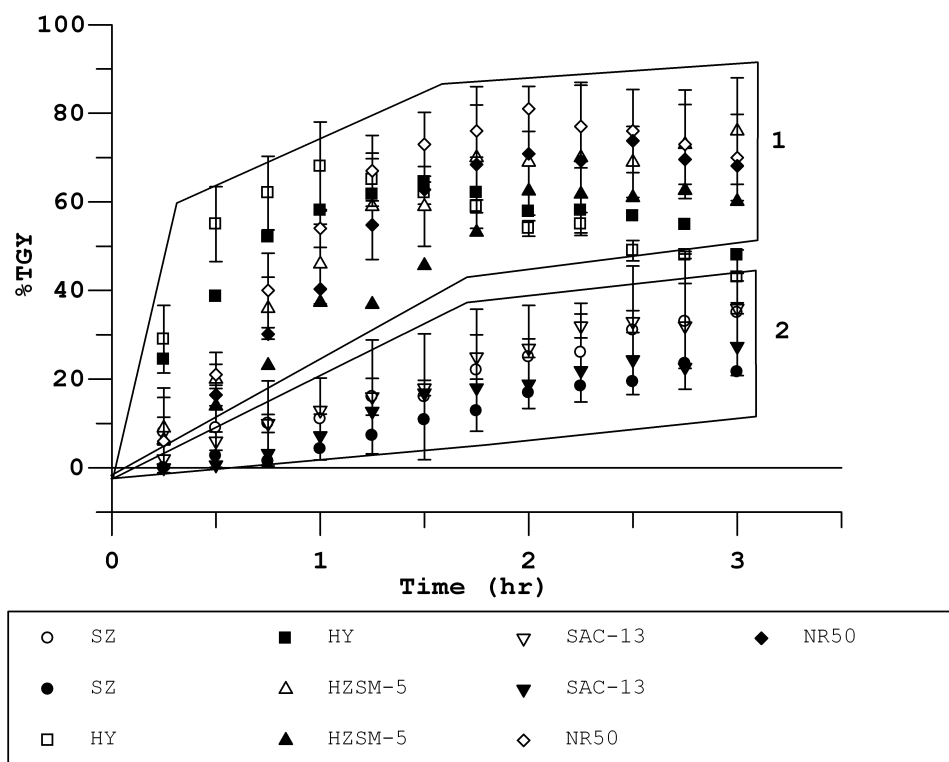
Figure 4.3 starch hydrolysis (black) as compared to cellulose hydrolysis (white) in ILM; error bars are on cellulose hydrolysis data

Although the amount of catalyst used (0.25 g) was kept constant, the amount of acid (mmol H^+ g^{-1}) varied for each catalyst. To compensate for this, the %TGY was scaled by the mmol H^+ employed. Scaled error bars on average ranged from 10-50, with a few outliers, but were omitted from plotted data for clarity (figure 4.4). Sulfated zirconia had about double the scaled error bars compared to the other SACs tested, and it is unclear as to why this may have occurred. Data for HY after 1hr was omitted due to the significant decrease in reducing sugar concentration. Because starch hydrolysis provided indistinguishable results to cellulose hydrolysis using the same SACs, scaled data for starch hydrolysis is not shown. The scaling values used here should not be confused with those used for ethyl acetate and starch hydrolysis in an aqueous medium, where the mmol H^+ was based on what was available in the fresh SAC, and not what was provided to the medium. Because SACs in water only media did not lose acidity to the hydrolysis medium, scaling values were determined by titration of fresh SACs (discussed in chapter 3). On the other hand, SACs in ILM did lose acidity to the hydrolysis medium.

Therefore, the scaling values used here accounted for the mmol H^+ based on what was provided to the medium. The mmol H^+ used for scaling was taken from table 4.1 (section 4.2), which lists the mmol H^+ provided by the various solid acid catalysts when exposed to [EMIM]Cl. To calculate the amount of H^+ transferred from the SAC to the reaction mixture, the mmol H^+ determined for SACs that had been exposed to [EMIM]Cl was subtracted from the mmol H^+ found for fresh SACs. The values reported in table 4.1 provided the following calculated amounts of solution acidity (mmol H^+) that were used for scaling the cellulose hydrolysis results from table 4.3: sulfated zirconia (0.08), HY (0.43), HZSM-5 (0.23), Nafion® SAC-13 (0.10), and Nafion® NR50 (0.25); where the values in parentheses are mmol H^+ provided to the reaction mixture. Under these conditions, similar activity was seen for all SACs when used for cellulose hydrolysis in [EMIM]Cl (figure 4.4). Based on these results, it was hypothesized that the total glucose yield from polysaccharide hydrolysis was a function of the solution H^+ concentration.
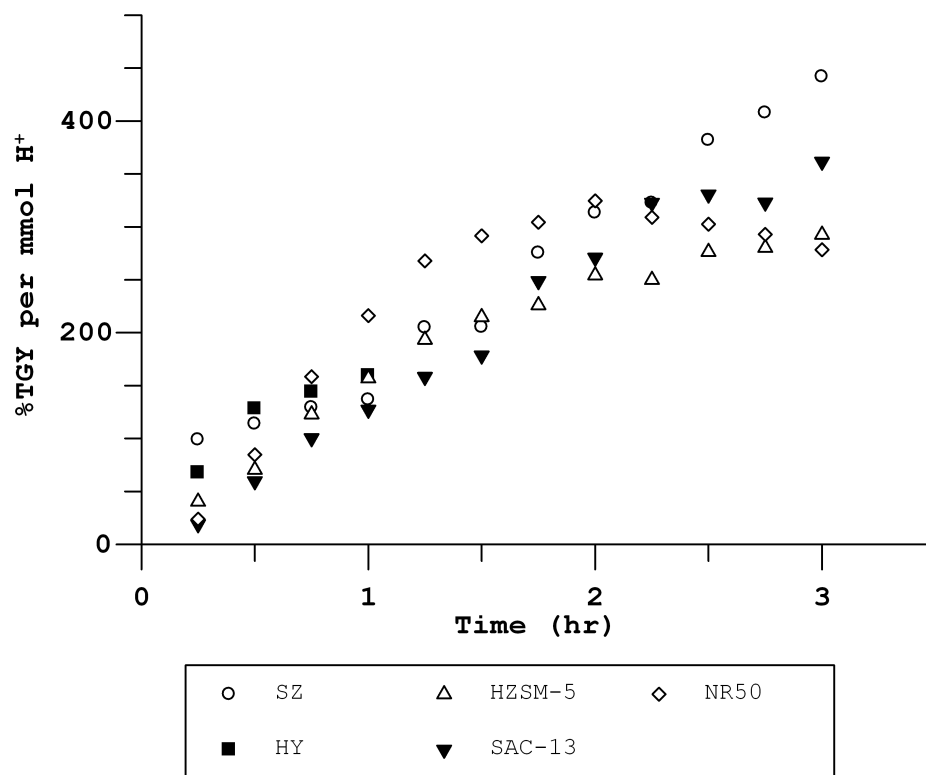
Figure 4.4 %TGY from cellulose hydrolysis scaled by the mmol H$^+$ employed in the ILM

SACs should perform similarly to a liquid acid when the values are scaled by the solution acidity, if the hypothesized dependence of solution H$^+$ concentration is true. To test this, hydrochloric acid (HCl) and HY were evaluated for cellulose hydrolysis in [EMIM]Cl under the same reaction conditions (105°C, 0.1 g cellulose, 2 g IL). Results are shown in figure 4.5. Errors were estimated to be ca. 10% from the original cellulose hydrolysis data in table 4.3, but were

149

omitted in the plotted data for clarity (figure 4.5). The %TGY values from cellulose hydrolysis were scaled based on the acid amount added to the ILM: HY (0.049 mmol H^+) and HCl (0.056 mmol H^+). Initially, hydrochloric acid had a slightly higher activity than HY (figure 4.5). Similar results have been reported when hydrochloric acid was compared to Amberlyst 15 DRY, which was shown to slowly release protons into the media within the first hour [158]. The slight differences seen here could also be due to the rate at which protons are released from the HY pores by ion exchange.
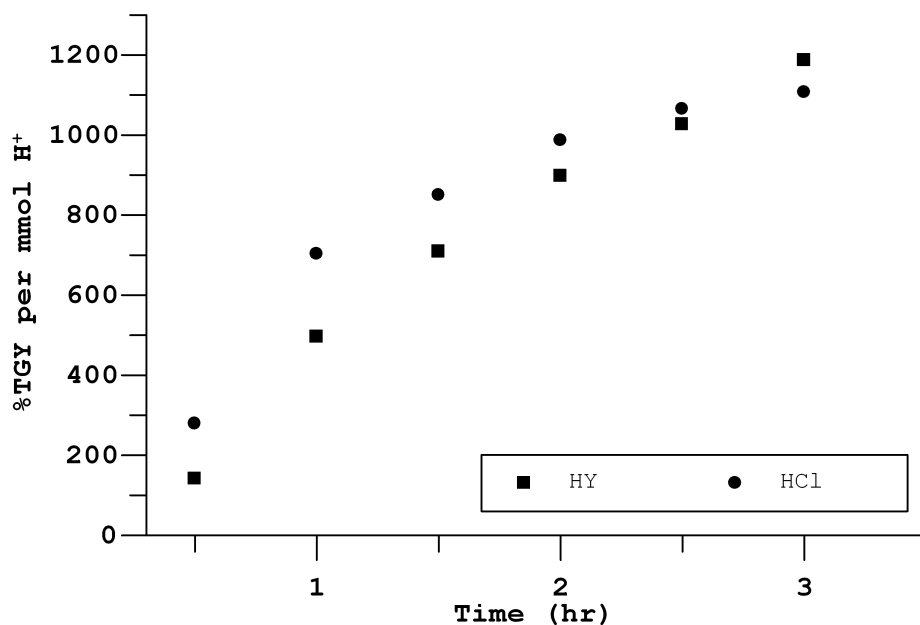
Figure 4.5 comparison of HY and HCl catalyzed cellulose hydrolysis scaled by the acid employed in the ILM

Based on these results, it would seem that after the proton is released from the surface of the solid catalyst into the ILM, it behaves similarly to hydrochloric acid catalysis. Whereas the amount of starting acidity does not appear to play as large of a role as initially anticipated for cellulose hydrolysis activity in [EMIM]Cl, the availability for the acidic proton to ion exchange with $EMIM^+$ appears to be a major contributor. Thus, solid acid catalyts are not equal for cellulose hydrolysis activity in [EMIM]Cl when the mmol H^+ on the fresh SAC is constant.

4.4.2 XRD Analysis of zeolites

Although all evidence thus far points to an ion exchange facilitated release of protons to increase catalytic activity of zeolites for polysaccharide hydrolysis, structural damage could also result in increased catalytic activity. As previous stated, the acid sites of zeolites are located within size restricting pores. If these pores are modified or destroyed, acid sites could become more readily available. X-ray diffraction (XRD) was used to determine if the structures of HY and HZSM-5 were modified after exposure to $EMIM^+$. Both fresh and spent catalysts (e.g. before and after cellulose hydrolysis in [EMIM]Cl respectively) were analyzed by Dr. Matt Miller at the Devon Energy NanoLab at the University of Oklahoma (Norman, OK, USA), on a Rigaku Ultima IV X-ray diffractometer. Samples were placed into a dry powder cavity without grinding and no solvents were used for mounting. The instrument settings were as follows: X-ray type (Cu Kα), tube voltage (40 kV), tube amperage (44 mA), tube load (1.26 KW), slit setting (variable slit), irradiated sample area (302 mm^2), step size (0.02° 2Θ), count time (2 seconds), 2Θ collection range

(2–70° 2Θ), sample rotation (12 rpm). Pattern fitting and mineral assignment were conducted by using MDI JADE 9 software.

The nearest match in the NanoLab's powder diffraction file database for HZSM-5 was card number 00-045-0191, which corresponded to synthetic ZSM-5 zeolite (thallium aluminum silicate hydrate), indicating an MFI framework. The difference in the charge balancing cation of TlZSM-5 (e.g. reference sample) and HZSM-5 (e.g. actual sample) should not significantly affect the structure of sample (e.g. MFI framework). Although the percent match to this database card was not provided, it was the closest match. These results indicated that the synthesized HZSM-5 did in fact have an MFI framework. Comparing the diffraction patterns for the fresh (figure 4.6A) and spent (figure 4.6B) HZSM-5 revealed a 98% similarity as calculated by MDI Jade version 9 software. This indicated that no significant structural changes were observed after HZSM-5 zeolite was exposed to [EMIM]Cl under polysaccharide hydrolysis conditions.
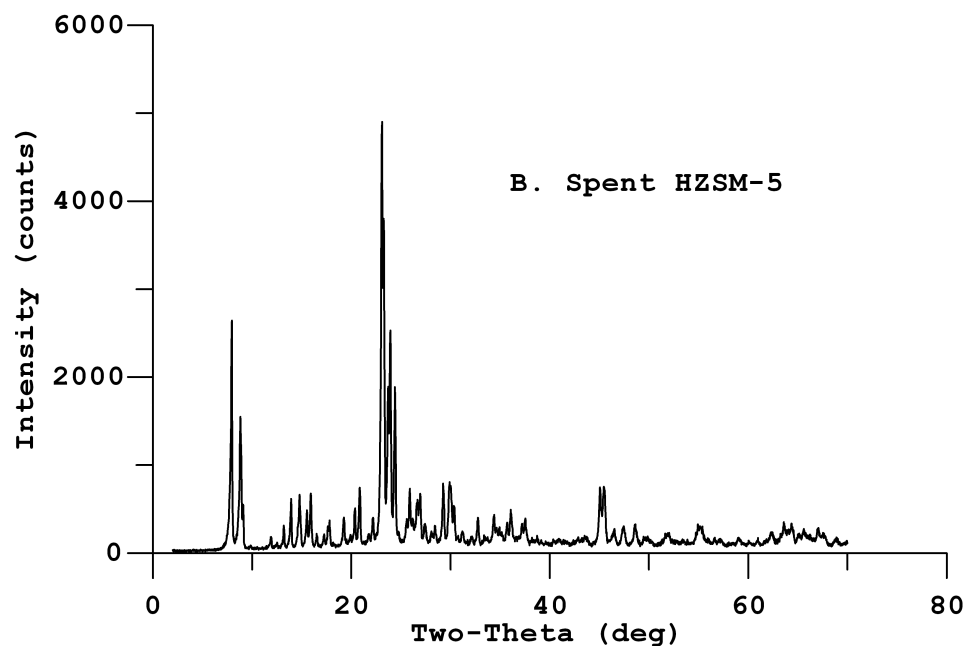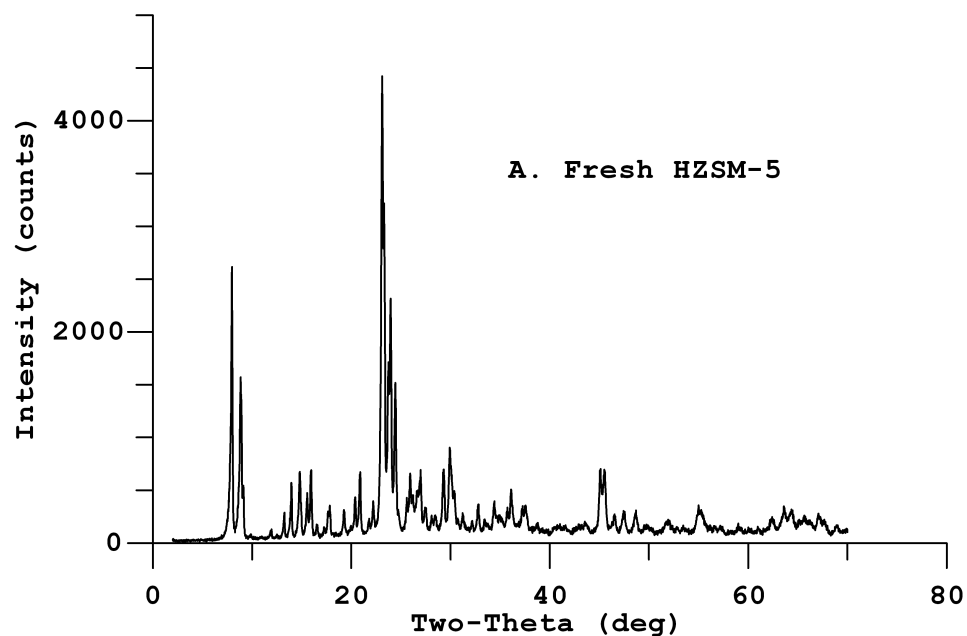
Figure 4.6 XRD spectra of A) fresh HZSM-5 catalyst and B) spent HZSM-5 catalyst

The nearest match in the NanoLab's powder diffraction file database for HY was card number 00-

039-1380, which corresponded to sodium-faujasite (NaY zeolite), indicating a faujasite framework; the percent match to this database card was also not provided. The diffraction patterns for fresh (figure 4.7A) and spent (figure 4.7B) HY show a 95% similarity as calculated by MDI Jade version 9 software, indicating that no significant structural changes occurred when HY was exposed to [EMIM]Cl under polysaccharide hydrolysis conditions. Therefore, it can be concluded that the increased activity of the zeolites in the ionic liquid was not due to catalyst structural changes.
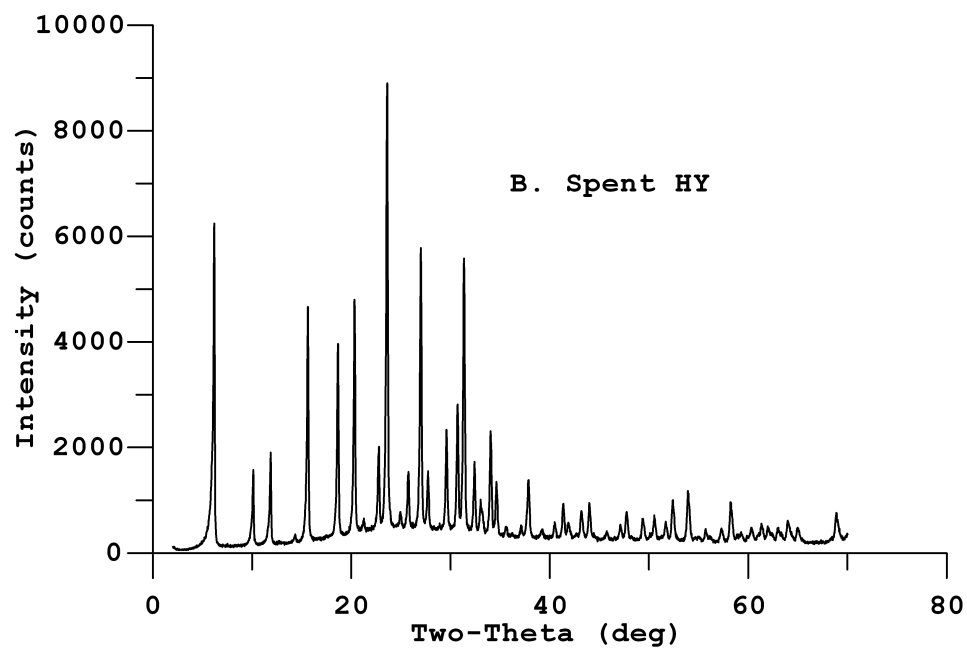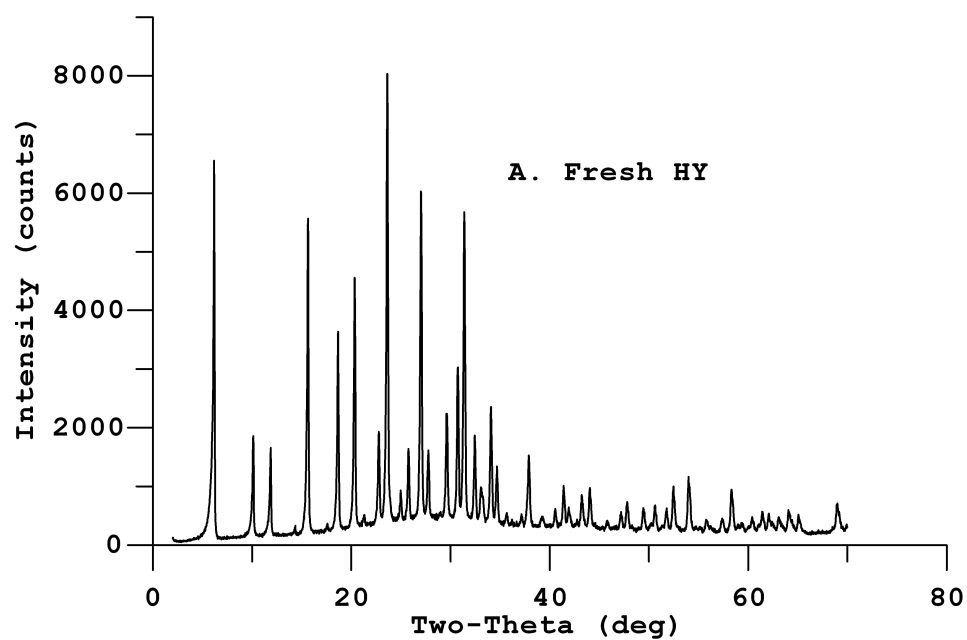
Figure 4.7 XRD spectra of A) fresh HY catalyst and B) spent HY catalyst

4.5 Catalyst Reusability for Cellulose Hydrolysis in [EMIM]Cl

Having the ability for SACs to be reused would make this method more cost effective than using liquid acid catalysis. However, ion exchange with $EMIM^+$ will decrease the catalysts abilities to be reused. Based on the results from table 4.1, there were various acid amounts (mmol H^+) remaining on the solid of the SACs after exposure to [EMIM]Cl. To determine reusability for each SAC, cellulose hydrolysis in [EMIM]Cl was performed with the same catalyst three separate times. The method used for preparing the hydrolysis samples was similar to that described in section 4.4. After each hydrolysis reaction, the solid acid catalyst was removed by filtering, rinsed with distilled water, and dried at room temperature. Because recovery was always less than 100%, the remaining catalyst was weighed (R.SAC) and the resulting weight was used to scale the amounts of ionic liquid (R.IL, equation 4.2), water (R.H_2O, equation 4.3), and polysaccharide (R.Poly, equation 4.4) that would be used for the next reaction in order to maintain the same relative concentrations of reactants. This method was repeated until the same

SAC was used three times for cellulose hydrolysis in [EMIM]Cl at 105°C.

$$\frac{2\,g\ IL}{0.25\,g\ SAC} \times g\ R.SAC = g\ R.IL \qquad \textbf{Equation 4.2}$$

$$\frac{0.3\,mL\ H_2O}{0.25\,g\ SAC} \times g\ R.SAC = mL\ R.H_2O \qquad \textbf{Equation 4.3}$$

$$\frac{0.1\,g\ Polysaccharide}{0.25\,g\ SAC} \times g\ R.SAC = g\ R.Poly \qquad \textbf{Equation 4.4}$$

For starch hydrolysis in an aqueous medium, it was found that the activity of sulfated zirconia significantly decreased with each repeated use. In contrast, for the ILM, it was found that sulfated zirconia was inactive when used a second time for cellulose hydrolysis. These results were not expected based on the results listed in table 4.1 (section 4.2), which show that fresh sulfated zirconia contained 0.27 mmol H^+, and after exposure to ionic liquid, 0.19 mmol H^+ still remained on the catalyst. The HZSM-5 and Nafion® SAC-13 catalysts were also not reusable for cellulose hydrolysis in [EMIM]Cl, which was consistent with the results reported in table 4.1 (section 4.2).

HZSM-5 and Nafion® SAC-13 were found to have only 0.05 mmol H^+ remaining on the solid after exposure to [EMIM]Cl, which was apparently not enough to provide detectable total glucose yield.

Although HY could be reused, the catalytic activity decreased with each consecutive use (figure 4.8). The decreased catalytic activity could be attributed to the loss of acidity from the solid. Titrations (method described in section 2.3) of the solid catalyst before each consecutive use indicated decreasing amounts of acidity on the solid: 1st use (0.37), 2nd use (0.16), 3rd use (0.11), where the values in parentheses are mmol H^+.
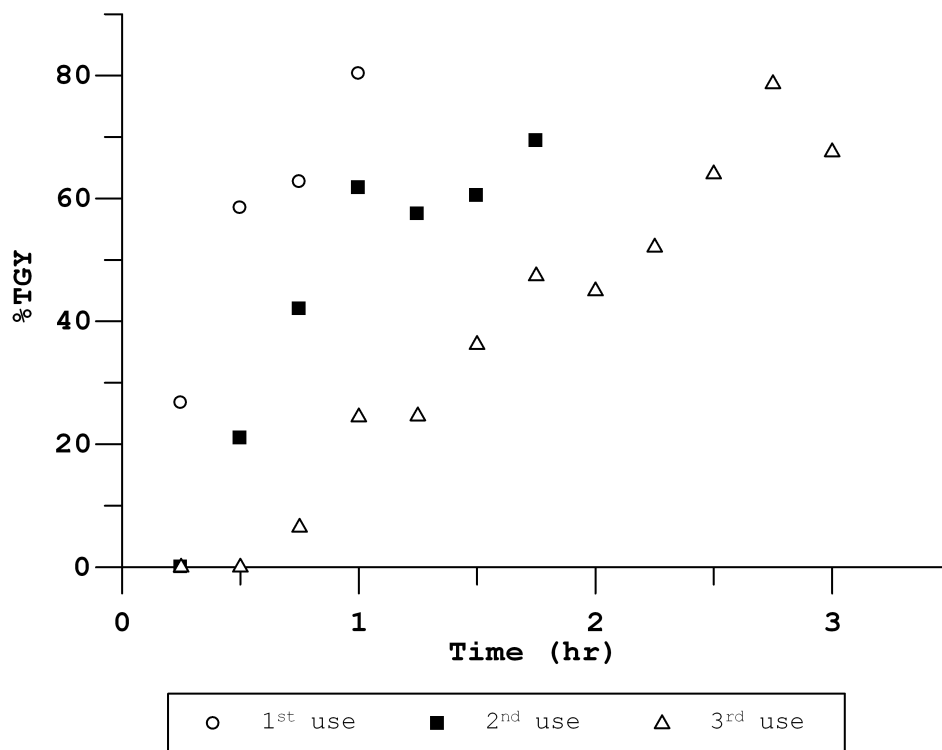
Figure 4.8 reusability of the HY catalyst for cellulose hydrolysis in ILM

Scaling the data from figure 4.8 by the mmol H^+ employed for each consecutive use indicated a similar HY activity after repeated use for cellulose hydrolysis in [EMIM]Cl (figure 4.9).
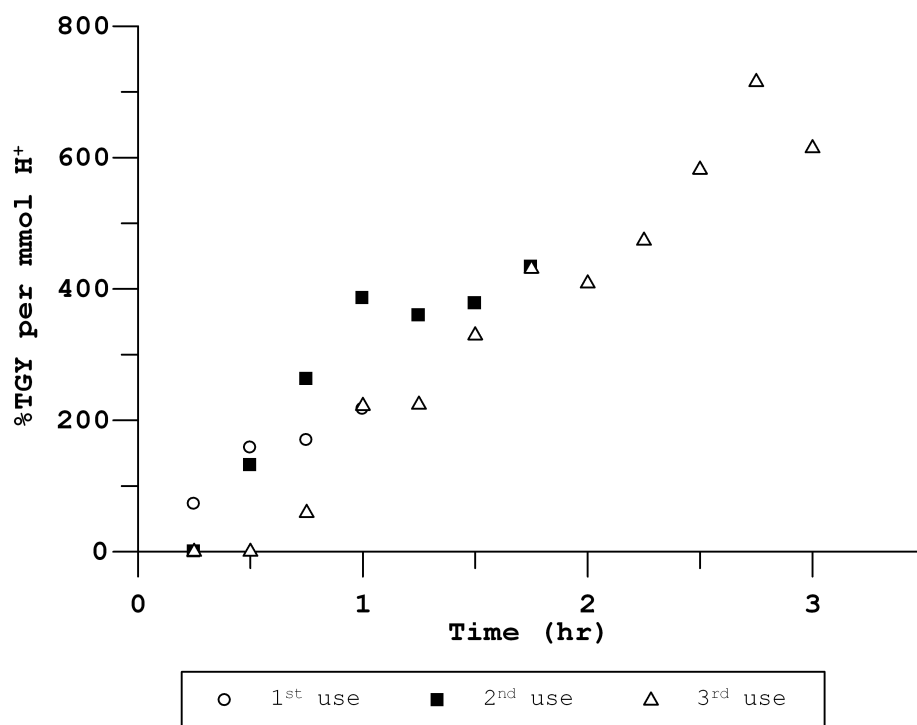
Figure 4.9 reusability of the HY catalyst for cellulose hydrolysis in ILM scaled by the mmol H$^+$ employed

Although Nafion® NR50 was capable of being used a second time, there was a significant induction period (1 hr) before any acidity was detected (figure 4.10), and no activity was detected for a third use after 2 hours. Induction periods for Nafion® NR50 have been previously attributed to the time required for the polymer to swell, which would allow ion exchange facilitated release of H$^+$ into the medium [166]. No induction period was observed for hydrolysis with fresh Nafion® NR50, which may be explained by the presence of

easily accessible acid sites on the surface. However, when used a second time, these acid sites may not be available and internal acid sites that are available only as a result of swelling may be responsible for catalyzing hydrolysis. Titration (method described in section 2.3) of the solid before each consecutive run indicated decreasing amounts of available acidity: 1st use (0.40), 2nd use (0.15), 3rd use (0.05), where the values in parentheses are mmol H^+. Based on these results, it appeared that 0.05 mmol H^+ did not provide enough acidity for detectable conversions of cellulose when Nafion® NR50 was used a third time. It may also be possible that the acid sites could be titrated by OH^-, but could not be accessed for ion exchange by the relatively larger $EMIM^+$ molecule.
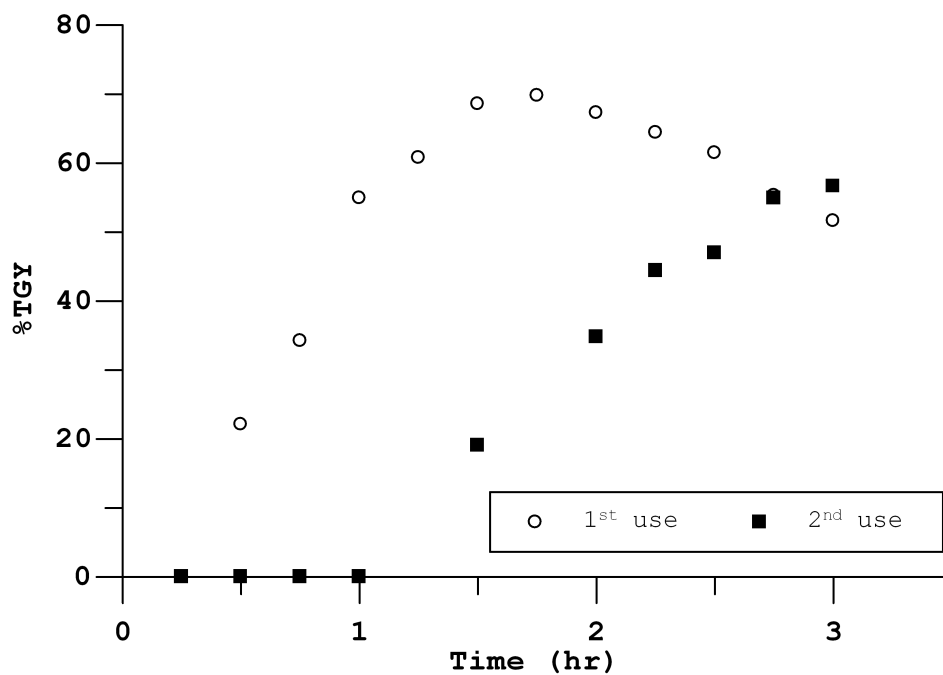
Figure 4.10 reusability of Nafion® NR50 for cellulose hydrolysis in ILM

Scaling only the linear portion of the data reported in figure 4.10 by the mmol H^+ showed similar activity for each consecutive use (figure 4.11). Based on these results, it could be concluded that the decreased activity was most likely due to a decreasing reaction media acid concentration.
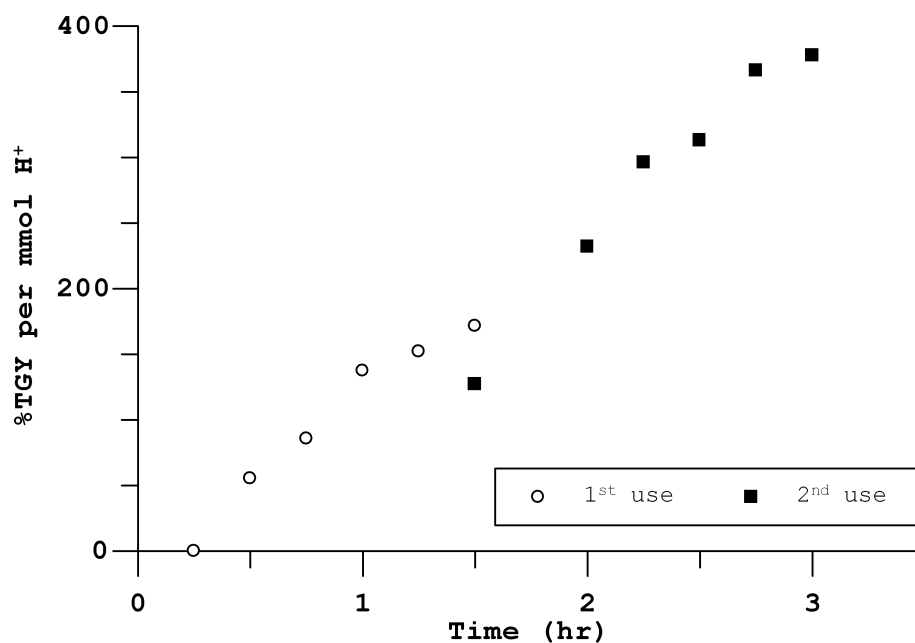
Figure 4.11 reusability of Nafion® NR50 for cellulose hydrolysis in ILM scaled by the acid amount employed

4.6 Regeneration of Zeolites

The zeolites tested were structurally different from the other SACs tested, in that their acid sites were located within size restricting pores. Although they were virtually inactive for starch hydrolysis in water, the addition of cations that could ion exchange with catalyst H^+ (e.g. $EMIM^+$) allowed for substantial cellulose hydrolysis activity. However, this also resulted in a significant loss of spent catalyst acidity. Studies were carried out to determine if this

acidity loss could be reversed and if the catalysts could be regenerated.

HY and HZSM-5 regeneration was tested by treatment with ammonium nitrate (NH_4NO_3), which was used for the preparation of the acid forms from the corresponding sodium form zeolites (procedure described in sections 2.3.3 and 2.3.4). In this case, NH_4^+ could ion exchange with the $EMIM^+$ found in the spent catalysts. The regeneration procedure consisted of heating the NH_4^+ treated SACs, which will evolve NH_3, leaving H^+ as the charge balancing cation. These studies were started by using fresh catalyst for cellulose hydrolysis in [EMIM]Cl, as described in section 4.4, for 2hrs at 105°C. The spent catalyst was then filtered, rinsed with distilled water, and dried at room temperature. Spent HY and HZSM-5 were separately placed in an ammonium nitrate solution (1 M) at room temperature with constant stirring over night. The catalysts were then filtered, rinsed, and calcined in a Thermolyne 47900 furnace at 550°C for 3 hours to produce a "regenerated" catalyst. The acidity of each fresh and regenerated solid acid catalyst was determined by titration (method described in section 2.3). Based on

acid content, HY could be completely regenerated, but HZSM-5 could only be partially regenerated by this process. In the case of HZSM-5, the acid concentration of the fresh catalyst was determined to be 1.10 mmol g^{-1} H^+ whereas, the regenerated catalyst was determined to be only 0.4 mmol g^{-1} H^+. This may be explained by the size of $EMIM^+$ relative to the size of the zeolite pores. Based on the cation size estimate provided in section 4.2.1 it would seem that $EMIM^+$ could fit into HY pores in any orientation, but this is not possible for HZSM-5. The pores of HZSM-5 are small enough that $EMIM^+$ might enter only when its orientation is within a narrow range. Therefore, it would be more likely that $EMIM^+$ would become trapped within the pores, hindering ion exchange with ammonium nitrate during the regeneration process. HY, on the other hand, should be able to expel virtually all $EMIM^+$ cations by ion exchange with ammonium nitrate. To further understand this process, diffuse reflectance Fourier transform spectroscopy (DRIFTS) was performed on catalyst samples.

4.6.1 DRIFTS analysis of zeolites

Diffuse reflectance infrared Fourier transform spectroscopy (DRIFTS) is a good method for detecting slight structural changes within a solid. DRIFTS analysis is based on the collection of diffusely scattered infrared radiation from powdered samples, after which a Fourier transform is applied to the data to obtain a spectrum. In diffuse reflectance spectroscopy, a beam of radiation interacts with the sample surface; during which the radiation can undergo absorption, transmission, and/or reflection. The relative amounts of reflection and transmission are based on the sample refractive index (η_2), the diluent media refractive index (η_1), and the radiation angle of incidence. For a monochromatic beam that has a normal angle of incidence (i.e. 90° to the surface), the reflectance $\rho(\lambda)$ can be determined by using equation 4.5 [167]. Predicting the reflectance of polychromatic radiation is more complicated because refractive indices for the sample and diluents change with radiation wavelength and the surface of a powdered sample is not smooth. Experimentally, measurements are separately made of a reference (i.e. pure diluents) and

sample, then the infrared reflectance spectrum is generated by calculating the ratio of the sample single beam spectrum to the reference single beam spectrum. This process effectively compensates for refractive index variations with wavelength. Samples were prepared for DRIFTS analysis according to the method described in section 2.5.5.

$$\rho(\lambda) = \frac{(\eta_2 - \eta_1)^2}{(\eta_2 + \eta_1)^2}$$

Equation 4.5

The purpose of these experiments was to test the hypothesis that EMIM$^+$ becomes trapped within the pores of HZSM-5, but not HY. Zeolites HY and HZSM-5 were analyzed by DRIFTS prior to [EMIM]Cl exposure (e.g. fresh catalyst), after [EMIM]Cl exposure, after ammonium nitrate exposure during catalyst regeneration, and after calcination. Fresh HY and HZSM-5 were also treated with ammonium nitrate in a similar manner as the ionic liquid treated catalysts to allow for spectral comparisons. There were two main regions of interest for this analysis (ca. 3000 and 3500 cm^{-1}). A cluster of bands around 3000 cm^{-1} were observed in the neat [EMIM]Cl spectrum (shown for reference in figures

4.12-4.17). These structural features represent C-H stretching vibrations for imidazole ring CH and CH_3, which are characteristic of [EMIM]Cl. Because the fresh zeolite catalysts did not exhibit any bands in this region, absorbance at 3000 cm^{-1} was an indication of the presence of [EMIM]Cl in samples. Two spectral bands that denote O-H stretching have been suggested to be indicative of BrØnsted acidity for HY: a low frequency band around 3550 cm^{-1} and a high frequency band around 3650 cm^{-1} [168-170]. Lavalley et al. suggested that the high frequency band represents acidity located in the supercages of HY [169]. For HZSM-5, it has been suggested that the presence of a band around 3600 cm^{-1} denotes O-H stretching for acid sites found in HZSM-5 [171].

After exposure to [EMIM]Cl, both HY and HZSM-5 spectra exhibited absorbance near 3000 cm^{-1} that could be assigned to $EMIM^+$. Spectral bands at 2980 cm^{-1} (CH_3) and at 3107 cm^{-1} and 3146 cm^{-1} (imidazole C-H) were observed in the HY spectrum after exposure to [EMIM]Cl (figure 4.12). The band shape in this region was similar to that obtained for HZSM-5, which contained spectral bands at 2988 cm^{-1}, 3123 cm^{-1}, and 3161 cm^{-1}

(figure 4.13).   The spectral band at 3123 cm^{-1} is overlapped by the band at 3161 cm^{-1}, and therefore appears as a shoulder on the 3161 cm^{-1} band.   Although spectral band frequencies are slightly different for HY and HZSM-5, the overall shape of the bands in this region was similar for both catalysts after exposure to [EMIM]Cl.   Furthermore, the band shapes observed in these spectra were different than that found in the neat [EMIM]Cl spectrum.   This suggests that the C–H vibrations are affected by interactions with the zeolites, which indicates that the ionic liquid is not simply mixed with the zeolites.   Because zeolites were thoroughly washed prior to DRIFTS analysis, the presence of the EMIM^{+} spectral bands indicates that the cation is strongly bound to the zeolites, most likely within the zeolite channels.   The similarity between the EMIM^{+} band shapes for HY and HZSM-5 suggests that the cation–zeolite interactions are similar for these two catalysts.

In addition to a gain of EMIM^{+} spectral features, O–H stretching vibration bands for both HY and HZSM-5 decreased in intensity after exposure to EMIM^{+}, suggesting ion exchange and a corresponding decrease in

acidity. In fresh HY catalyst, the absorbance band intensities for bands at 3551 cm^{-1} and 3636 cm^{-1} are approximately equal. However, significant absorbance was observed only for the band at 3551 cm^{-1} in the spectrum obtained for HY after exposure to the ionic liquid. As previously mentioned, the absorbance band near 3650 cm^{-1} is attributed to acidity located in HY supercages [169]. Similarly, the spectrum obtained after exposure of HZSM-5 to the ionic liquid exhibited significant loss of absorbance at 3605 cm^{-1}. These results suggest that $EMIM^+$ replaces H^+ when HY and HZSM-5 catalysts are immersed in [EMIM]Cl.
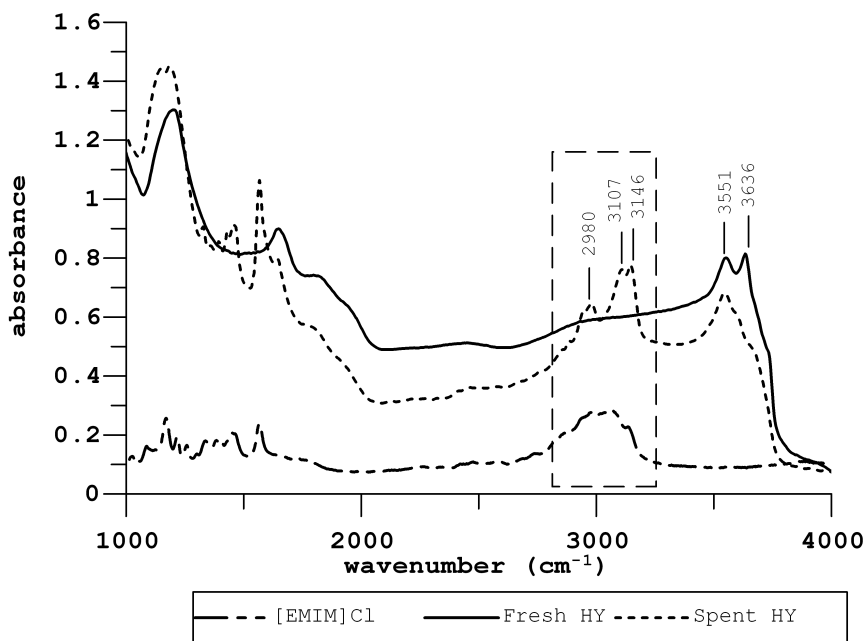
Figure 4.12 DRIFTS spectra for [EMIM]Cl, fresh catalyst, and spent catalyst; HY zeolite
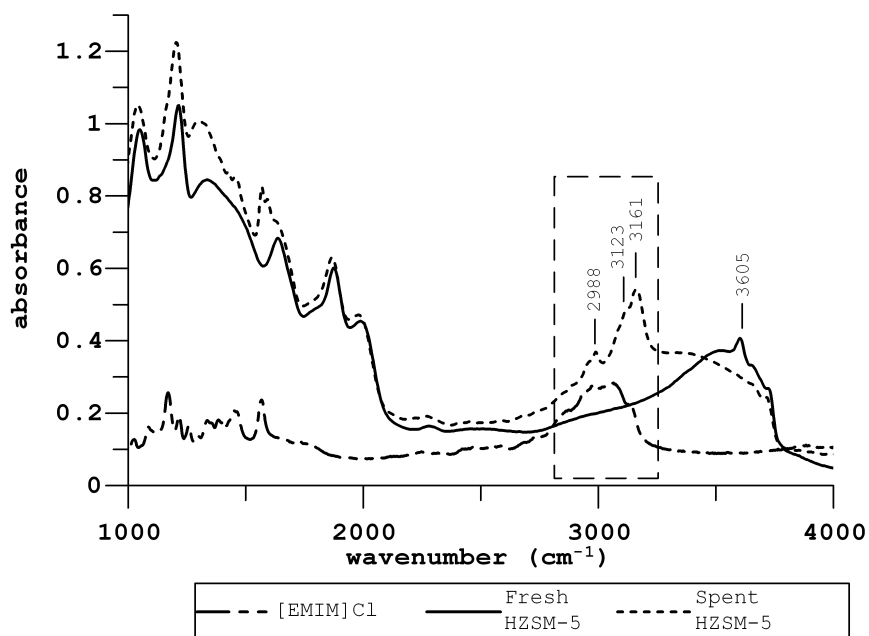
Figure 4.13 DRIFTS spectra for [EMIM]Cl, fresh catalyst, and spent catalyst; HZSM-5 zeolite

DRIFTS analysis was also used to characterize HY and HZSM-5 samples that had been exposed to [EMIM]Cl after soaking them in an ammonium nitrate solution, which is the first step in the catalyst regeneration process. If the ammonium ion can displace $EMIM^+$, no bands near 3000 cm^{-1} should be observed in DRIFTS spectra. In fact, the distinct bands at 2980 cm^{-1}, 3107 cm^{-1}, and 3146 cm^{-1} observed in the HY spectrum after exposure to [EMIM]Cl (figure 4.12) were not observed

after soaking the catalyst in ammonium nitrate solution. Instead, a broad feature, ranging from ca. 2500 cm^{-1} to 3500 cm^{-1}, was observed (figure 4.14). To verify that this feature was due to NH_4^+ adsorption, fresh HY was treated with ammonium nitrate in a similar manner. Similar spectra were obtained for the fresh and [EMIM]Cl treated HY samples after exposure to NH_4^+. Furthermore, no significant absorbance was observed at ca. 3636 cm^{-1}, indicating that ion exchange occurred, effectively removing $EMIM^+$ from the catalyst (figure 4.14).
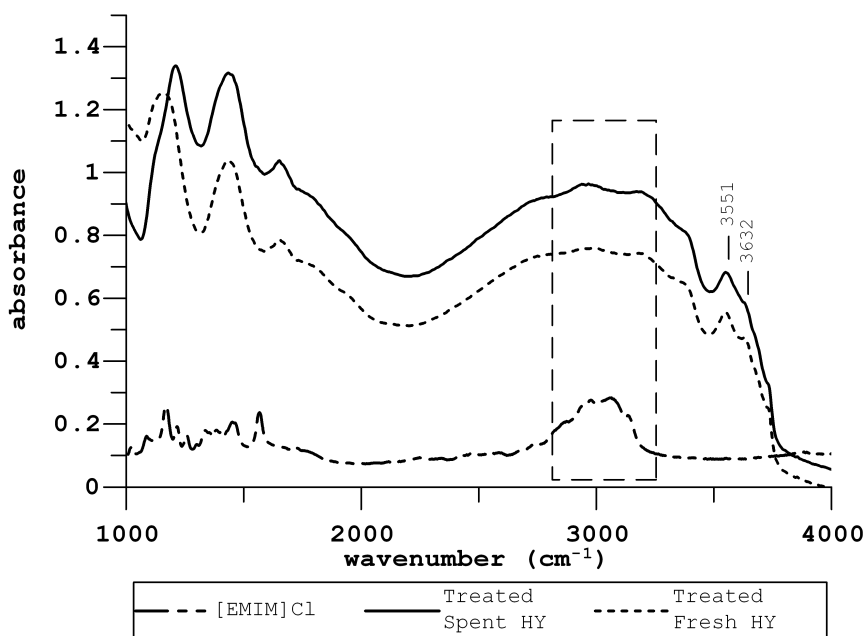
Figure 4.14 DRIFTS spectra for [EMIM]Cl, ammonium nitrate treated spent catalyst, and ammonium nitrate treated fresh catalyst; HY zeolite

In contrast, after soaking the HZSM-5 catalyst in ammonium nitrate solution after it had been exposed to ionic liquid, the DRIFTS spectrum still contained distinct bands at 2988 cm^{-1}, 3123 cm^{-1}, and 3161 cm^{-1}, which indicates that at least some $EMIM^+$ remained (figure 4.15). These results indicate incomplete exchange of $EMIM^+$ for NH_4^+. DRIFTS findings are consistent with the titration results, which indicate that HY could be fully regenerated, but that HZSM-5 was only partially regenerated, regaining ca. 36% of the original acidity. Based on these results, it appears that removal of $EMIM^+$ by NH_4^+ ion exchange was more difficult for HZSM-5 than for HY. This may be attributed to a greater steric hindrance for removal of $EMIM^+$ from the smaller pores found in HZSM-5.
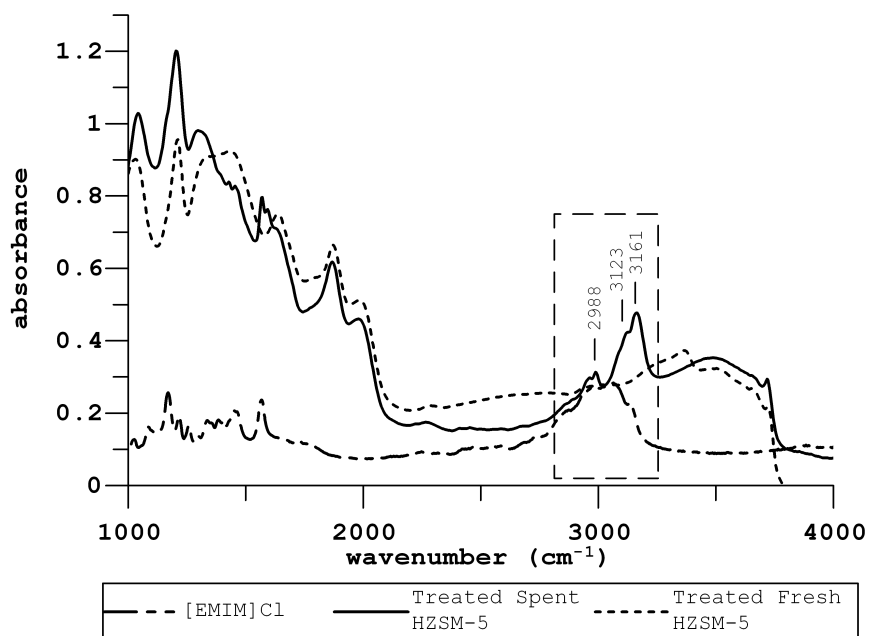
Figure 4.15 DRIFTS spectra for [EMIM]Cl, ammonium nitrate treated spent catalyst, and ammonium nitrate treated fresh catalyst; HZSM-5 zeolite

After treatment with ammonium nitrate, the HY and HZSM-5 catalysts that had been exposed to [EMIM]Cl were calcined at 550°C for 3 hrs, and then DRIFTS was performed on the calcined samples. Based on the absence of $EMIM^+$ spectral features in the NH_4^+ treated HY spectrum, essentially 100% regeneration was expected for HY (figure 4.16). As expected, absorbance bands at 3551 cm^{-1} and 3636 cm^{-1} were observed in the HY calcined spectrum. However, the relative intensities of these two bands were somewhat different from those in the fresh HY DRIFTS spectrum. Although the two bands were

approximately equal intensity in the fresh HY spectrum, the absorbance band at 3636 cm^{-1} was slightly smaller than the band at 3551 cm^{-1} in the regenerated HY spectrum. Based on spectral data alone, it would seem that HY was not fully regenerated. However, titration of the solid indicated that essentially 100% of the acid sites were recovered.
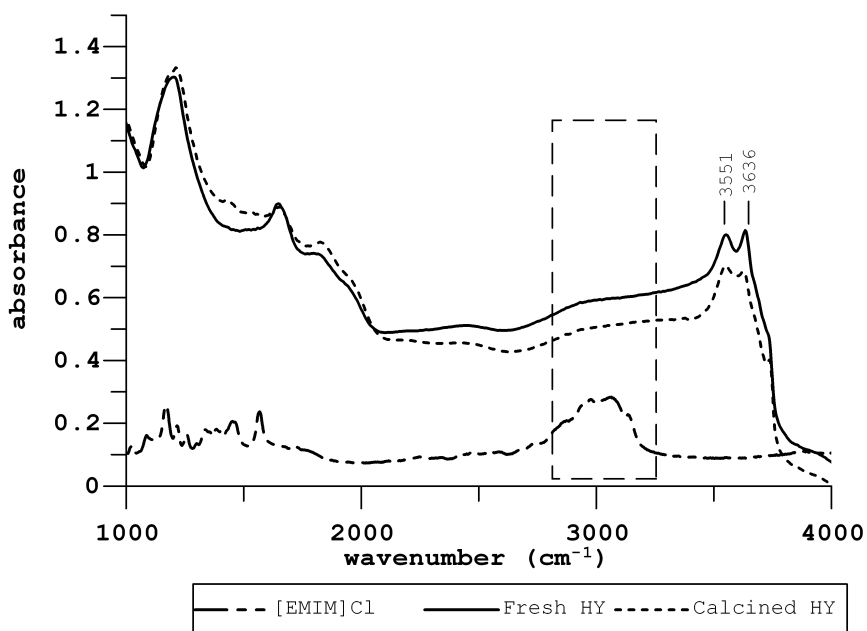
Figure 4.16 DRIFTS spectra for [EMIM]Cl, fresh catalyst, and calcined catalyst; HY zeolite

In contrast to the results obtained for HY, the NH$_4^+$ treated spectrum for HZSM-5 still contained features representative of EMIM$^+$ (e.g. bands at 2988

cm^{-1}, 3123 cm^{-1}, and 3161 cm^{-1}), suggesting incomplete ion exchange with NH_4^+. However, these peaks disappeared in the subsequently calcined spectrum, suggesting that $EMIM^+$ decomposed when the material was heated. Furthermore, the band at 3605 cm^{-1}, which was found in the fresh HZSM-5 spectrum, was observed in the regenerated HZSM-5 spectrum (figure 4.17). Based on these spectral results, it appears that the HZSM-5 acid sites were restored. However, titration of the HZSM-5 solid after "regeneration" revealed that only ca. 36% of the original acidity was recovered. Based on these results, it seems that the $EMIM^+$ decomposed when the sample was calcined, but that the decomposition process did not result in a charge-balancing acidic proton, despite the fact that the O-H stretching vibration commonly associated with BrØnsted acidity reappeared in the DRIFTS spectrum.
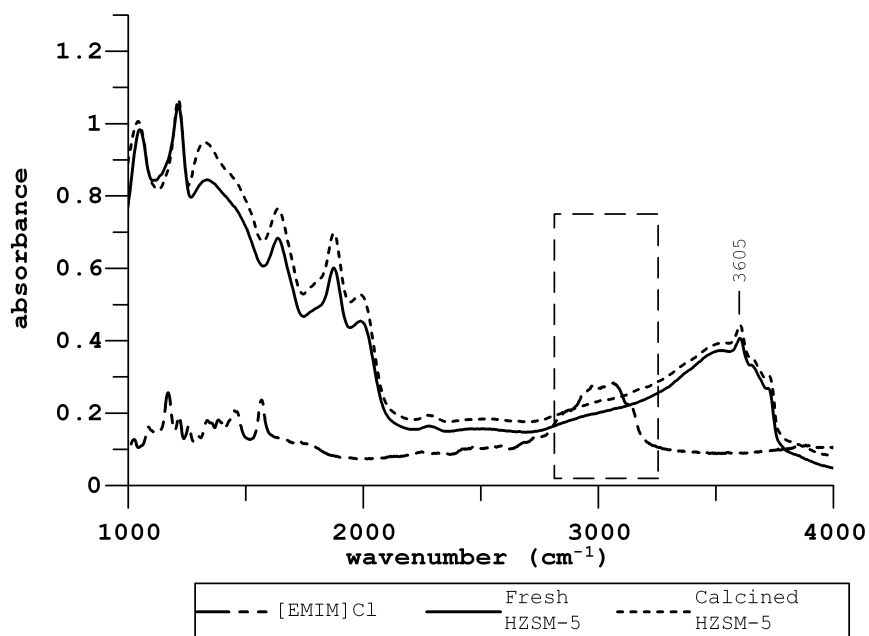
Figure 4.17 DRIFTS spectra for [EMIM]Cl, fresh catalyst, and calcined catalyst; HZSM-5 zeolite

The DRIFTS results are summarized in table 4.4, where each stage of the catalyst regeneration process is characterized by the presence of [EMIM]Cl. To summarize, the results of these studies support the theory that ion exchange with $EMIM^+$ results in the irreversible release of H^+ from HY and HZSM-5, which is responsible for the observed polysaccharide hydrolysis catalytic activity. Although this allows the zeolites to be useful for cellulose hydrolysis, it inherently limits reusability without catalyst regeneration. Furthermore, greater steric hindrance in HZSM-5 reduced

acid site recovery (36% recovered) compared to HY (100% recovered).

Table 4.4 summary of DRIFTS results

Catalyst	Fresh	Spent[a]	NH$_4$NO$_3$[b]	Calcined
Presence of [EMIM]Cl				
HY	NO	YES	NO	NO
HZSM-5	NO	YES	YES	NO

[a]after exposure to [EMIM]Cl
[b]after ammonium nitrate ion exchange

4.7 Cellulose Hydrolysis in [EMIM]Cl/OS medium

Rinaldi et al. suggested the use of an ionic liquid (IL) and organic solvent (OS) mixture for improved cellulose dissolution. By using various organic solvents with 1-butyl-3-methylimidazolium chloride [BMIM]Cl, it was found that cellulose could be dissolved in less than 3 minutes and at temperatures below 100°C [172]. For comparison, 30 minutes at 120°C are required to dissolve cellulose in pure 1-ethyl-3-methylimidazolium chloride [EMIM]Cl. Lower temperature requirements for cellulose dissolution based on using

an organic solvent in combination with ionic liquid would be beneficial for cellulose hydrolysis and possibly result in decreased glucose decomposition. In addition, the use of an IL/OS medium may reduce the cost of glucose production from cellulose by requiring less ionic liquid (ca. $0.34 per gram [EMIM]Cl). Clearly, assuming that acid catalyzed cellulose hydrolysis could be performed, IL/OS could be a better reaction medium than pure ILM.

Studies were carried out to test the effects of an [EMIM]Cl/OS medium on the acid catalyzed hydrolysis of cellulose. Experiments were conducted with hydrochloric acid rather than SACs to elucidate effects that could be attributed to the medium without complications of effects due to interactions between the SAC and reaction media. The organic solvents studied included t-butanol, dimethyl sulfoxide (DMSO), and dimethylformamide (DMF), and structures are shown in figure 4.18.

dimethyl sulfoxide   t-butanol   dimethylformamide
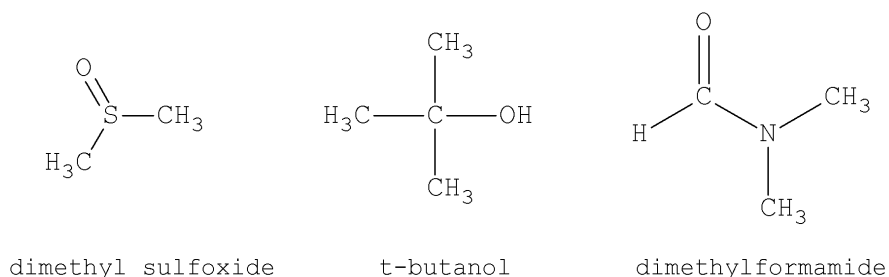
Figure 4.18 structures of the organic solvents

Cellulose (0.05 g) was first placed in the organic solvent for one minute, after which [EMIM]Cl was added to obtain a total volume of 1.5 mL. The [EMIM]Cl/OS ratio needed to dissolve cellulose (0.05 g) was determined by varying the amount of OS and visually observing cellulose dissolution. The percent ionic liquid was calculated (equation 4.6) by using the same method as Rinaldi et. al [172], where n is the number of moles of [EMIM]Cl (IL) and organic solvent (OS).

$$\%IL = \frac{n_{IL}}{(n_{OS}+n_{IL})} \qquad \textbf{Equation 4.6}$$

Cellulose hydrolysis was carried out by placing the samples into a temperature controlled oil bath at 105°C for 1hr. Aliquots (0.05 mL) from the hydrolysis reaction mixture were taken throughout the experiment and tested for reducing sugars with Benedict's reagent,

181

according to the method described in section 2.4. Relevant properties for the organic solvents used for these studies are given in table 4.5.

Table 4.5 organic solvent properties

Organic Solvent	Boiling Point (°C)	%IL[a]
t-butanol	82	0.49
DMSO	189	0.21
DMF	153	0.35

[a]calculated with equation 4.6

Although cellulose could be dissolved in [EMIM]Cl/t-butanol (0.49 %IL), the low boiling point of t-butanol (82°C), caused evaporation during cellulose hydrolysis when reaction temperatures were above 80°C. Lowering the reaction temperature caused the solution to become increasingly viscous and more difficult to stir. Furthermore, no conversion was detected at room temperature for cellulose hydrolysis in an [EMIM]Cl/t-butanol medium. Based on these results, t-butanol was too volatile to be used as an organic solvent additive with the testing procedure employed here.

Both [EMIM]Cl/DMSO (0.21 %IL) and [EMIM]Cl/DMF (0.35 %IL) could dissolve cellulose, and the high

boiling points of DMSO (189°C) and DMF (153°C) allowed for cellulose hydrolysis at 100°C. Comparing %TGY from cellulose hydrolysis in [EMIM]Cl and [EMIM]Cl/OS, slower reaction rates and lower activities were observed when the reaction medium was [EMIM]Cl/OS; where OS was either DMSO or DMF (figure 4.19).
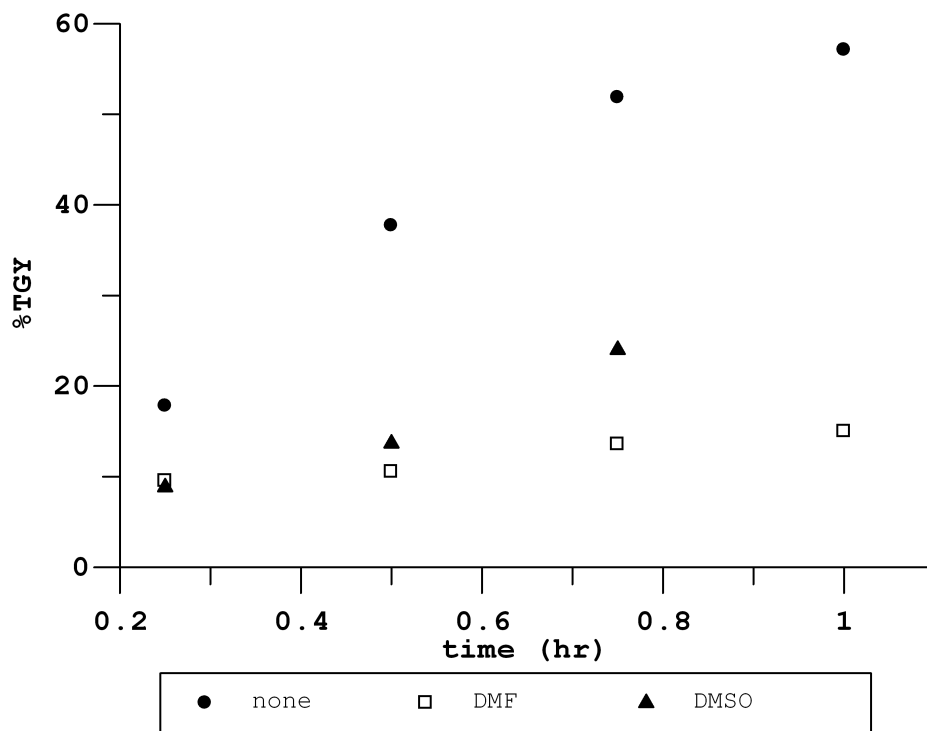
Figure 4.19 cellulose hydrolysis in [EMIM]Cl with organic solvent additives (none, DMF, and DMSO) at 100°C for 1hr.

The lower yields obtained with [EMIM]Cl/OS media could be explained by effects from the basicity of the organic solvents used. For example, Slivko et al.

suggested that in the presence of acid, the oxygen of the sulfoxide group in DMSO (figure 4.18) could be protonated [173]. The same could be expected of the oxygen in DMF, although no literature references were found to confirm this. On the other hand, the oxygen in t-butanol (figure 4.18) is already protonated and therefore, would not be expected to interact with acidic protons. This reaction results in loss of acid equivalents that otherwise could have catalyzed cellulose hydrolysis. According to the results presented in the literature, cellulose dissolution improves when the solvent basicity increases [22, 172]. Unfortunately, slightly basic organic solvents can compete with the hydrolysis substrate for the catalyst acidity (H^+), lowering the catalyst activity. Thus, the addition of slightly basic OS to the ILM resulted in lower %TGY compared to pure ILM. Thus, reduced cellulose hydrolysis activity in IL/OS mixtures makes organic solvent additives less attractive for use with acid catalyzed cellulose hydrolysis.

4.8 Summary

Because cellulose is virtually insoluble in water but can be dissolved at moderate temperatures in an ionic liquid, studies of the effects of [EMIM]Cl ionic liquid on SACs and on hydrolysis reactions were carried out. SACs characterized after exposure to [EMIM]Cl showed a significant loss of acidity. Sulfated zirconia, HY, and Nafion® NR50 lost about half of their original acidity to the ILM. HZSM-5 and Nafion® SAC-13 lost almost all of their initial acidity to the ILM. The mmol H^+ lost from each solid to the ILM was dependent on the catalyst acid site location and its availability to $EMIM^+$ cations. Although the addition of organic solvents to the ILM increased cellulose solubility, they were not useful for acid catalyzed reactions because the solvents that are most effective at dissolving cellulose are also weak bases. For polysaccharide hydrolysis in ILM, ion exchange induced proton release resulted in an observed catalytic activity for cellulose hydrolysis for all SACs tested (HY, HZSM-5, sulfated zirconia, Nafion® SAC-13, and Nafion® NR50). Scaling the %TGY from cellulose hydrolysis by the mmol H^+ released to the ILM resulted

185

in similar scaled values for all SACs tested. Therefore, it can be concluded that after H^+ is released into the ILM, the resultant catalytic activity is comparable to having added an equivalent amount of a liquid acid and it is not dependent upon the SAC from which the acid equivalents were derived.

Ion exchange cations $EMIM^+$ also affected the reusability of the catalysts. HY was the only catalyst tested that could be reused for two cellulose hydrolysis reactions. Although HY was inactive in aqueous media, the presence of ion exchange cations ($EMIM^+$) resulted in protons being released into the ILM, which provided catalytic activity. DRIFTS analysis confirmed that ion exchange of H^+ with $EMIM^+$ occurred in spent HY. Regeneration of spent HY with NH_4^+ followed by calcining resulted in 100% renewal to the original solid acidity, but the same process applied to HZSM-5 only regenerated some of the initial acid sites.

Chapter 5 : CELLULOSE TO ETHANOL CONVERSION BY USING SOLID ACID CATALYSIS

5.1 Industrial Implications

Although starch and cellulose hydrolysis mechanisms are the subjects of the work described here, ultimately it is desired to obtain ethanol from wood, straw and other sources of lignocellulosic materials. Production of bioethanol from lignocellulosic materials is a relatively recent area of interest. Consequently, the development of improved methodologies that can be used for large scale production are actively being sought. To make bioethanol a competitive alternative to gasoline, bioethanol production efficiency needs to be optimized. Several literature reviews have been published relating to this topic [4, 149, 174–178]. Currently, there are only a few pilot/demonstration plants producing bioethanol from cellulose. The National Renewable Energy Laboratory (NREL) published a document in 2011 that summarizes the requirements for commercial production of cellulosic ethanol, which is shown in figure 5.1 [179]. Raw feedstock is first brought to the feed handling area, where it is milled

and stored until it is subjected to pretreatment and conditioning. Cellulosic feedstocks are composed of lignin, hemicellulose, and cellulose. Hemicellulose and cellulose can be hydrolyzed into sugars, but lignin cannot. The cellulosic feedstock is treated with dilute sulfuric acid to liberate cellulose and hemicellulose from the lignin. This slurry is flash-cooled, resulting in condensed water, which is collected and treated in the "Wastewater Treatment" area, and subsequently reused. Prior to enzymatic hydrolysis, ammonia is added to the biomass slurry to increase the pH of the mixture. Cellulose hydrolysis is then performed by using cellulase enzymes that are prepared on-site. The hydrolysis products are fermented with *Zymomonas mobilis* for five days, which can simultaneously ferment glucose and xylose to ethanol. The resulting products are distilled to recover ethanol, which is then purified by vapor-phase molecular sieve adsorption. Solid-liquid separation removes residual solids (e.g. lignin) that are transported to the "Burner/Boiler & Turbogenerator" area, which is used to produce steam and electricity for the production plant. The liquid portion is pumped

to the "Wastewater Treatment" area, where the water is recycled and reused in the production process.

CELLULOSIC ETHANOL PRODUCTION
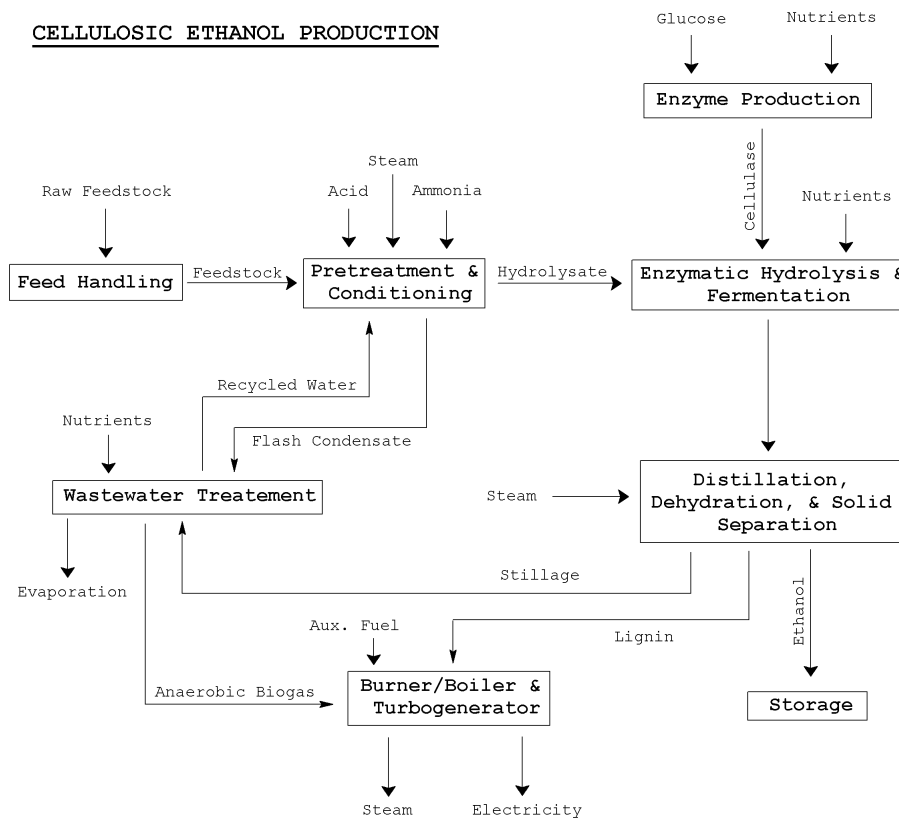
Figure 5.1 cellulosic ethanol production flowchart
derived from ref. [179]

There are three main processes that should be optimized to decrease ethanol production costs and increase production efficiency: biomass pretreatment, hydrolysis, and fermentation. In addition to process optimizations, reductions in the number of sequential

process steps would also be beneficial to streamlining overall bioethanol production.

5.1.1 Lignocellulosic Hydrolysis

Several studies have evaluated various pretreatment methods for preparing lignocellulosic materials for hydrolysis [22, 180-183]. However, the use of ionic liquids for lignocellulosic dissolution could potentially eliminate the need for any pretreatment processes. Fort et al. showed that 5 wt% untreated soft wood chips (e.g. oak, eucalyptus, poplar, and pine) could be dissolved in [C_4MIM]Cl at 100°C within 12-24hrs [23]. Other published studies have also demonstrated dissolution of lignocellulosic materials in various types of ionic liquids [32, 184, 185]. After the lignocellulosic material has been dissolved, hydrolysis can be performed in the ionic liquid medium to produce fermentable sugars [32]. The pilot/demonstration plants producing bioethanol currently employ enzymatic catalysis for lignocellulosic hydrolysis. However, solid acids are also being evaluated for potential hydrolysis catalysts. Current trends in biomass hydrolysis

process development are detailed in chapter 1 and thus will not be described further here.

5.1.2 Fermentation to Ethanol

The use of lignocellulosic feedstocks as hydrolysis substrates with ionic liquid solvents complicates the fermentation process, requiring new methodologies. Lignocellulosic hydrolysis products include sugars such as xylose, which cannot be fermented by S. cerevisiae, which is typically used for fermentation of cornstarch hydrolysis products (e.g. glucose). Consequently, new fermentation microbes and enzymes are currently being developed that can tolerate the ionic liquids used to dissolve cellulose. In addition, improved fermentation methodologies should withstand higher alcohol concentrations and fermenting sugars other than glucose [175, 186–189]. Engineering microbes that can better tolerate ionic liquids would eliminate the need for dilution or IL removal prior to fermentation.

5.1.3 Potential Industrial Scale Removal of Ionic

Liquid

Due to the high cost of ionic liquids ($0.34-$4/gram), it would be beneficial to be able to recycle and reuse the ILM. Rinaldi et al. reported that cellulose conversions using recycled [BMIM]Cl were comparable to cellulose conversions using fresh [BMIM]Cl [158]. Although their recycling method included procedures for removal of acidity (by neutralization) and water (by evaporation), they had difficulty removing soluble hydrolysis waste products from the ILM. However, their results indicated that these waste products did not affect the reusability of [BMIM]Cl [158].

On an industrial scale, waste products may build up until they do affect the conversion process. To avoid this, a technology called simulated moving bed chromatography (SMB), which is commercially available from Amalgamated Research, could be used to remove ionic liquids on a large scale [190]. Prior to SMB, any un-reacted cellulose would be precipitated by addition of water, and solids (e.g. SACs) would be removed by filtration. In SMB theory, there would be

two opposing flows: water, and ion exchange resin. The
ILM containing hydrolysates would be continuously fed
into opposing flows, wherein the ionic liquid would be
attracted to the ion exchange resin and the hydrolysis
products would be attracted to the water. Separate
downstream exit ports for the ionic liquid and the
water-soluble products would complete the separation
process (figure 5.2).
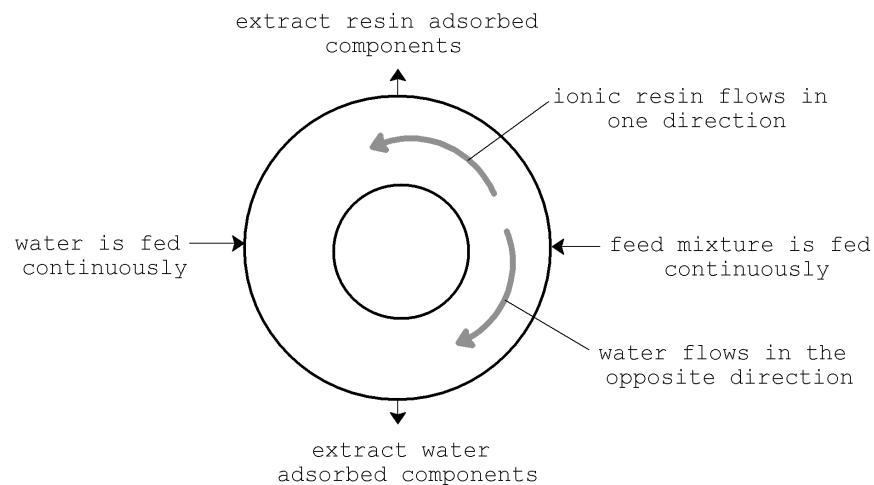
Figure 5.2 theory of SMB derived from ref. [191]

In practice, a series of columns (figure 5.3a) are
arranged in a manner that simulates the opposing
circular flow paths (figure 5.3b). Using circulation
pumps, a continuous flow of water can be established
through the columns. Although the resin inside each

193

column is stationary, ion exchange resin movement in a direction opposite to that of the water flow can be simulated by switching the connections designated by A, B, C, and D in figure 5.3b. For example, the connections might initially be positioned so that: A=feed mixture, B=extract resin, C=water, D=extract products. Next, automatic valves would be used to simultaneously switch these connections so that: A=extract products, B=feed mixture, C=extract resin, and D=water, which effectively moves the resin beds in the opposite direction from the water flow.
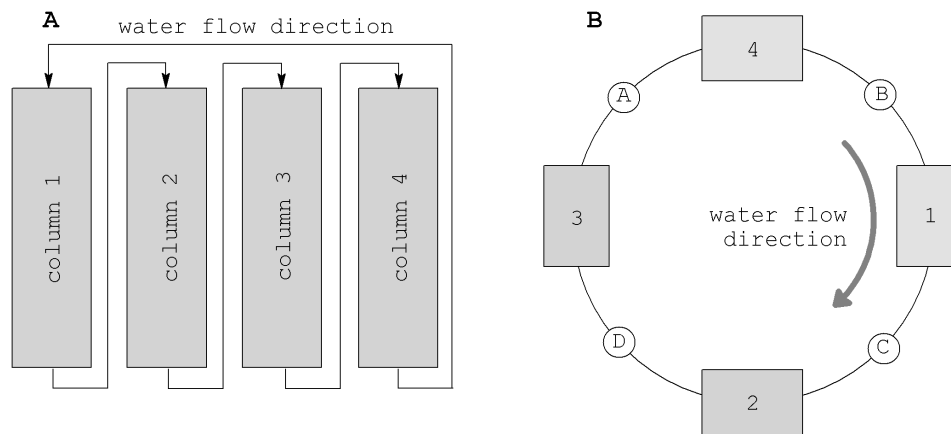
Figure 5.3 a) inline columns in SMB chromatography, b) inline columns in SMB chromatography shown in a circular orientation; derived from ref. [191]

5.2 Experimental Production of Ethanol

In the experiments described here, cellulose hydrolysis products were assayed by using the Benedict's test for reducing sugars, so any reducing sugar would yield a positive reading. An experiment was designed to test if it was possible to obtain ethanol by fermentation of SAC derived cellulose hydrolysates in the ILM. Although conversion of glucose to ethanol by fermentation in aqueous media is well established and has been optimized using yeasts (e.g. S. cerevisiae), the corresponding process in the presence of ionic liquid solvent has been much less studied. In water, fermenting yeasts have been shown to provide high yields (90% conversion, 10–14 wt% ethanol) at reasonable rates (1.5 g L^{-1} h^{-1}) [175]. However, the use of cellulose feedstock requires dissolution in ionic liquid media. Sendovski et al. showed that Saccharomyces cerevisiae could grow in up to 20% ionic liquid solutions, but compatibility with the ionic liquid decreased when longer alkyl side chains were attached to the ionic liquid imidazolium ring [192]. Ionic liquid concentrations exceeding 20% caused the yeast to die prematurely.

5.2.1 Effect of [EMIM]Cl on S. Cerevisiae Fermentation of Glucose

To evaluate the effect of [EMIM]Cl on the fermentation of glucose to ethanol, a study was performed in which the concentration of [EMIM]Cl was systematically varied. The yeast used for this study was Saccharomyces cerevisiae, and was prepared by dissolving S. cerevisiae (1.5 g) in warm distilled water (15 mL). Glucose (0.122 g) was dissolved in 10mL of [EMIM]Cl/H_2O (0-20 %vol [EMIM]Cl) and S. cerevisiae solution (1 mL) was added. Ethanol concentrations were determined after the mixture was at room temperature for 24 hours. Calibration standards and fermentation products were prepared according to the methods described in section 2.5.6. Values reported were vol% ethanol detected based on calibration standards. Results indicated that less than 5% [EMIM]Cl/H_2O provided maximum fermentation activity (figure 5.4). Above 5% [EMIM]Cl/H_2O, the fermentation activity decreased. When 20% [EMIM]Cl/H_2O was employed, ethanol yields were only 30% of what was obtained when no [EMIM]Cl was used. Although a 5% IL solution would provide a higher total ethanol yield than a 20% IL

196

solution, more water must be added to obtain a 5% IL solution, which decreases the ethanol concentration. In an industrial setting, minimizing the amount of water used would also minimize the amount of water that would have to be removed to reuse the ILM. Therefore, solutions were diluted to 20% [EMIM]Cl/H$_2$O prior to fermentation to determine if ethanol could be produced under these high IL concentration conditions.
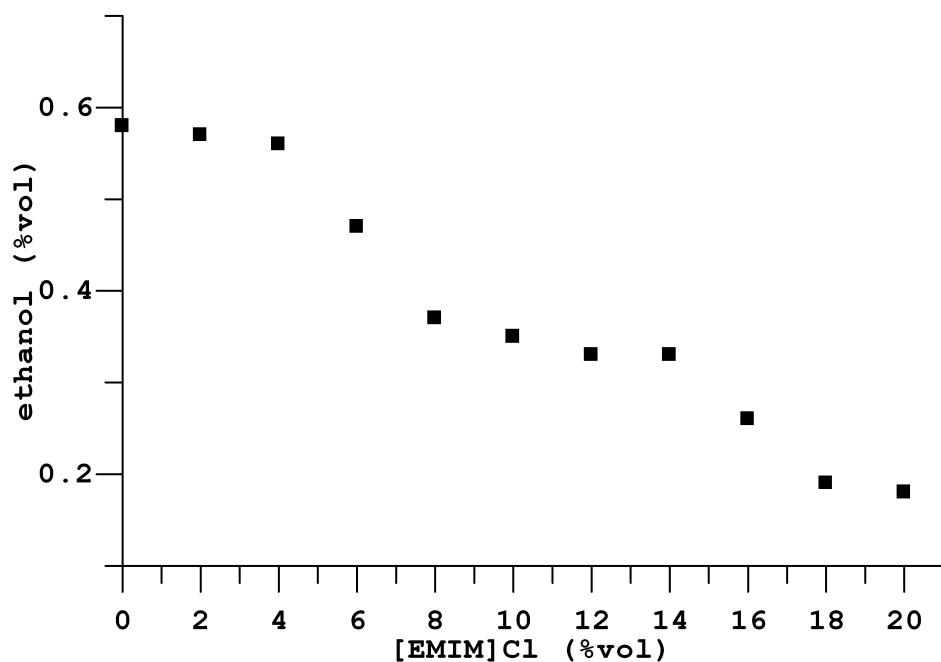
Figure 5.4 effect of [EMIM]Cl concentration on the fermentation activity of S. cerevisiae

5.2.2 In-Situ Production of Ethanol from Cellulose

As previously stated, the purpose of this experiment was to determine if cellulose could be hydrolyzed in ILM with solid acid catalysis, and then if the resulting hydrolysis products could be fermented to produce ethanol. Assuming that cellulose (0.1 g) is completely converted to glucose, the equivalent amount of glucose in grams can be calculated by using equation 5.1, where RU is the repeat unit described in section 4.4.

$$(\text{g cellulose})\left(\frac{\text{mol RU}}{162\text{ g}}\right)\left(\frac{1\text{ mol glucose}}{1\text{ mol RU}}\right)\left(\frac{180.16\text{ g glucose}}{\text{mol}}\right) \quad \textbf{Equation 5.1}$$

Based on the amount of glucose calculated when 0.1 g of cellulose is converted to glucose (0.111 g), equation 5.2 gives the theoretical amount of ethanol that would be produced to be 1.23 mmol.

Equation 5.2

$$(\text{g glucose})\left(\frac{\text{mol}}{180.16\text{ g}}\right)\left(\frac{2\text{ mol EtOH}}{1\text{ mol glucose}}\right)\left(\frac{1000\text{ mmol}}{1\text{ mol}}\right) = \text{mmol EtOH}$$

Prior to fermenting cellulose hydrolysis products, the S. cerevisiae that was used for fermentation was

tested in aqueous media and the ILM. These tests were carried out by adding 0.111 g of glucose, which would theoretically produce 1.23 mmol ethanol, into either distilled water (10 mL) or 20% [EMIM]Cl/H_2O along with 1 mL of the S. cerevisiae (1.5 g per 15 mL H_2O) solution. The amounts of ethanol produced were determined to be 0.99 mmol and 0.38 mmol in aqueous media and ILM respectively. Although 100% fermentation was not achieved, the S. cerevisiae used for these studies was significantly more effective in aqueous media (0.99 mmol). The lower ethanol yield obtained in 20% [EMIM]Cl/H_2O (0.38 mmol) indicated that S. cerevisiae activity for fermentation of glucose was significantly hindered. Therefore, the best possible result expected for fermentation of cellulose hydrolysis products in 20% [EMIM]Cl/H_2O would be 0.38 mmol. Based on the results from section 4.4.1, HY provided the highest %TGY from cellulose hydrolysis when catalyst weight was constant. Therefore, the cellulose hydrolysis products subjected to fermentation were obtained by using the HY acid catalyst. Cellulose hydrolysis was performed as described in section 4.4 with HY at 90°C for 3 hours and at 105°C for 1 hour. These reaction parameters were

chosen because although the percent total glucose yield for each was similar (82% and 75% respectively), the amount of fermentable sugars may have been different, because higher temperatures cause increased glucose degradation. After hydrolysis, each sample was diluted to 10 mL, and 1 mL Saccharomyces cerevisiae solution (1.5 g per 15mL H_2O) was added to the mixture. Fermentation proceeded at room temperature for 72 hours.   The resulting products were analyzed for ethanol by gas chromatography with mass spectrometry detection and calibration standards were used to determine ethanol yields (method described in section 2.5.6).

There was very little difference between cellulose hydrolysis performed at 90°C (3 hr) and 105°C (1 hr), which yielded 0.24 mmol (±0.02) and 0.29 mmol (±0.04) ethanol respectively. When comparing these results to those obtained for the ILM glucose reference sample (0.38 mmol ±0.08) yields of 63% and 76% relative to the glucose standard are obtained respectively.   These results confirm the presence of glucose in the cellulose hydrolysis products.   If these results are instead compared to the aqueous media glucose standard,

yields of only 20% and 24% are obtained. Thus, although the amount of ionic liquid present in the hydrolysis medium significantly reduces ethanol yields, it was clear that ethanol could be produced from HY catalyzed cellulose hydrolysis products by simply diluting (rather than removing) the ionic liquid.

5.3 Conclusions and Future Implications

The energy crisis is a world-wide problem, and although making bioethanol production a more cost effective process may not completely solve this problem, it would be a step in the right direction. Additionally, increasing the cost effectiveness of bioethanol production can help reduce the U.S. dependence on foreign countries for fuel. The ability to use cellulosic biomass instead of starch for ethanol production will make bioethanol an even more attractive renewable fuel. Several solid acid catalysts (SACs) were evaluated here for their activity for both starch and cellulose hydrolysis. Whereas starch hydrolysis could be performed in aqueous media, cellulose hydrolysis required dissolution in ionic liquid media (ILM). The studies described here show dramatically

different behaviors of the SACs in aqueous media versus ILM. This was primarily attributed to effects from the ion exchange cation (EMIM$^+$) associated with the ILM. Ion exchange allowed access to acidic protons within size-restricted areas in the solid catalysts that were too small for penetration by polysaccharide substrates. The locations of acid sites determined their availability for ion exchange with EMIM$^+$, but after H$^+$ was released into the ILM, the media behaved in a similar manner to hydrochloric acid, and it did not matter from which SAC the protons came from. This irreversible release of acidic protons inevitably made repeated use of the SACs impractical. Sulfated zirconia, HZSM-5, Nafion® SAC-13, and Nafion® NR50 could not be used more than 1-2 times, whereas HY was found to be reusable for three hydrolysis reactions, and then could be fully regenerated to its original acidity. Whereas the SACs tested here may not be viable alternatives to liquid acids, several crucial factors for development of more effective SACs were determined from the studies described here. First, when acidic protons are exposed to ionic liquids, ion exchange can increase proton mobility by releasing them

from solid acid surfaces. Thus, reusable solid acid catalysts should be engineered so that their structure limits the release of acidic protons by ion exchange. Second, polysaccharides and water should have easy access to acidic protons. Thus, if the catalyst is porous, pores should be large enough that minimal steric interactions exist. Third, SAC surface protons should return to their original site after hydrolysis. This could be accomplished by minimizing exposure of acidic protons to ion exchanging cations. Based on these suggestions, a theoretical porous solid acid catalyst would have channels large enough to allow dissolved cellulose to pass through, with all acid sites located within the channels. Channel openings could be positively charged to repel ILM cations from entering the channel, preventing ion exchange with the acidic protons (figure 5.5). In theory, this SAC would allow cellulose to be hydrolyzed to glucose without loss of catalytic activity due to ion exchange with ILM cations.
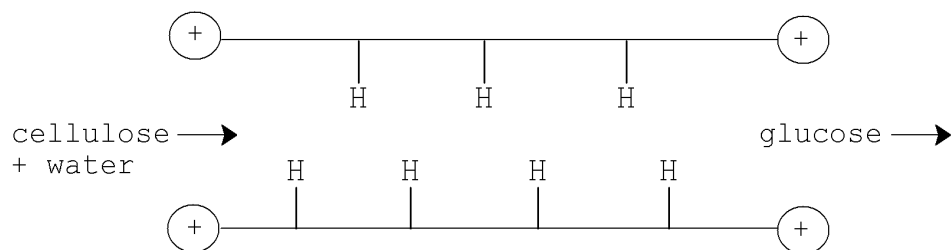
Figure 5.5 theoretical solid acid catalyst for cellulose hydrolysis in ILM

Recent literature publications have reported on novel cellulase mimetic solid acid catalysts. These catalysts are similar to cellulase enzymes in that they contain both a cellulose-binding domain (CBD) and a catalysis domain (CD). The cellulose substrate is adsorbed on the catalyst surface through hydrogen bonding between the cellulose and the cellulose-binding domain. Then, the catalysis domain breaks the glycosidic bond and the resulting product desorbs (figure 5.6).
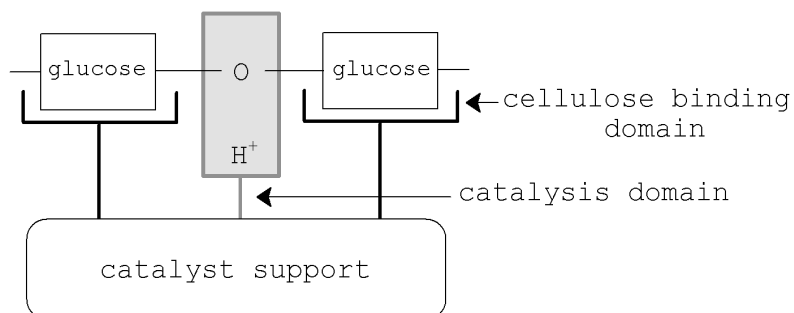
Figure 5.6 diagram of a cellulase mimetic solid acid catalyst

For example, Guo et al. reported a 73% yield of total reducing sugars when sulfonated carbon material ($C-SO_3H$) was used for cellulose hydrolysis after 4 hours in [BMIM]Cl at 110°C [193]. For this catalyst, the cellulose binding domain is reported to contain rigid —COOH and phenolic —OH groups whereas —SO_3H groups are located in the catalysis domain. This $C-SO_3H$ catalyst was reported to be reused 5 times without significant loss of catalytic activity [193]. Li and Xuejun reported glucose yields up to 93% by using a sulfonated chloromethyl polystyrene resin ($CP-SO_3H$) catalyst and Avicel (microcrystalline cellulose) [194]. Hydrolysis was carried out in an aqueous medium at 120°C for 10 hours. It was suggested that the cellulose forms hydrogen bonds with the CBD (-Cl), which disrupts the crystalline cellulose hydrogen bond system, making glycosidic bonds more accessible to the CD (-SO_3H). The activation energy for hydrolysis of cellulose with $CP-SO_3H$ (83 kJ mol^{-1}) was significantly lower than that obtained with sulfuric acid (170 kJ mol^{-1}) [194]. Zhang et al. also developed a novel cellulase mimetic catalyst, which is an ionic liquid functionalized biochar sulfonic acid ($BC-SO_3H-IL$), containing a CBD (-

Cl) and CD (-SO$_3$H). In contrast to the C-SO$_3$H catalyst

(Guo et al.) and the CP-SO$_3$H catalyst (Li and Xuejun),

which are rigid, BC-SO$_3$H-IL (Zhang et al.) is reported

to have a flexible region allowing for easier access to

the CBD (figure 5.7). Reducing sugar yields of 33%

and 65% were reported for cellulose hydrolysis in water

and [BMIM]Cl medium respectively at 90°C after 2 hours

[195]. Furthermore, BC-SO$_3$H-IL could be reused 4 times

without loss of catalytic activity.
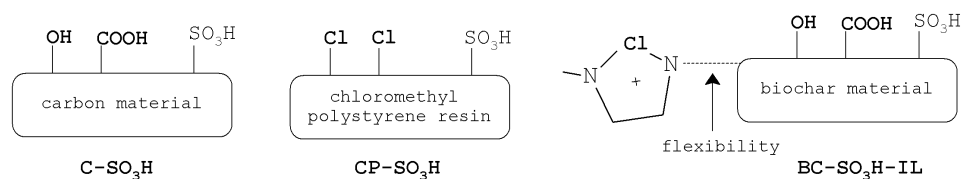
Figure 5.7 simplified structures of example cellulase mimetic catalysts

Results from experiments described here indicate

that polysaccharide hydrolysis can be enhanced by ion

exchange when inaccessible protons are transported from

the catalyst to the reaction medium. However, this

apparently does not occur for cellulase mimetic solid

acid catalysts. The main difference between the

catalysts tested for the studies described here and

cellulase mimetic catalysts is the cellulose binding

domain, which makes the solid catalyst surfaces hydrophilic. Zhang et al. reported minimal loss of catalytic activity after repeated use of BC-SO$_3$H-IL (from 34-33% TRS), whereas the same catalyst without the IL functionality (i.e. -Cl cellulose binding domain) showed a more significant decrease in catalytic activity after being used four times (from 27-17% TRS) [195]. It should be pointed out that the relative decrease in catalytic activity reported by Zhang et al. is less than those reported here, where most SACs tested lost most of their activity after the first run. One possible explanation for this difference may involve the lack of hydrophilic surfaces at which cellulose can bind. However, there may be other explanations for the catalytic stability reported for cellulase mimetic catalysts, and these should be investigated further when designing even more effective new solid acid catalysts.

References

1. DOE. *U.S. Energy Information Administration*. Independent Statistics and Analysis 2012 [cited http://www.eia.gov.

2. Gomez, L.D., C.G. Steele-King, and S.J. McQueen-Mason, *Sustainable liquid biofuels from biomass: the writing's on the walls.* New Phytologist, 2008. **178**(3): p. 473-485.

3. Granda, C.B., L. Zhu, and M.T. Holtzapple, *Sustainable liquid biofuels and their environmental impact.* Environmental Progress, 2007. **26**: p. 233-250.

4. Standlee, C., *2010 Ethanol Industry Outlook: Climate of Opportunity*, in *Renewable Fuels Association* 2010.

5. Rinaldi, R. and F. Schuth, *Acid Hydrolysis of Cellulose as the Entry Point into Biorefinery Schemes.* Chemsuschem, 2009. **2**(12): p. 1096-1107.

6. Taherzadeh, M.J. and K. Karimi, *ACID-BASED HYDROLYSIS PROCESSES FOR ETHANOL FROM LIGNOCELLULOSIC MATERIALS: A REVIEW.* Bioresources, 2007. **2**(3): p. 472-499.

7. Strachan, J., *Solubility of cellulose in water.* Nature, 1938. **141**: p. 332-333.

8. Hinterstoisser, B. and L. Salmen, *Two-dimensional step-scan FTIR: a tool to unravel the OH-valency-range of the spectrum of Cellulose I.* Cellulose, 1999. **6**(3): p. 251-263.

9.   Marechal, Y. and H. Chanzy, *The hydrogen bond network in I-beta cellulose as observed by infrared spectrometry.* Journal of Molecular Structure, 2000. **523**: p. 183–196.

10.   Kokot, S., B. Czarnik-Matusewicz, and Y. Ozaki, *Two-dimensional correlation spectroscopy and principal component analysis studies of temperature-dependent IR spectra of cotton-cellulose.* Biopolymers, 2002. **67**(6): p. 456–469.

11.   Ito, T., et al., *Hydrogen bond and crystal deformation of cellulose in sub/super-critical water.* Japanese Journal of Applied Physics Part 1-Regular Papers Short Notes & Review Papers, 2002. **41**(9): p. 5809–5814.

12.   Sukhov, D.A., *Hydrogen bonds in natural and mercerized cellulose fibres based on Raman spectroscopic data.* Fibre Chemistry, 2003. **35**(4): p. 277–282.

13.   Bochek, A.M., *Effect of hydrogen bonding on cellulose solubility in aqueous and nonaqueous solvents.* Russian Journal of Applied Chemistry, 2003. **76**(11): p. 1711–1719.

14.   Watanabe, A., S. Morita, and Y. Ozaki, *Study on temperature-dependent changes in hydrogen bonds in cellulose I beta by infrared spectroscopy with perturbation-correlation moving-window two-dimensional correlation spectroscopy.* Biomacromolecules, 2006. **7**(11): p. 3164–3170.

15.   Yu, Y., X. Lou, and H.W. Wu, *Some recent advances in hydrolysis of biomass in hot-compressed, water and its comparisons with other hydrolysis methods.* Energy & Fuels, 2008. **22**(1): p. 46–60.

16.   Ehara, K. and S. Saka, *Decomposition behavior of cellulose in supercritical water, subcritical*

water, and their combined treatments. Journal of Wood Science, 2005. **51**(2): p. 148–153.

17. Deguchi, S., K. Tsujii, and K. Horikoshi, *Cooking cellulose in hot and compressed water.* Chemical Communications, 2006(31): p. 3293–3295.

18. vanWyk, J.P.H., *Cellulose hydrolysis and cellulase adsorption after pretreatment of cellulose materials.* Biotechnology Techniques, 1997. **11**(6): p. 443–445.

19. Zheng, Y.Z., H.M. Lin, and G.T. Tsao, *Pretreatment for cellulose hydrolysis by carbon dioxide explosion.* Biotechnology Progress, 1998. **14**(6): p. 890–896.

20. Onda, A., T. Ochi, and K. Yanagisawa, *Selective hydrolysis of cellulose into glucose over solid acid catalysts.* Green Chemistry, 2008. **10**(10): p. 1033–1037.

21. Onda, A., T. Ochi, and K. Yanagisawa, *Hydrolysis of Cellulose Selectively into Glucose Over Sulfonated Activated-Carbon Catalyst Under Hydrothermal Conditions.* Topics in Catalysis, 2009. **52**(6–7): p. 801–807.

22. Brandt, A., et al., *The effect of the ionic liquid anion in the pretreatment of pine wood chips.* Green Chemistry, 2010. **12**(4): p. 672–679.

23. Fort, D.A., et al., *Can ionic liquids dissolve wood? Processing and analysis of lignocellulosic materials with 1-n-butyl-3-methylimidazolium chloride.* Green Chemistry, 2007. **9**(1): p. 63–69.

24. Kosan, B., C. Michels, and F. Meister, *Dissolution and forming of cellulose with ionic liquids.* Cellulose, 2008. **15**(1): p. 59–66.

25. Ohno, H. and Y. Fukaya, *Task Specific Ionic Liquids for Cellulose Technology.* Chemistry Letters, 2009. **38**(1): p. 2-7.

26. Remsing, R.C., et al., *Mechanism of cellulose dissolution in the ionic liquid 1-n-butyl-3-methylimidazolium chloride: a C-13 and Cl-35/37 NMR relaxation study on model systems.* Chemical Communications, 2006(12): p. 1271-1273.

27. Swatloski, R.P., et al., *Ionic liquids: New solvents for non-derivitized cellulose dissolution.* Abstracts of Papers of the American Chemical Society, 2002. **224**: p. 076-IEC.

28. Swatloski, R.P., et al., *Ionic liquids as green solvents for the dissolution and regeneration of cellulose.* Abstracts of Papers of the American Chemical Society, 2003. **225**: p. 131-CELL.

29. Li, C.Z., Q. Wang, and Z.K. Zhao, *Acid in ionic liquid: An efficient system for hydrolysis of lignocellulose.* Green Chemistry, 2008. **10**(2): p. 177-182.

30. Li, C.Z. and Z.K.B. Zhao, *Efficient acid-catalyzed hydrolysis of cellulose in ionic liquid.* Advanced Synthesis & Catalysis, 2007. **349**: p. 1847-1850.

31. Rinaldi, R., et al., *An Integrated Catalytic Approach to Fermentable Sugars from Cellulose.* Chemsuschem, 2010. **3**(10): p. 1151-1153.

32. Sievers, C., et al., *Ionic-Liquid-Phase Hydrolysis of Pine Wood.* Industrial & Engineering Chemistry Research, 2009. **48**(3): p. 1277-1286.

33. Moiseev, Y.V.K., N.A.; Zaikov, G.E., *The mechanism of the acid-catalysed hydrolysis of*

polysaccharides. Carbohydrate Research, 1976. **51:** p. 39–54.

34. Kim, J.S., Y.Y. Lee, and R.W. Torget, *Cellulose hydrolysis under extremely low sulfuric acid and high-temperature conditions.* Applied Biochemistry and Biotechnology, 2001. **91-3:** p. 331–340.

35. Shimizu, K., et al., *Effects of Bronsted and Lewis acidities on activity and selectivity of heteropolyacid-based catalysts for hydrolysis of cellobiose and cellulose.* Green Chemistry, 2009. **11**(10): p. 1627–1632.

36. Xiang, Q., et al., *Heterogeneous aspects of acid hydrolysis of alpha-cellulose.* Applied Biochemistry and Biotechnology, 2003. **105:** p. 505–514.

37. Choi, J.H. and S.B. Kim, *EFFECT OF ULTRASOUND ON SULFURIC ACID-CATALYZED HYDROLYSIS OF STARCH.* Korean Journal of Chemical Engineering, 1994. **11**(3): p. 178–184.

38. Torget, R.W., J.S. Kim, and Y.Y. Lee, *Fundamental aspects of dilute acid hydrolysis/fractionation kinetics of hardwood carbohydrates. 1. Cellulose hydrolysis.* Industrial & Engineering Chemistry Research, 2000. **39**(8): p. 2817–2825.

39. Bej, B., R.K. Basu, and S.N. Ash, *Kinetic studies on acid catalysed hydrolysis of starch.* Journal of Scientific & Industrial Research, 2008. **67**(4): p. 295–298.

40. Harris, E.E. and B.G. Lang, *HYDROLYSIS OF WOOD CELLULOSE AND DECOMPOSITION OF SUGAR IN DILUTE PHOSPHORIC ACID.* Journal of Physical and Colloid Chemistry, 1947. **51**(6): p. 1430–1441.

41. Hamelinck, C.N., G. van Hooijdonk, and A.P.C. Faaij, *Ethanol from lignocellulosic biomass: techno-economic performance in short-, middle- and long-term.* Biomass & Bioenergy, 2005. **28**(4): p. 384-410.

42. Lourvanij, K. and G.L. Rorrer, *REACTIONS OF AQUEOUS GLUCOSE SOLUTIONS OVER SOLID-ACID Y-ZEOLITE CATALYST AT 110-160 DEGREES-C.* Industrial & Engineering Chemistry Research, 1993. **32**(1): p. 11-19.

43. Brown, T., et al., *Chemistry: the central science.* 10th ed2006, Upper Saddle River: Prentice Hall.

44. Allen, S.G., et al., *Fractionation of sugar cane with hot, compressed, liquid water.* Industrial & Engineering Chemistry Research, 1996. **35**(8): p. 2709-2715.

45. Matsumura, Y., et al., *Supercritical water treatment of biomass for energy and material recovery.* Combustion Science and Technology, 2006. **178**(1-3): p. 509-536.

46. Minowa, T., et al., *Decomposition of cellulose and glucose in hot-compressed water under catalyst-free conditions.* Journal of Chemical Engineering of Japan, 1998. **31**(1): p. 131-134.

47. Sakaki, T., et al., *Saccharification of cellulose using a hot-compressed water-folw reactor.* Industrial & Engineering Chemistry Research, 2002. **41**(4): p. 661-665.

48. Bobleter, O. and G. Pape, *HYDROTHERMAL DEGRADATION OF GLUCOSE.* Monatshefte Fur Chemie, 1968. **99**(4): p. 1560-&.

49. Kabyemela, B.M., et al., *Kinetics of glucose epimerization and decomposition in subcritical and supercritical water.* Industrial & Engineering Chemistry Research, 1997. **36**(5): p. 1552-1558.

50. Mansfield, S.D., C. Mooney, and J.N. Saddler, *substrate and enzyme characteristics that limit cellulose hydrolysis.* Biotechnology Progress, 1999. **15**: p. 804-816.

51. Bobleter, O., *HYDROTHERMAL DEGRADATION OF POLYMERS DERIVED FROM PLANTS.* Progress in Polymer Science, 1994. **19**(5): p. 797-841.

52. Bootsma, J.A. and B.H. Shanks, *Cellobiose hydrolysis using organic-inorganic hybrid mesoporous silica catalysts.* Applied Catalysis a-General, 2007. **327**(1): p. 44-51.

53. Klein-Marcuschamer, D., et al., *The challenge of enzyme cost in the production of lignocellulosic biofuels.* Biotechnology and Bioengineering, 2011. **109**(4): p. 1083-1087.

54. Tagusagawa, C., et al., *Highly Active Mesoporous Nb-W Oxide Solid-Acid Catalyst.* Angewandte Chemie-International Edition, 2010. **49**(6): p. 1128-1132.

55. Dhepe, P.L., et al., *Hydrolysis of sugars catalyzed by water-tolerant sulfonated mesoporous silicas.* Catalysis Letters, 2005. **102**(3-4): p. 163-169.

56. Bootsma, J.A., et al., *Hydrolysis of oligosaccharides from distillers grains using organic-inorganic hybrid mesoporous silica catalysts.* Bioresource Technology, 2008. **99**(12): p. 5226-5231.

57. Degirmenci, V., et al., *Sulfated Zirconia Modified SBA-15 Catalysts for Cellobiose Hydrolysis.* Catalysis Letters, 2011. **141**(1): p. 33-42.

58. Jiang, Y.J., et al., *Acid functionalized, highly dispersed carbonaceous spheres: an effective solid acid for hydrolysis of polysaccharides.* Journal of Nanoparticle Research, 2011. **13**(2): p. 463-469.

59. Rinaldi, R., R. Palkovits, and F. Schuth, *Depolymerization of Cellulose Using Solid Catalysts in Ionic Liquids.* Angewandte Chemie-International Edition, 2008. **47**(42): p. 8047-8050.

60. Holm, V.C., Bailey, G, *Sulfate-treated zirconia-gel catalyst*, in *US 3032599*, DOCDB, Editor 1962: US.

61. Katada, N.E., J.; Notsu, K.; Yasunobu, N.; Naito, N.; Niwa, M., *Superacidity and catalytic activity of sulfated zirconia.* Journal of Physical Chemistry B, 2000. **104**: p. 10321-10328.

62. Zhang, L., et al., *Sulfated Zirconia-A Superacid.* Progress in Chemistry, 2011. **23**(5): p. 860-873.

63. Song, X.M. and A. Sayari, *Sulfated zirconia-based strong solid-acid catalysts: Recent progress.* Catalysis Reviews-Science and Engineering, 1996. **38**(3): p. 329-412.

64. Chen, F., X.J. Meng, and F.S. Xiao, *Mesoporous Solid Acid Catalysts.* Catalysis Surveys from Asia, 2011. **15**(1): p. 37-48.

65. Yamaguchi, T., *RECENT PROGRESS IN SOLID SUPERACID.* Applied Catalysis, 1990. **61**(1): p. 1-25.

66. Yamaguchi, D., et al., *Hydrolysis of Cellulose by a Solid Acid Catalyst under Optimal Reaction Conditions.* Journal of Physical Chemistry C, 2009. **113**(8): p. 3181-3188.

67. Hino, M., et al., *The surface structure of sulfated zirconia: Studies of XPS and thermal analysis.* Thermochimica Acta, 2006. **441**(1): p. 35-41.

68. Clearfield, A., G.P.D. Serrette, and A.H. Khazisyed, *NATURE OF HYDROUS ZIRCONIA AND SULFATED HYDROUS ZIRCONIA.* Catalysis Today, 1994. **20**(2): p. 295-312.

69. Adeeva, V., et al., *ACID SITES IN SULFATED AND METAL-PROMOTED ZIRCONIUM DIOXIDE CATALYSTS.* Journal of Catalysis, 1995. **151**(2): p. 364-372.

70. Morterra, C., et al., *BRONSTED ACIDITY OF A SUPERACID SULFATE-DOPED ZRO2 SYSTEM.* Journal of Physical Chemistry, 1994. **98**(47): p. 12373-12381.

71. Riemer, T., et al., *SUPERACID PROPERTIES OF SULFATED ZIRCONIA AS MEASURED BY RAMAN AND H-1 MBS NMR-SPECTROSCOPY.* Journal of the Chemical Society-Chemical Communications, 1994(10): p. 1181-1182.

72. White, R.L., et al., *Potential role of penta-coordinated sulfur in the acid site structure of sulfated zirconia.* Journal of Catalysis, 1995. **157**(2): p. 755-758.

73. Babou, F., G. Coudurier, and J.C. Vedrine, *Acidic properties of sulfated zirconia - an infrared spectroscopic study.* Journal of Catalysis, 1995. **152**(2): p. 341-349.

74. Arata, K. and M. Hino, *PREPARATION OF SUPERACIDS BY METAL-OXIDES AND THEIR CATALYTIC ACTION.*

Materials Chemistry and Physics, 1990. **26**(3-4): p. 213-237.

75. Laizet, J.B., et al., *Influence of sulfation and structure of zirconia on catalytic isomerization of n-hexane.* Topics in Catalysis, 2000. **10**(1-2): p. 89-97.

76. Auari, R., et al., *Synthesis and characterization of mesoporous silica-supported nano-crystalline sulfated zirconia catalysts prepared by a sol-gel process: Effect of the S/Zr molar ratio.* Applied Catalysis a-General, 2007. **328**(1): p. 43-51.

77. Connoly, D.J.G., W.F., *Fluorocarbon vinyl ether polymers*, 1966: US.

78. Olah, G.A., P.S. Iyer, and G.K.S. Prakash, *PERFLUORINATED RESINSULFONIC ACID (NAFION-H) CATALYSIS IN SYNTHESIS.* Synthesis-Stuttgart, 1986(7): p. 513-531.

79. Rajagopal, G., Lee, H., Kim, S.S., *Nafion SAC-13: heterogeneous and reusable catalyst for the activation of HMDS for efficient and selective O-silylation reactions under solvent-free condition.* Tetrahedron, 2009. **65**: p. 4735-4741.

80. Arata, K., *Solid superacids.* Advances in Catalysis, 1990. **37**: p. 165-211.

81. Rorvik, T., Dahl, I.M., Mostad, H.B., *Nafion-H as catalyst for isobutane/2-butene alkylation compared with a cerium exchange Y zeolite.* Catalysis Letters, 1995. **33**: p. 127-134.

82. Harmer, M.A., Farneth, W.E., Sun, Q., *High surface area Nafion resin/silica nanocomposites: a new class of solid acid catalyst.* Journal of the

American Chemical Society, 1996. **118**(33): p. 7708–7715.

83. Sun, Q., Harmer, M.A., Farneth, W.E., *But-1-ene isomerization over Nafion resin/silica composite catalyst.* Chemical Communications, 1996. **1996**(10): p. 1201–1202.

84. Heidekum, A., Harmer, M.A., Hoelderich, W.F., *Highly selective fries rearrangement over zeolites and Nafion in silica composite catalysts: a comparison.* Journal of Catalysis, 1998. **176**(1): p. 260–263.

85. Lopez, D.E.G., J.B.; Bruce, D.A., *Transesterification of triacetin with methanol on Nafion acid resins.* Journal of Catalysis, 2007. **245**: p. 381–391.

86. Flanigen, E., r. Broach, and S. Wilson, *Introduction*, in *Zeolites in industrial separation and catalysis*, S. Kulprathipanja, Editor 2010, Wiley-VCH: Weinheim.

87. Okuhara, T., *Water-tolerant solid acid catalysts.* Chemical Reviews, 2002. **102**(10): p. 3641–3665.

88. Abdo, S., *Bond breaking and rearrangement*, in *Zeolites in Industrial Separation and Catalysis*, S. Kulprathipanja, Editor 2010, Wiley-VCH: Weinheim. p. 307–327.

89. Bauer, J., et al., *Indsustrial isomerization*, in *Zeolites in Industrial Separation and Catalysis*, S. Kulprathipanja, Editor 2010, Wiley-VCH: Weinheim. p. 307–327.

90. Jan, D.Y. and P. Barger, *Processes on industrial C-C bond formation*, in *Zeolites in Industrial*

Separation and Catalysis, S. Kulprathipanja, Editor 2010, Wiley-VCH: Weinheim. p. 307-327.

91.   O'Brien-Abraham, J., Lin, J.Y, *Zeolite membrane separations*, in *Zeolites in Industrial Separation and Catalysis*, S. Kulprathipanja, Editor 2010, Wiley-VCH: Weinheim. p. 307-327.

92.   Young, G.J., *Interaction of water vapor with silica surfaces.* Journal of Colloid Science, 1958. **13**(1): p. 67-85.

93.   McCusker, C.B.a.L.B. *Database of Zeolite Structures*. Available from: http://www.iza-structure.org/databases/.

94.   Broach, R.W., *Zeolite types and structures*, in *Zeolites in industrial separation and catalysis*, S. Kulprathipanja, Editor 2010, Wiley-VCH: Weinheim.

95.   Baerlocher, C., *Atlas of zeolite framework types*. 6th ed, ed. L. McCusker, et al.2007, Boston: Elsevier.

96.   Frising, T. and P. Leflaive, *Extraframework cation distributions in X and Y faujasite zeolites: A review.* Microporous and Mesoporous Materials, 2008. **114**(1-3): p. 27-63.

97.   Olson, D.H., et al., *CRYSTAL-STRUCTURE AND STRUCTURE-RELATED PROPERTIES OF ZSM-5.* Journal of Physical Chemistry, 1981. **85**(15): p. 2238-2243.

98.   Mentzen, B.F., *Crystallographic determination of the positions of the monovalent H, Li, Na, K, Rb, and Tl cations in fully dehydrated MFI type zeolites.* Journal of Physical Chemistry C, 2007. **111**(51): p. 18932-18941.

99. Weingarten, R., et al., *Design of solid acid catalysts for aqueous-phse dehydration of carbohydrates: the role of Lewis and Bronsted acid sites.* Journal of Catalysis, 2011. **279**: p. 174–182.

100. Katada, N. and M. Niwa, *Analysis of acidic properties of zeolitic and non-zeolitic solid acid catalysts using temperature-programmed desorption of ammonia.* Chemistry and Materials Science, 2004. **8**(3): p. 161–170.

101. Corma, A. and H. Garcia, *Organic reactions catalysed over solid catalysts.* Catalysis Today, 1997. **38**: p. 257–308.

102. Chai, F., et al., *Transesterification of vegetable oil to biodiesel using a heteropolyacid solid catalyst.* Advanced Synthesis & Catalysis, 2007. **349**: p. 1057–1065.

103. Sikabwe, C.E., *Investigations of the effects of iron, manganese, and nickel on the properties of sulfated zirconia catalysts*, in *Chemistry and Biochemistry*1997, University of Oklahoma: Norman.

104. Hesse, n., *In-Situ analysis of volatiles obtained by catalytic cracking of polyethylene with HZSM-5, HY, and HMCM-41*, in *Chemistry and Biochemistry*2002, University of Oklahoma: Norman.

105. Argauer, R., *Crystalline zeolite zsm-5 and method of preparing the same*, in *DOCDB*1972.

106. Hesse, N.D., et al., *In situ analysis of volatiles obtained from the catalytic cracking of polyethylene.* Journal of Applied Polymer Science, 2001. **82**(12): p. 3118–3125.

107. Benedict, S.R., *A reagent for the detection of reducing sugars.* Journal of Biological Chemistry, 1909. **5**(5): p. 485-487.

108. Forni, L., *Comparison of the methods for the determination of surface acidity of solid catalysts.* Catalysis Reviews-Science and Engineering, 1974. **8**(1): p. 65-115.

109. Glazneva, T., N. Kotsarenko, and E. Paukshtis, *Surface acidity and basicity of oxide catalysts: from aqueous suspensions to in situ measurements.* Kinetics and Catalysis, 2008. **49**(6): p. 906-915.

110. Kamiya, Y., et al., *Zirconium phosphate with a high surface area as a water-tolerant solid acid.* Catalysis Letters, 2004. **94**(1-2): p. 45-47.

111. Horita, N., et al., *CS2.5H0.5PW12O40 bonded to an amine functionalized SiO2 as an excellent water-tolerant solid acid.* Chemistry Letters, 2005. **34**(10): p. 1376-1377.

112. Tarafdar, A., et al., *Synthesis of spherical mesostructured zirconium phosphate with acidic properties.* Microporous and Mesoporous Materials, 2006. **95**(1-3): p. 360-365.

113. Inumaru, K., et al., *Water-tolerant, highly active solid acid catalysts composed of the Keggin-type polyoxometalate H3PW12O40 immobilized in hydrophobic nanospaces of organomodified mesoporous silica.* Angewandte Chemie-International Edition, 2007. **46**(40): p. 7625-7628.

114. Li, L.S., Y. Yoshinaga, and T. Okuhara, *Unusual acceleration of acid-catalyzed reactions by water in the presence of Mo/Zr mixed oxides calcined at high temperatures.* Physical Chemistry Chemical Physics, 2002. **4**(24): p. 6129-6136.

115. Okuyama, K., et al., *Water-tolerant catalysis of a silica composite of a sulfonic acid resin, Aciplex.* Applied Catalysis a-General, 2000. **190**(1-2): p. 253-260.

116. Chuntanapum, A., T. Shii, and Y. Matsumura, *Acid-Catalyzed char formation of 5-HMF in subcritical water.* Journal of Chemical Engineering of Japan, 2011. **44**(6): p. 431-436.

117. Bandura, A. and S. Lvov, *The ionization constant of water over wide ranges of temperature and density.* Journal of Physical Chemistry Reference Data, 2006. **35**(1): p. 15-30.

118. Ando, H., et al., *Decomposition behavior of plant biomass in hot-compressed water.* Industrial & Engineering Chemistry Research, 2000. **39**: p. 3688-3693.

119. Marshall, W. and W. Franck, *New international formulation and its background.* Journal of Physical Chemistry Reference Data, 1981. **10**(2): p. 295-304.

120. Kimura, M., T. Nakato, and T. Okuhara, *Water-tolerant solid acid catalysis of Cs2.5H0.5PW12O40 for hydrolysis of esters in the presence of excess water.* Applied Catalysis a-General, 1997. **165**: p. 227-240.

121. Namba, S., N. Hosonuma, and T. Yashima, *CATALYTIC APPLICATION OF HYDROPHOBIC PROPERTIES OF HIGH-SILICA ZEOLITES .1. HYDROLYSIS OF ETHYL-ACETATE IN AQUEOUS-SOLUTION.* Journal of Catalysis, 1981. **72**(1): p. 16-20.

122. Kasprzyk-Hordern, B., *Chemistry of alumina, reaction in aqueous solution and its application in water treatment.* Advances in Colloid and Interface Science, 2004. **110**: p. 19-48.

123. Parker, L., D. Bibby, and G. Burns, *Interaction of water with the zeolite HY, studies by FTIR.* Zeolites, 1991. **11:** p. 293-297.

124. Parker, L., D. Bibby, and G. Burns, *an infrared study of H2O and D2O on HZSM-5 and DZSM-5.* Zeolites, 1993. **13**(2): p. 107-112.

125. Lohse, U., et al., *Hydroxyl groups of the non-framework aluminium species in dealuminated Y zeolites.* Zeolites, 1987. **7**(1): p. 11-13.

126. Manjare, S. and A. Ghoshal, *Comparison of adsorption of ethyl acetate on activated carbon and molecular sieves 5A and 13X.* Journal of Chemical & Engineering Data, 2006. **51:** p. 1185-1189.

127. Kerr, G., *Some comments on Bolton's "deammination ammonium Y" zeolite.* Journal of Catalysis, 1974. **35:** p. 476-477.

128. Olson, D.H., Haag, W.O., Lago, R.M., *Chemical and physical properties of the ZSM-5 substitutional series.* Journal of Catalysis, 1980. **61**(6): p. 390-396.

129. Nakamoto, H., Takahashi, H., *Hydrophobic natures of zeolites ZSM-5.* Zeolites, 1982. **2**(2): p. 67-68.

130. Li, L., Y. Yoshinaga, and T. Okuhara, *Water-tolerance catalysis by Mo-Zr mixed oxides calcined at high temperatures.* Physical Chemistry Chemical Physics, 1999. **1:** p. 4913-4918.

131. Yamada, T. and T. Okuhara, *Hydrophobicity of water-tolerant solid acids characterized by adsorption of water and benzene.* Langmuir, 2000. **16:** p. 2321-2325.

132. van Bekkum, H., Flanigen, E.M, Jacobs, P.A., Jansen, J.C., *Introduction to zeolite science and practice*. 2nd ed2011, Amsterdam: Elsevier Science.

133. Hattori, T., Yashima, T., *Studies in surface science and catalysis: Zeolites and microporous crystals.* 1994. **83:** p. xxi.

134. Wright, P., *Microporous Framework Solids*2008, Cambridge: Royal Society of Chemistry.

135. Okuhara, T., M. Kimura, and T. Nakato, *A water-tolerant solid acid, Cs2.5H0.5PW12O40, for hydrolysis of esters in water* Applied Catalysis a-General, 1997. **155**(1): p. L9-L13.

136. Palinko, I., et al., *Surface characterization of variously treated Nafion-H, Nafion-H supported on silica and Nafion-H silica nanocomposite catalysts by infrared microscopy.* Applied Catalysis a-General, 1998. **174:** p. 147-153.

137. Omota, F., A.C. Dimian, and A. Bliek, *Fatty acid esterification by reactive distillation: Part 2 – Kinetics-based desing for sulphated zirconia catalysts.* Chemical Engineering Science, 2003. **58**(14): p. 3175-3185.

138. Lopez, D., J. Goodwin, and B. Bruce, *Transesterification of triacetin with methanol on Nafion acid resins.* Journal of Catalysis, 2007. **245**(2): p. 381-391.

139. Gebel, G., P. Aldebert, and M. Pineri, *Swelling study of perfluorosulphonated ionomer membranes.* Polymer, 1993. **34**(2): p. 333-339.

140. Nivarthy, G., K. Seshan, and J. Lercher, *The influence of acidity on zeolite H-BEA catalyzed*

isobutane/n-butene   alkylation.   Microporous   and
Mesoporous Materials, 1998. **22:** p. 379.

141. Silva, B., et al., *Evaluation of ion exchange-
     modified   Y   and   ZSM-5   zeolites   in   Cr(VI)
     biosorption and catalytic oxidation of ethyl
     acetate.* Applied Catalysis B: Environmental, 2012.
     117-118: p. 406-413.

142. Kielland, J., *Individual activity coefficients of
     ions in aqueous solutions.* Journal of American
     Chemical Society, 1937. **59:** p. 1675-1678.

143. Harris, D., *Quantitative Chemical Analysis*. 7th
     ed2007, New York: W.H. Freeman and Company.

144. Alberti, A. and A. Martucci, *Proton transfer
     mediated by water: experimental evidence by
     neutron diffraction.* Journal of Physical Chemistry
     C, 2010. **114:** p. 7767-7773.

145. P. Sarv, T.T., E. Lippmaa, K. Keskinen, A. Root,
     *Mobility of the acidic proton in broensted sites
     of H-Y, H-Mordenite, and H-ZSM-5 zeolites, studied
     by   high-temperature   1H   MAS   NMR.*   Journal   of
     Physical Chemistry, 1995. **99**(38): p. 13763-13768.

146. Baba, T., et al., *Mobility of the acidic protons
     in H-ZSM-5 as studied by variable temperature 1H
     MAS NMR.* Journal of Physical Chemistry B, 1998.
     102(5): p. 804-808.

147. Sierka, M. and J. Sauer, *Proton mobility in
     chabazite, faujasite, and ZSM-5 zeolite catalysts.
     Comparion based on ab initio calculations.* The
     Journal of Physical Chemistry B, 2001. **105**(8): p.
     1603-1613.

148. Ryder, J., A. Chakraborty, and A. Bell, *Density
     functional   theory   study   of   proton   mobility   in*

zeolites: proton migration and hydrogen exchange in ZSM-5. Journal of PHysical Chemistry B, 2000. **104**(30): p. 6998-7011.

149. Hattori, T. and S. Morita, *Energy Crops for Sustainable Bioethanol Production; Which, Where and How?* Plant Production Science, 2010. **13**(3): p. 221-234.

150. Hashaikeh, R., et al., *Hydrothermal dissolution of willow in hot compressed water as a model for biomass conversion.* Fuel, 2007. **86**(10-11): p. 1614-1622.

151. Pinkert, A., et al., *Ionic Liquids and Their Interaction with Cellulose.* Chemical Reviews, 2009. **109**(12): p. 6712-6728.

152. Singh, S., B.A. Simmons, and K.P. Vogel, *Visualization of Biomass Solubilization and Cellulose Regeneration During Ionic Liquid Pretreatment of Switchgrass.* Biotechnology and Bioengineering, 2009. **104**(1): p. 68-75.

153. Dorn, S., et al., *Interactions of Ionic Liquids with Polysaccharides-7: Thermal Stability of Cellulose in Ionic Liquids and N-Methylmorpholine-N-oxide.* Macromolecular Materials and Engineering, 2008. **293**(11): p. 907-913.

154. Dadi, A.P., S. Varanasi, and C.A. Schall, *Enhancement of cellulose saccharification kinetics using an ionic liquid pretreatment step.* Biotechnology and Bioengineering, 2006. **95**(5): p. 904-910.

155. Li, Q., et al., *Improving enzymatic hydrolysis of wheat straw using ionic liquid 1-ethyl-3-methyl imidazolium diethyl phosphate pretreatment.* Bioresource Technology, 2009. **100**(14): p. 3570-3575.

156.   Zhang, Y.T., et al., *Ionic Liquid–Water Mixtures: Enhanced K-w for Efficient Cellulosic Biomass Conversion.* Energy & Fuels, 2010. **24:** p. 2410–2417.

157.   Binder, J.B. and R.T. Raines, *Fermentable sugars by chemical hydrolysis of biomass.* Proceedings of the National Academy of Sciences of the United States of America, 2010. **107**(10): p. 4516–4521.

158.   Rinaldi, R., et al., *Which Controls the Depolymerization of Cellulose in Ionic Liquids: The Solid Acid Catalyst or Cellulose?* Chemsuschem, 2010. **3**(2): p. 266–276.

159.   Vitz, J., et al., *Extended dissolution studies of cellulose in imidazolium based ionic liquids.* Green Chemistry, 2009. **11**(3): p. 417–424.

160.   Sievers, C., et al., *Acid–Catalyzed Conversion of Sugars and Furfurals in an Ionic-Liquid Phase.* Chemsuschem, 2009. **2**(7): p. 665–671.

161.   Vanoye, L., et al., *Kinetic model for the hydrolysis of lignocellulosic biomass in the ionic liquid, 1–ethyl–3–methyl–imidazolium chloride.* Green Chemistry, 2009. **11**(3): p. 390–396.

162.   Zhang, Z.H. and Z.B.K. Zhao, *Solid acid and microwave-assisted hydrolysis of cellulose in ionic liquid.* Carbohydrate Research, 2009. **344**(15): p. 2069–2072.

163.   Rinaldi, R. and F. Schuth, *Design of solid catalysts for the conversion of biomass.* Energy & Environmental Science, 2009. **2**(6): p. 610–626.

164.   Zhang, D.L., et al., *Separation of ethyl acetate-ethanol azeotropic mixture using hydrophilic ionic*

liquids. Industrial & Engineering Chemistry Research, 2008. **47**(6): p. 1995-2001.

165. Crosthwaite, J.M., et al., *Liquid phase behavior of imidazolium-based ionic liquids with alcohols.* Journal of Physical Chemistry B, 2004. **108**(16): p. 5113-5119.

166. Dwiatmoko, A.A., et al., *Understanding the role of halogen-containing ionic liquids in the hydrolysis of cellobiose catalyzed by acid resins.* Applied Catalysis a-General, 2010. **387**(1-2): p. 209-214.

167. Ingle, J. and S. Crouch, *Spectrochemical Analysis*1988, Upper Saddle River: Prentice Hall.

168. Santen, R.A.v., *Theory of Bronsted acidity in zeolites.* Advanced Zeolite Science and Applications, 1994. **85:** p. 273-294.

169. J. Lavalley, R.A., J. Czyzniewska, M. Ziolek, *Use of pyridine as a probe for the determination, by IR spectroscopy, of the Bronsted acid strength of M(I)HNaY zeolites.* Journal of the chemical Society-Faraday Transactions, 1996. **92**(7): p. 1263-1266.

170. P. Jacobs, J.U., *Assignment of the hydroxyl bands in the infrared spectra of zeolites X and Y.* Journal of the chemical Society-Faraday Transactions, 1972. **69:** p. 359-372.

171. Jacobs, P.A. and R. Vonballmoos, *FRAMEWORK HYDROXYL-GROUPS OF H-ZSM-5 ZEOLITES.* Journal of Physical Chemistry, 1982. **86**(15): p. 3050-3052.

172. Rinaldi, R., *Instantaneous dissolution of cellulose in organic electrolyte solutions.* Chemical Communications, 2011. **47**(1): p. 511-513.

173. Slivko, S.A., M.A. Sarukhanov, and N.N. Kulikova, *STRUCTURE OF THE DIMETHYLSULFOXIDE MOLECULE IN NEUTRAL, ACID, AND ALKALINE MEDIA.* Journal of Structural Chemistry, 1993. **34**(3): p. 363–366.

174. Brethauer, S. and C.E. Wyman, *Review: Continuous hydrolysis and fermentation for cellulosic ethanol production.* Bioresource Technology, 2010. **101**(13): p. 4862–4874.

175. DOE, *Breaking the biological barriers to cellulosic ethanol: a joint research agenda*, G. Office of Biological and Environmental Research, Editor 2006: Rockville.

176. Girio, F.M., et al., *Hemicelluloses for fuel ethanol: A review.* Bioresource Technology, 2010. **101**(13): p. 4775–4800.

177. Service, R.F., *Is There a Road Ahead For Cellulosic Ethanol?* Science, 2010. **329**(5993): p. 784–785.

178. Wyman, C.E., *What is (and is not) vital to advancing cellulosic ethanol.* Trends in Biotechnology, 2007. **25**(4): p. 153–157.

179. Humbird, D., et al., *Process design and economics for biochemical conversion of lignocellulosic biomass to ethanol*, NREL, Editor 2011: Golden, Colorado.

180. Zhu, J.Y., X.J. Pan, and R.S. Zalesny, *Pretreatment of woody biomass for biofuel production: energy efficiency, technologies, and recalcitrance.* Applied Microbiology and Biotechnology, 2010. **87**(3): p. 847–857.

181. Arslan, Y. and N. Eken-Saracoglu, *Effects of pretreatment methods for hazelnut shell*

hydrolysate fermentation with Pichia Stipitis to ethanol. Bioresource Technology, 2010. **101**(22): p. 8664–8670.

182. Alvira, P., et al., *Pretreatment technologies for an efficient bioethanol production process based on enzymatic hydrolysis: A review.* Bioresource Technology, 2010. **101**(13): p. 4851–4861.

183. Kumar, P., et al., *Methods for Pretreatment of Lignocellulosic Biomass for Efficient Hydrolysis and Biofuel Production.* Industrial & Engineering Chemistry Research, 2009. **48**(8): p. 3713–3729.

184. Lee, S.H., et al., *Ionic Liquid-Mediated Selective Extraction of Lignin From Wood Leading to Enhanced Enzymatic Cellulose Hydrolysis.* Biotechnology and Bioengineering, 2009. **102**(5): p. 1368–1376.

185. Zavrel, M., et al., *High-throughput screening for ionic liquids dissolving (ligno-)cellulose.* Bioresource Technology, 2009. **100**(9): p. 2580–2587.

186. Dien, B.S., M.A. Cotta, and T.W. Jeffries, *Bacteria engineered for fuel ethanol production: current status.* Applied Microbiology and Biotechnology, 2003. **63**: p. 258–266.

187. Payen, F., et al., *CHED 192-Bacterial metabolism of ionic-liquid-pretreated lignocellulose: Production of biofuels.* Abstracts of Papers of the American Chemical Society, 2009. **238**(192-CHED).

188. Yanase, H., et al., *Ethanol production from wood hydrolysate using genetically engineered Zymomonas mobilis.* Applied Microbiology and Biotechnology, 2012. **94**(6): p. 1667–1678.

189. Chandel, A. and O. Singh, *Weedy lignocellulosic feedstock and microbial metabolic engineering: advancing the generation of 'biofuel'.* Applied Microbiology and Biotechnology, 2011. **89**(5): p. 1289-1303.

190. Mai, N.L., et al., *Recovery of ionic liquid and sugars from hydrolyzed biomass using ion exclusion simulated moving bed chromatography.* Journal of Chromatography A, 2011. **1227**: p. 67-72.

191. Amalgamated. *What is simulated moving bed chromatography (SMB chromatography).* http://www.arifractal.com.

192. Sendovski, M., N. Nir, and A. Fishman, *Bioproduction of 2-Phenylethanol in a Biphasic Ionic Liquid Aqueous System.* Journal of Agricultural and Food Chemistry, 2010. **58**(4): p. 2260-2265.

193. Guo, H., et al., *Hydrolysis of cellulose over functionalized glucose-derived carbon catalyst in ionic liquid.* Bioresource Technology, 2012. **116**: p. 355-359.

194. Shuai, L. and X. Pan, *Hydrolysis of cellulose by cellulase-mimetic solid catalyst.* Energy & Environmental Science, 2012. **5**(5): p. 6889-6894.

195. Zhang, C., et al., *Ionic liquid-functionalized biochar sulfonic acid as a biomimetic catalyst for hydrolysis of cellulose and bamboo under microwave irradiation.* Green Chemistry, 2012. **14**(7): p. 1928-1934.